Establishing the CRISPR/Cas13a genome editing system in *Nicotiana benthamiana* for RNA targeting applications

by

Gaëlle Robertson

Thesis presented in partial fulfilment of the requirements for the degree of Master of Science in the Faculty of Science at Stellenbosch University

Supervisor: Professor Johan Burger

Co-supervisor: Dr Manuela Campa

December 2021

DECLARATION

By submitting this thesis electronically, I declare that the entirety of the work contained therein is my own, original work, that I am the sole author thereof (save to the extent explicitly otherwise stated), that reproduction and publication thereof by Stellenbosch University will not infringe any third party rights and that I have not previously in its entirety or in part submitted it for obtaining any qualification.

Gaëlle Robertson

December 2021

ABSTRACT

Globally, grapevine (*Vitis vinifera*) is a widely cultivated fruit crop and makes a vital contribution to the South African agricultural sector. Highly susceptible to a plethora of virus species, grapevine faces severe constraints to overall crop productivity and durable antiviral strategies are necessary to control the spread of viral diseases. The CRISPR/Cas (clustered regularly interspaced short palindromic repeats/CRISPR associated) technology has emerged as a valuable genetic engineering tool for plant breeding purposes. Recently, genome editing by the CRISPR/Cas system has been expanded beyond DNA targeting. A novel class 2 Cas effector, Cas13a, has been revealed as a programmable RNA-targeting nuclease. Using CRISPR/Cas13a, this study therefore aimed to investigate the potential of this system to mediate targeted RNA cleavage and viral RNA interference in *Nicotiana benthamiana*. The choice of this model plant allowed for an immediate test of the functionality and efficacy of this system. For this, binary Cas13a vectors targeting regions of an annotated mRNA transcript from the carotenoid pathway were assembled and transgenic *N. benthamiana* lines were established. A CRISPR/Cas13a-based down-regulation of gene expression was not observed in these lines. However, after improving the cellular localisation of the Cas13a/crRNA constructs, a transgenic line expressing a cytoplasmic-localised Cas13a/crRNA vector showed a significant two-fold reduction in target gene expression, further correlated with a lowered concentration of total carotenoid content from a preliminary measurement. To demonstrate virus inhibition, a modified tobacco mosaic virus (TMV) system expressing a green fluorescent protein (TRBO-GFP), was used to visually and molecularly measure CRISPR/Cas13a-mediated interference activity in *N. benthamiana*. A LwaCas13a/crRNA vector targeting a conserved region of the reporter mRNA was assembled and after performing a series of transient assays, phenotypic quantifications of GFP signal intensity confirmed a significant attenuation (~50%) in virus accumulation. However, RT-qPCR analyses showed that GFP mRNA abundance was not directly proportional to that of the observed GFP signal intensity, suggesting a possible limitation in the method of molecular quantification of the GFP mRNA transcript levels. Overall, the results provide insight into the functionality of the CRISPR/Cas13a system for RNA targeting of both an endogenous transcript and a viral genome in plants. Further optimisation of crRNA design features and the method of CRISPR component delivery are highlighted for future studies, especially for an application in grapevine.

OPSOMMING

Wingerd (*Vitis vinifera*) is wêreldwyd 'n algemeen-verboude vrugtegewas en maak 'n belangrike bydrae tot die Suid-Afrikaanse landbousektor. Aangesien wingerd hoogs vatbaar is vir 'n groot aantal virusspesies, staar die bedryf ernstige beperkings in die gesig ten opsigte van produktiwiteit, en word duur virus-beheerstrategieë benodig om die verspreiding van virussiektes te beheer. Die CRISPR/Cas (gegroepeerde eweredig-gespasieërde kort palindromiese herhalings/CRISPR-geassosieerde) tegnologie het as 'n genetiese manipulasie toepassing vir planttelingsdoeleindes na vore gekom. Onlangs is genoom-redigering deur middel van CRISPR/Cas verder as net DNS as teiken uitgebrei. Die nuwe klas-2 Cas effektor, Cas13a, het as ‘n programmeerbare RNS-teiken nuklease te voorskyn gekom. Die doel van hierdie studie was om die potensiaal van CRISPR/Cas13a op geteikende RNS kliewing en virus-RNS inhibisie in *Nicotiana benthamiana*, te ondersoek. Die keuse van hierdie modelplant het die vinnige toets van beide funksionaliteit en doeltreffendheid van hierdie stelsel moontlik gemaak. Hiervoor is binêre Cas13a vektore ontwikkel wat areas van ‘n geannoteerde bRNS transkrip van die karotenoïed-weg teiken, en transgeniese *N. benthamiana* lyne is daargestel. 'n CRISPR/Cas13a-gebaseerde afregulering van geenuitdrukking was nie in hierdie lyne waargeneem nie. Na die verbetering van die sellulêre lokalisering van die Cas13a/crRNS konstrukte egter, is 'n transgeniese lyn, wat 'n sitoplasmies-gelokaliseerde Cas13a/crRNA vektor uitdruk, ontwikkel wat 'n beduidende tweevoudige vermindering in teiken geenuitdrukking getoon het, en wat ook goed gekorreleer het met 'n verlaagde konsentrasie van totale karotenoïed-inhoud. Om virus-inhibisie te demonstreer, is 'n gemodifiseerde tabak mosaïek virus (TMV) stelsel, wat 'n groen-fluoresserende proteïen uitdruk (TRBO-GFP), gebruik om die CRISPR/Cas13a-gemedieërde inhibisie-aktiwiteit in *N. benthamiana*, beide visueel en molekulêr, te meet. 'n Cas13a/crRNS vektor wat 'n gekonserveerde streek van die merker-geen mRNS teiken, was ontwikkel wat in ‘n reeks tydelike uitdrukkingseksperimente ‘n beduidende verswakking (~50%) in virus-akkumulasie bevestig het. Kwantitatiewe molekulêre ontledings van GFP bRNS uitdrukking kon egter nie ‘n direkte korrelasie met die waargenome GFP sein-intensiteit aantoon nie, wat moontlik dui op 'n beperking van die molekulêre kwantifiseringsmetode. Saamgevat, gee die resultate ‘n insig in die funksionaliteit van die CRISPR/Cas13a stelsel vir RNS teikening van beide 'n endogene transkrip asook 'n virusgenoom in plante. Verdere optimisering van crRNS ontwerp en die metode van CRISPR-komponent toediening word benodig vir toekomstige studies, veral vir toepassings in wingerd.

ACKNOWLEDGEMENTS

I would like to acknowledge and express my sincere gratitude towards the following individuals and institutions:

The **Wine Industry Network of Expertise and Technology (Winetech)** and **Stellenbosch University**, for research funding and financial support.

Prof Johan Burger, for your exceptional guidance, insight and encouragement over the course of my MSc. I consider myself very lucky that I ended up in your research group three years ago and to have had you as a supervisor.

Dr Manuela Campa, the greatest mentor anyone could ever ask for. Thank you for the unwavering support you provide for all your students you supervise. Your unparalleled dedication to your work is truly inspiring and your kind nature is genuine. Beyond every skill, technique and concept you patiently taught me, you also instilled a true appreciation for plant biotechnology in me.

All the members of the **Vitis lab**, for providing a very enjoyable work environment and always being ready to lend a helping hand or (mostly) chat away our trials and triumphs.

Dr Rachelle Bester, for organising plant material and lending us greenhouse space at the farm.

Dr Justin Lashbrooke and **Dr Philip Young**, for your assistance in using the facilities at the Institute of Wine Biotechnology (IWBT) for some of the analyses.

Finally, my **friends** and **family**, for being forever supportive from both near and far. Without your constant words of encouragement and unconditional love, I would never have been able to complete this. And of course, **Gideon**, my sounding board, thank you for always being there to give me perspective.

TABLE OF CONTENTS

LIST OF FIGURES

LIST OF TABLES

LIST OF ABBREVIATIONS

AGO	Argonaute
BAP	6-Benzylaminopurine
BLAST	Basic Local Alignment Search Tool
CAF	Central Analytical Facility
Cas	CRISPR-associated proteins
cDNA	complementary DNA
CI	Confidence interval
CRISPR	Clustered regularly interspaced short palindromic repeat
crRNA	CRISPR RNA
CTAB	Cetyltrimethylammonium bromide
CTCF	Corrected total cell fluorescence
DBD	DNA-binding domain
dCas	catalytically inactive Cas protein
DCL	Dicer-like
DNA	Deoxyribonucleic acid
DNase	deoxyribonuclease
DSB	Double-stranded break
dsDNA	double-stranded DNA
dsRNA	double-stranded RNA
ELISA	Enzyme-linked immunosorbent assay
GFP	Green fluorescent protein
gRNA	guide RNA
HDR	Homology-directed repair
HEPN	Higher eukaryotes and prokaryotes nucleotide-binding
LB	Luria-Bertani
LCYB	Lycopene β-cyclase
LCYE	Lycopene ε-cyclase
MES	2-(N-morpholino) ethanesulfonic acid
miRNA	micro-RNA

mRNA	messenger ribonucleic acid
MS	Murashige and Skoog
msfGFP	monomeric superfolder GFP
NES	Nuclear export signal
NHEJ	Non-homologous end-joining
NLS	Nuclear localisation signal
nt	nucleotide
PAM	Protospacer adjacent motif
PAMmer	PAM-presenting oligonucleotide
PCR	Polymerase chain reaction
PDR	Pathogen-derived resistance
PDS	Phytoene desaturase
PEG	Polyethylene glycol
PFS	Protospacer flanking sequence
pgRNA	polyvalent gRNA
pre-crRNA	precursor CRISPR RNA
PTGS	Post-transcriptional gene silencing
RdDM	RNA-directed DNA methylation
REPAIR	RNA Editing for Programmable A-to-I Replacement
RISC	RNA-induced silencing complex
RNA	Ribonucleic acid
RNAi	RNA interference
Rnase	Ribonuclease
RNP	Ribonucleoprotein
RT-PCR	Reverse transcriptase PCR
RT-qPCR	Reverse transcriptase quantitative PCR
scaRNA	small CRISPR/Cas-associated RNA
SDN	Site-directed nuclease
sgRNA	single guide RNA
SHERLOCK	Specific High-Sensitivity Enzymatic Reporter UnLOCKing

siRNA	small interfering RNA
ssRNA	Single-stranded RNA
TALENs	Transcription activator-like effector nucleases
TGS	Transcriptional gene silencing
tracrRNA	trans-activating crRNA
TRBO	Tobacco mosaic virus RNA-based overexpression
v/v	volume per volume
VSR	Viral suppressors of RNA silencing
w/v	weight per volume
YEB	Yeast extract broth
ZNFs	Zinc-finger nucleases

CHAPTER 1: INTRODUCTION

1.1 General background

One of the world's most important fruit crops is grapevine (*Vitis vinifera*). With the global area of grapevines cultivated exceeding 7.4 million ha in 2018, viticulture has become part of the world's major horticultural industries (OIV, 2018). According to the latest statistics, South Africa is the ninth largest wine-producing country in the world, accounting for 3.3% of the annual global wine production (SAWIS, 2018). However, the future economic viability of the grapevine industry is constantly challenged by abiotic and biotic stresses, causing severe losses in crop yields and quality. Like most crops, substantial harvest losses occur due to the plant's susceptibility to a wide range of viral pathogens (Louime et al., 2010).

Currently, more than 70 different virus species have been reported to infect grapevine globally, the most known for any perennial crop (Reynolds, 2017). Many of these viruses, frequently in combinations, are responsible for serious diseases that might have detrimental effects on vines (Zherdev et al., 2018). Four main viral diseases namely leafroll, rugose wood, fleck disease and infectious degeneration are of major economic importance worldwide and are attributed to the virus families *Closteroviridae*, *Betaflexiviridae*, *Tymoviridae* and *Comoviridae,* respectively (Basso et al., 2017; Maliogka et al., 2015; Martelli, 2019). Of these, grapevine leafroll disease is the most widespread and economically damaging viral disease of grapevine, occurring in most viticultural areas of the world (Naidu et al., 2014).

Since agriculture became a vital practice worldwide, innovative methods are consistently being introduced to increase the yield and quality of crops. Genetic engineering emerged as a way of modifying the plant genome by introducing functional genes in plants to improve crop productivity under adverse environmental conditions. The latest technology that can be exploited to achieve this is the CRISPR/Cas (clustered regularly interspaced short palindromic repeats/CRISPR-associated proteins) system, a tool that has quickly become the most widely-used approach for genome editing research over the past decade (Duensing et al., 2018). Shown to be simpler and more versatile than other techniques such as ZNFs (zinc-finger nucleases) and TALENs (transcription activator-like effector nucleases), the CRISPR/Cas system offers a powerful alternative to classical breeding approaches (Gupta and Musunuru, 2014).

The most utilised CRISPR platform to date is CRISPR/Cas9, developed to easily produce site-specific mutations in eukaryotic genomes. This procedure is predominantly used for the disruption of genes to perform important functional analyses, or for the improvement of crop traits (Pacher and Puchta, 2017; Scheben et al., 2017). The proven success of CRISPR/Cas9 technology in plant breeding to

generate plants with desirable traits has stimulated a different application of this technology to engineer plants with durable resistance to DNA viruses (Mahas and Mahfouz, 2018). However, the majority of plant pathogenic viruses possess RNA genomes, restricting the applicability of Cas9 for engineering plant immunity against these viruses.

Recent computational efforts to identify new CRISPR systems revealed a unique effector called Cas13. It is the first effector identified to act exclusively on single-stranded RNA (Abudayyeh et al., 2016; East-Seletsky et al., 2016). Since the discovery of the Cas13 nuclease, a range of orthologues (a-d) were identified and re-programmed for targeted RNA cleavage, precise base editing, live-cell transcript imaging and nucleic acid detection in mammalian, human, bacterial and plant cells, as well as more recently in animal models (Burmistrz et al., 2020). To date, the RNA binding and cleaving activity of the CRISPR/Cas13 system has mainly been employed for its use as an antiviral defence mechanism in plants (Aman et al., 2018a, 2018b; Zhan et al., 2019; Zhang et al., 2018b).

1.2 Project rationale

Grapevine is classified as a highly susceptible species to viral diseases, where low or no resistant phenotypes have been delineated and chemical agents are limited in their use for targeting insect pests and bacterial or fungal diseases, but not viral diseases. Thus, the development of genetic tools and resources for the sustainable control of grapevine viruses has become critically important. The CRISPR/Cas13 system presents itself as a novel option for applications based on programmable RNA targeting in plants. As opposed to a complete gene knockout, the Cas13 effector targets the mRNA transcript and hence results in gene silencing. By re-purposing this unique ability of the CRISPR/Cas13 platform, the RNA genome of a plant pathogenic virus can be directly targeted to attenuate viral replication. This technology may therefore provide an opportunity to contribute to crop improvement strategies interested in developing grapevine cultivars resistant to economically important viruses. To present the feasibility of this application for grapevine, the intrinsic properties of a model plant species makes them the ideal candidate to practically demonstrate the CRISPR/Cas13-mediated targeting of an mRNA transcript and a viral RNA genome.

1.2 Aim and objectives

Chapter 3: To provide a proof-of-concept for the CRISPR/Cas13a-mediated cleavage of an endogenous mRNA transcript using the model plant *Nicotiana benthamiana*.

To achieve this aim, the following objectives were formulated:

i. To select and generate crRNA(s) that target an mRNA transcript conserved across both *N. benthamiana* and grapevine (*Vitis vinifera*).

ii. To assemble expression construct(s) for CRISPR/Cas13a-based editing of the selected mRNA transcript using the Golden Gate and Gibson assembly techniques.
iii. To perform *Agrobacterium*-mediated transformation in *N. benthamiana* and establish transgenic lines from the regenerated *N. benthamiana* plantlets using molecular analyses.
iv. To evaluate the gene expression levels of the targeted mRNA transcript in the transgenic plants using quantitative molecular analyses.

Chapter 4: To investigate the potential of the CRISPR/Cas13a system to confer interference activity against an RNA virus using *N. benthamiana*.

To achieve this aim, the following objectives were formulated:

i. To select a crRNA and assemble an expression construct for CRISPR/Cas13a-based editing of a pre-assembled infectious virus clone tagged with a reporter gene.
ii. To perform transient *Agrobacterium*-mediated transformation assays in *N. benthamiana*.
iii. To evaluate the level of CRISPR/Cas13a-mediated viral interference in the plants post-infiltration using quantitative molecular analyses.

1.3 Overview of chapters

Firstly, in **Chapter 2,** existing literature on previous and recent methods to engineer resistance to viruses in plants is reviewed. An evaluation of the various CRISPR/Cas systems and their predominant functions is provided, along with an overview of their applications for CRISPR/Cas-based resistance against DNA and RNA viruses in plants.

In **Chapter 3**, CRISPR/Cas13a-based plant expression vector(s) targeting an mRNA transcript are assembled and introduced into *N. benthamiana* using *Agrobacterium*-mediated transformation. The regenerated transgenic plants are molecularly characterised to assess if the target transcript was effectively cleaved to reduce gene expression.

Chapter 4 describes the transient experiment(s) conducted by co-infiltrating *N. benthamiana* plants with a CRISPR/Cas13a-based vector and an infectious clone harbouring a GFP reporter gene. Thereafter, the interference activity of the CRISPR/Cas13a system against the virus is visualised using GFP screening and the accumulation of the virus genome is molecularly assessed.

Finally, **Chapter 5** summarises the major findings of each study and provides both limitations and suggestions for future consideration.

CHAPTER 2: LITERATURE REVIEW

2.1 A brief background of plant viruses

Plant viruses are nucleoprotein complexes that rely mostly on host cells for their propagation. A large fraction of emerging plant diseases are caused by viruses, mostly because of their ability to adapt to changing environmental conditions and their effective dissemination facilitated by vector transmission (Anderson et al., 2004). Most economically important crops get infected with viruses, causing serious viral diseases that are responsible for significant decreases in both the yield and quality of harvests worldwide. It is estimated that 15% of the global crop production is lost due to plant diseases, of which one third is accounted for by viruses (Boualem et al., 2016; Yadav and Chhibbar, 2018). Plant viruses, therefore, threaten global food security and agricultural productivity for the ever-increasing world population.

Most viruses that infect plants have positive-sense single-stranded RNA (+ssRNA) genomes and encode for conserved genes such as the coat protein, movement protein and RNA-dependant RNA polymerase (Awasthi et al., 2016). Viral replication and transcription is dependent on the host's cellular machinery, making plant viruses obligate parasites. Plant viruses are transmitted by exposure to wounds, seeds, pollen or by a diverse range of vectors including insects, nematodes, soil fungi or mites (Bragard et al., 2013; Lefeuvre et al., 2019). Unlike other plant pathogens, viruses cannot be controlled directly by chemical applications on infected material, making preventative sanitary measures the only approach to manage infections. Currently, control measures include planting virus-free material, the eradication of infected material that was detected early enough, crop rotation and pesticides to control transmission vectors (Fereres and Raccah, 2015; Tavazza et al., 2017). While agricultural practices often depend on pesticides, the extensive use of these has shown to have many adverse effects on the environment and given rise to insecticide resistance in virus-vector populations (Bragard et al., 2013).

The use of plant varieties that have natural genetic resistance factors constitutes the most efficient and sustainable approach to control viral infections. The first virus resistance gene was cloned and isolated from *Nicotiana glutinosa* infected with tobacco mosaic virus (TMV). Named the *N* gene of tobacco, it was reported to confer a gene-for-gene resistance to the viral pathogen TMV in both tobacco and tomato transgenics (Whitham et al., 1994, 1996). This ultimately led to a better understanding of plant virus immune systems. By introgression of resistance genes from wild to cultivated plants, a number of these plants were improved over the past decades and made commercially available. Unfortunately, for many plant- virus combinations, the transfer of a resistance

trait to a desired cultivar faces complex genetic constraints, such as linkage drag and high levels of heterozygosity (Kang et al., 2005). In addition, this approach requires a long generation time and is not cost-effective for breeding programs. Viruses are unique in the sense that they are able to evolve rapidly through recombination, mutations and reassortment, making the molecular advances in providing new tools for crop improvement vital.

In the 1980s, when alternative transgenic approaches were being explored, it was discovered that the inhibition of gene expression could be engineered by the expression of antisense RNA in plant cells, a phenomenon named pathogen-derived resistance (PDR) (Sanford and Johnston, 1985). As further studies were conducted, resistance was obtained through the expression of partial or non-coding virus sequences, leading to successful developments of virus-resistant crops (Lomonossoff, 1995; Wilson, 1993), even though the mechanisms behind PDR were not completely understood (Baulcombe, 1996). The RNA-mediated mechanism behind PDR was later shown to be an antivirus response from plants, a strategy termed as RNA silencing (Tenllado, 2004). By means of regulating gene expression, the RNA silencing strategy was a breakthrough for antiviral breeding and has since been used to engineer resistance in many crops. In the past decade, genome editing technology has emerged and introduced new methods that can change the way plant virus resistance is approached.

2.2 RNA silencing-based strategy

RNA gene silencing is a gene regulatory mechanism that limits transcript levels by either suppressing transcription (transcriptional gene silencing [TGS]), or by activating a sequence-specific RNA degradation process (post-transcriptional gene silencing [PTGS]), otherwise known as RNA interference (RNAi) (Petrov et al., 2019). The natural phenomenon of RNA silencing in plants was first discovered in 1990 and has since been characterised in several other eukaryotic organisms (Gaudet et al., 1996; Napoli et al., 1990; Romano and Macino, 1992). Initially demonstrated in nematodes, RNAi is a biological response triggered by the presence of foreign double-stranded RNA (dsRNA) and mediates the suppression of protein-coding gene expression (Fire et al., 1998; Hannon, 2002). The RNA silencing pathway has diversified in plants to cope with important regulatory roles in growth, development and antiviral defence.

Depending on the precursor source, RNA silencing is classified by three overlapping but considerably distinct pathways: the micro-RNA (miRNA) pathway, small interfering RNA (siRNA) pathway and RNA-directed DNA methylation (RdDM) pathway (Wang and Metzlaff, 2012). These control the expression of key regulatory genes, play a role in host antiviral defence and mediate transcriptional silencing, respectively.

The basic RNA silencing pathway is induced by precursor dsRNAs derived either from endogenous sequences, such as precursor miRNAs (pre-miRNA) generated in the nucleus, or exogenous sequences supplied via experimental manipulation or viruses (Figure 2.1). The long dsRNA or pre-miRNA is processed in the cytoplasm by a Dicer or Dicer-like (DCL) protein to generate small non-coding RNAs called siRNA or miRNA, respectively. One strand of the RNA duplex is incorporated into an Argonaute (AGO) endonuclease and forms an RNA-induced silencing complex (RISC). This guide RNA strand remains bound to the RISC complex and directs it to bind to a complementary mRNA target for mRNA degradation or the inhibition of translation, leading to sequence-specific gene silencing (Baulcombe, 2004; Hannon, 2002).

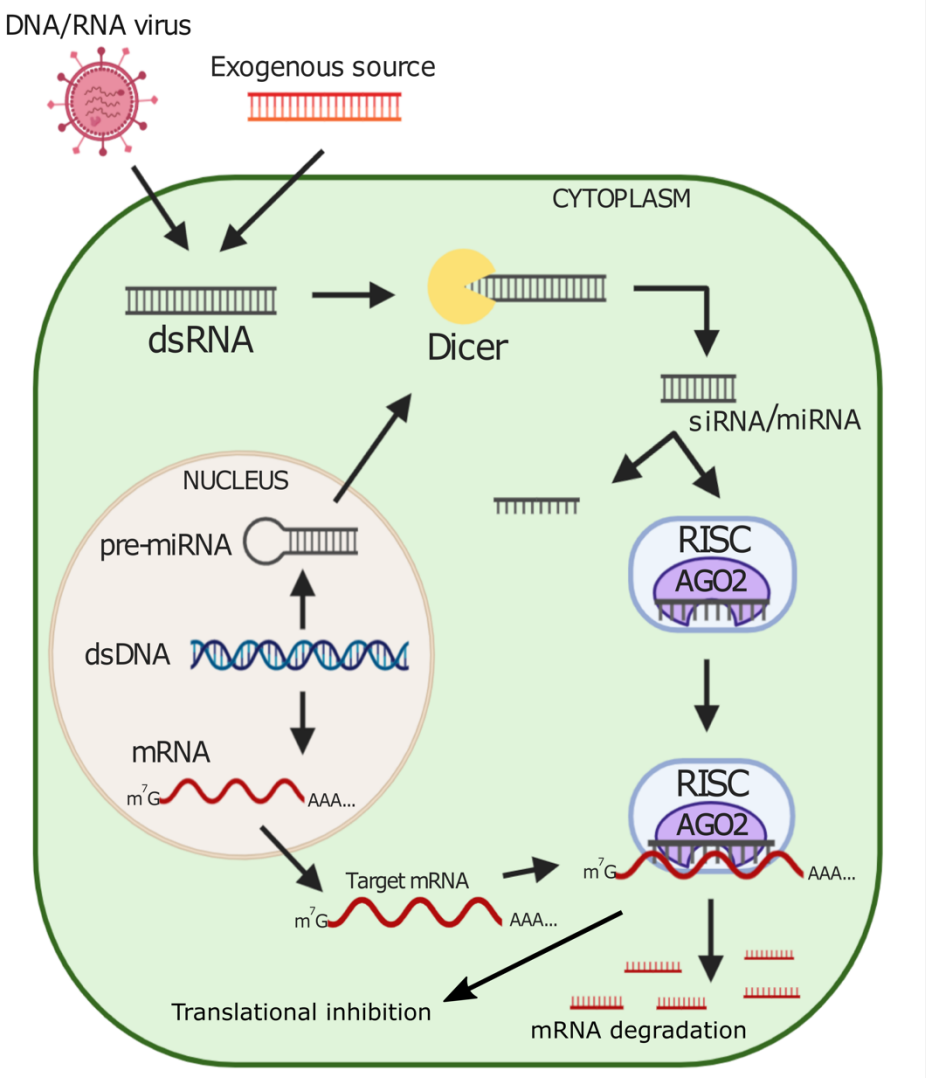

Figure 2.1. A schematic representation of the pathway involved in the generation of small regulatory RNAs (siRNAs or miRNAs) and their role in the general mechanism of RNA interference. The siRNA/miRNA duplexes are loaded into Argonaute protein (AGO) in the RNA-induced silencing complex (RISC), where one strand is selected to be the guide strand. When the RISC-bound guide RNA binds to the target of the complementary RNA, the degradation or the translational inhibition of the target RNA occurs. This figure was created using Biorender.

The specificity of the Watson-Crick base pairing between the dsRNA and the target RNA is the leading advantage of the RNAi technology and can be reprogrammed for a wide range of applications (Agrawal et al., 2003; Rosa et al., 2018). Since its role in antiviral immunity was discovered, RNAi has been successfully applied to target several plant virus species such as maize streak virus (MSV) (Shepherd et al., 2007), papaya ringspot virus (PRSV) (Bau et al., 2003; Fitch et al., 1992), potato virus Y (PVY) (Missiou et al., 2004; Tabassum et al., 2016) and tomato yellow leaf curl virus (TYLCV) (Fuentes et al., 2006), to name a few. A transgenic plant RNAi-based virus resistance approach is usually designed by producing a dsRNA transcript that is homologous to a specific region of a viral genome, such as the coat protein. Different forms of RNAi inducers have been developed for diverse targeting approaches, including long/short hairpin RNA, sense/antisense RNA and artificial miRNA precursors (Simón-Mateo and García, 2011).

Transgenic overexpression of viral RNA has been used to generate a number of virus-resistant genetically engineered crops, many of which have been approved for commercialisation (Guo et al., 2016; Rosa et al., 2018). While these transgenic approaches were successful, the process is time-consuming, expensive and faces strict risk assessments before approval (Casacuberta et al., 2015). To circumvent the genetic transformation of plant material, progress has been made in establishing direct-spray applications of dsRNA to target viral pathogens for non-transgenic crop protection. The durability and stability of exogenously applied dsRNA was successfully demonstrated in tobacco plants by using double hydroxide nanosheet carriers for the dsRNA (Mitter et al., 2017).

A limitation in RNA silencing approaches is the evolutionary development of counter-defensive measures from plant viruses, one of which is encoded viral suppressors of RNA silencing (VSR). These VSRs inhibit various steps of the RNA silencing pathway, targeting siRNAs or effectors such as AGO and DCL proteins (Roth et al., 2004). As many crops are susceptible to mixed viral infections, an infection with a non-target virus could disrupt the immunity conferred by RNA silencing (Kung et al., 2015; Mitter et al., 2001; Simón-Mateo and García, 2011). Since this has been shown to occur in some cases only, further understanding of the factors that affect RNA silencing-mediated resistance is required. Therefore, over the last 10 years other biotechnology approaches have been gaining attention for their ability to manipulate more stable gene modifications and improve broad-spectrum resistance in plants. These are referred to as genome editing methods.

2.3 Plant genome editing technologies

Since the emergence of genome editing technology a decade ago, the advances achieved using this approach have revolutionised the fields of functional genomics and crop improvement. Essentially, genome editing technology is the use of sequence-specific nucleases for recognising specific DNA

sequences and producing DNA double-stranded breaks (DSBs) at targeted sites in chromosomal loci (Yin and Qiu, 2019). In almost all cell and organism types, a nuclease-induced break is repaired via either non-homologous end-joining (NHEJ) or homology-directed repair (HDR) (Sonoda et al., 2006). These two pathways differ between their efficiency and the mechanisms they require to repair the chromosome. If a repair template is absent, the error-prone NHEJ operates, resulting in the introduction of a single or multiple insertion/deletion (indel) mutations after a DSB (Figure 2.2). These indels can cause a frameshift mutation as they either disrupt a translational reading frame or the binding sites of trans-acting factors. Therefore, gene knockouts are created (Song et al., 2016). Alternatively, the high-fidelity HDR method uses an intact homologous sequence as a donor template to enable sequence insertions or introduce point mutations by means of loci recombination (Belhaj et al., 2013).

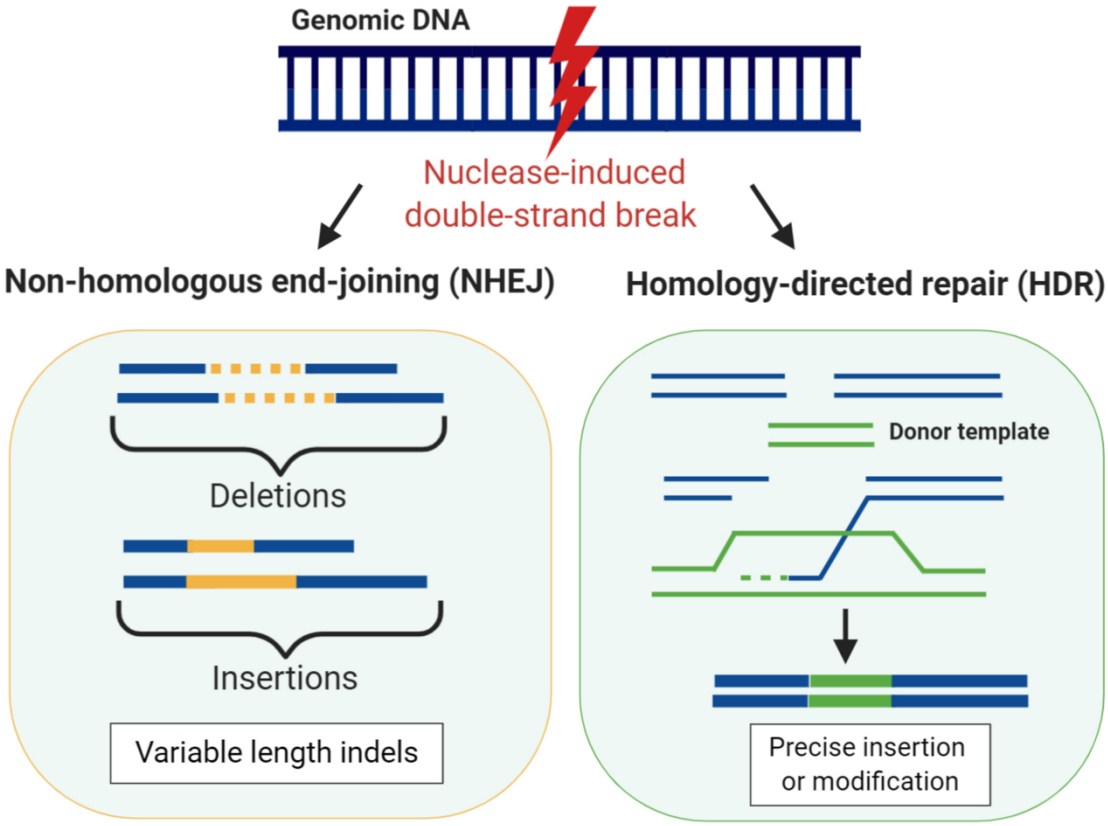

Figure 2.2 Repair pathways for nuclease-induced double-stranded breaks. Non-homologous end-joining (NHEJ) leads to the introduction of random indel (insertion/deletion) mutations, whereas homology-directed repair (HDR) can introduce point mutations or sequence insertions through recombination with a donor template. This figure was created using Biorender.

Previously, the leading genome editing tools available were zinc finger nucleases (ZFNs) and transcription activator-like effector nucleases (TALENs) (Boch et al., 2009; Kim et al., 1996). Both of these nucleases are chimeric proteins created by fusing their respective DNA-binding domains (DBD)

with the DNA cleavage domain of the *Fok*I restriction enzyme. Sequence specificity of the target DNA is conferred by the DBD and the *Fok*I cleavage domain produces the DSBs in the targeted site (Christian et al., 2010; Kim et al., 1996). ZFN- and TALENS-based genome editing has used with variable success in several plant species (Cai et al., 2009; Curtin et al., 2011; Zhang et al., 2013a, 2013b). Although the use of ZFNs and TALENs led to important advances, the customisation of these two genome editing platforms requires protein engineering for each new target, making it a time-consuming and resource-intensive process (Gaj et al., 2013). During the last decade, a new genome editing platform naturally surpassed ZFNs and TALENs and their applications in plants.

2.3.1 CRISPR/Cas systems

Clustered regularly interspaced short palindromic repeats (CRISPR), and CRISPR-associated (Cas) proteins form the CRISPR-Cas system, which is used by many archaea and bacteria as an adaptive prokaryotic immune defence system against invading foreign nucleic acids originating from viral or plasmid pathogens (Barrangou and Marraffini, 2014; Barrangou et al., 2007; Brouns et al., 2008). The mechanism of CRISPR/Cas-mediated immunity consists of three main steps: acquisition of spacers from the invaders genome; the transcription of the CRISPR array and maturation of the guide RNA (gRNA) molecules; and targeted interference against the invaders genome (Figure 2.3) (Makarova et al., 2011; van der Oost et al., 2009). During adaptation, a complex of Cas proteins cleaves a fragment of invading genetic material and incorporates it into the CRISPR array. At the expression stage, the CRISPR array is transcribed as a single transcript called the precursor CRISPR RNA (pre-crRNA) and it is processed into mature crRNAs (crRNAs). Finally, the crRNA guides the Cas nuclease to bind and cleave to the invading sequence it recognises. The interest in CRISPR/Cas systems grew from a practical concept that looked at exploiting the complementarity between the gRNA and target sequence for target recognition, together with the nuclease activity of the Cas nuclease for specific target cleavage.

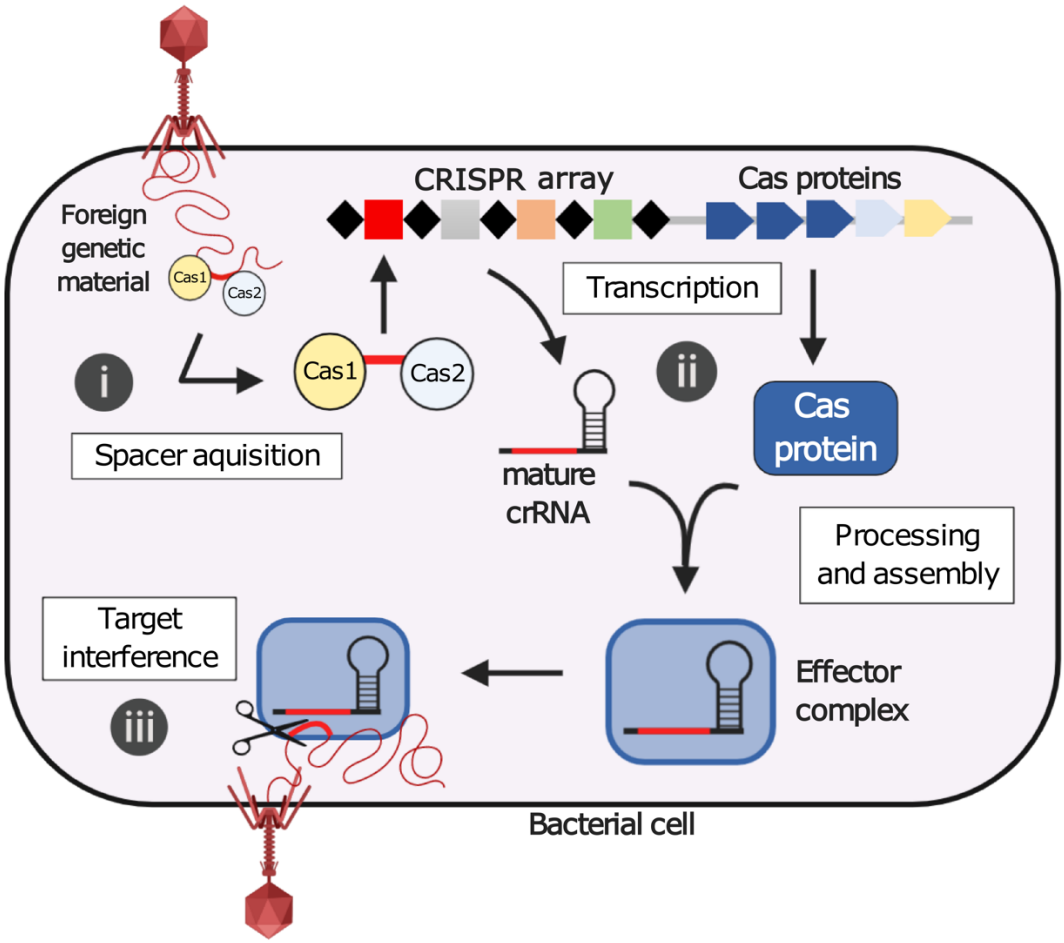

Figure 2.3 The three stages of CRISPR/Cas adaptive immunity in bacterial cells. (**i**) The first process termed adaptation is where the foreign genetic material is acquired by Cas1-Cas2 and integrated into the CRISPR array. (**ii**) The associated Cas proteins are expressed and the CRISPR array is processed into mature crRNA to provide targeting specificity. (**iii**) The crRNA guides the effector nucleases to foreign genetic elements, leading to target interference and immunity. This figure was created using Biorender.

Currently known CRISPR/Cas systems are divided into two main classes (Class 1 and 2), which are further classified into six types and several subtypes. The two classes are differentiated by the architecture of the effector modules involved in crRNA maturation and interference: Class 1 systems are composed of multi-effector protein complexes (Type I, III, and IV), whereas class 2 (Type II, V, and VI) systems are single-effector proteins (Koonin et al., 2017; Shmakov et al., 2015).

2.3.2 Class 2 CRISPR/Cas systems

Generally, Class 2 CRISPR/Cas systems are less abundant than Class 1 CRISPR/Cas systems and are predominantly discovered in bacterial organisms. These systems use an RNA-guided Cas protein to cleave a target sequence and can be reprogrammed to target a defined sequence of interest, making them a more attractive genome editing tool (Shmakov et al., 2017).

2.3.2.1 CRISPR/Cas9

The class 2 type II endonuclease Cas9 from *Streptococcus pyogenes* (SpCas9) was the first Cas effector to be adapted as a genome engineering tool. In the natural system, the pre-crRNA is processed into mature crRNAs by a trans-activating crRNA (tracrRNA) and the bacterial RNase III. An RNA complex comprised of a crRNA and tracrRNA then directs a cluster of Cas9 nuclease proteins to cleave invading double-stranded DNA (dsDNA), which essentially gives rise to a target interference (Oost et al., 2014). For genome editing, the crRNA-tracrRNA complex is reduced to a single guide RNA (sgRNA) with a specific 20 nt spacer sequence complementary to a DNA target (Figure 2.4 A). A pre-requisite for Cas9 cleavage is the presence of a short G-rich protospacer adjacent motif (PAM), found immediately adjacent to a DNA target sequence. The Cas9 protein is comprised of two nuclease domains, RuvC and HNH, both responsible for the blunt cleavage of each strand of the dsDNA target (Ran et al., 2013; Sander and Joung, 2014).

Several online bioinformatic software tools have been developed to predict the effectiveness of gRNAs from whole genome information. A well-designed sgRNA should be specific to the DNA target, meaning it should tolerate as few mismatches as possible, to lower the off-target activity (Zhang et al., 2015). Both the number and type of nucleotides that compose a sgRNA can affect target binding (Uniyal et al., 2019). When applying the CRISPR/Cas9 system, it is still a concern that higher frequencies of off-target mutations than on-target mutations may cause genomic instability (Wolt et al., 2016; Manghwar et al., 2020).

The cleavage action of the Cas9 protein is a crucial step in targeted genome editing as this is the introduction of a double-stranded break (DSB) in the genomic sequence of interest. Owing to its higher mutation efficiency and design simplicity, the CRISPR/Cas9 system has been implemented for more applications in plants than ZFNs and TALENs. Initially, CRISPR/Cas9-mediated genome editing was typically used to target one or two gene loci at the same time. In order to target multiple genomic loci simultaneously, multiplex CRISPR/Cas9 systems are designed to allow the co-expression of several sgRNAs (Mushtaq et al., 2018). This multiplex genome editing approach is valuable for functional gene knockouts in plants.

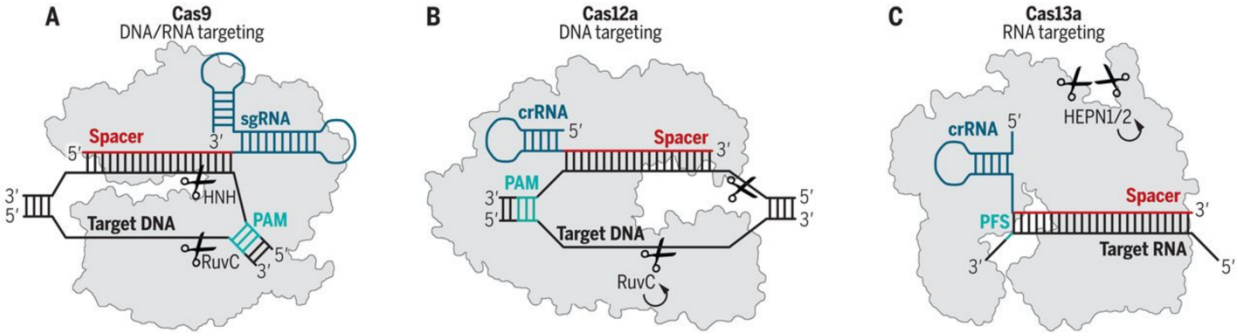

Figure 2.4. A schematic comparison of the class 2 CRISPR/Cas systems. (**A**) Cas9 represents a type II system and is guided by a sgRNA encoding a spacer bound to a dsDNA target adjacent to a PAM. The HNH and RuvC nuclease domains are activated when the correct base-pairing occurs and cleave both DNA strands (**B**) Cas12a represents a type V system and binds to the DNA sequence complementary to the single crRNA spacer and adjacent to a PAM. The RuvC nuclease domain is activated when the correct base-pairing occurs and ssDNase activity cleaves both strands (**C**) Cas13 represents a type VI system and binds to a ssRNA sequence complementary to the crRNA spacer. The HEPN domains are activated when the correct base-pairing occurs for ssRNase activity. Adapted from (Knott and Doudna, 2018).

2.3.2.2 CRISPR/Cas12a

A second class 2 effector, Cas12a (formerly Cpf1), was later identified and categorised as a type V CRISPR/Cas. In contrast to Cas9, Cas12a contains a RuvC domain but not an HNH domain and generates a staggered DSB distal from a T-rich PAM located upstream from the guide sequence (Makarova et al., 2015; Zetsche et al., 2015). The staggered DSB is situated close to the 3'-end of the complementary target sequence, creating a 5'-overhang. The production of DSBs with staggered ends by Cas12a may be advantageous for knock-in applications such as integrating DNA sequences in precise positions by using complementary DNA ends through HDR. Furthermore, Cas12a requires a shorter crRNA than Cas9 and there is no evidence that a tracrRNA is required (Fonfara et al., 2016). Guided by a single crRNA, the Cas12a effector can target either ssDNA or dsDNA. As shown in Figure 2.4 B, the crRNA scaffold is located on the 5'-end, as opposed to the 3'-end in type II CRISPR/Cas systems. The Cas12a proteins also have RNase activity, used to process pre-crRNAs into mature crRNAs (Jeon et al., 2018). This crRNA processing feature can be exploited to simplify multiplexed genome editing through the use of a single customised crRNA array. The potential of Cas12a as an alternative to the Cas9 endonuclease has been demonstrated in mammalian, plant, and microbial cells (Yan et al., 2017; Zaidi et al., 2017; Zetsche et al., 2015).

2.3.2.3 CRISPR/Cas13a

After using data mining and bioinformatic approaches, three novel Class 2 CRISPR systems besides the common Cas9 effector were discovered, namely C2c1, C2c2 and C2c3 (Shmakov et al., 2015). Similar to Cas12a, C2c1 and C2c3 contained RuvC-like endonucleases and were therefore classified as type V-

B Cas12b and type V-C Cas12c, respectively. Notably, C2c2 was shown to have unique properties compared with all other Cas proteins. Thereafter designated as Cas13a, the putative effector was assigned to a novel type, class 2 type VI-A (Shmakov et al., 2017). Cas13a was the first class 2 effector found to solely function as a single RNA-guided RNA-targeting protein (Bhushan, 2018). Analysis of the Cas13a protein sequence resulted in the detection of two "higher eukaryotes and prokaryotes nucleotide-binding" (HEPN) domains, which are exclusively associated with RNase activity (Anantharaman et al., 2013). The two structurally different HEPN domains, HEPN1 and HEPN2, are located on the outer surface and when activated, lead to the cleavage of the target RNA outside of the binding region (Figure 2.4 C). The exposed catalytic site of HEPN is available to all RNAs in a solution, thus explaining why unspecific cleavage of RNA was detected in bacterial cells (Liu et al., 2017a). Further characterisation of the RNA cleavage activity of Cas13a elucidated that Cas13a is guided by a crRNA containing a 28-nt spacer sequence, an interaction maintained by the presence of a protospacer flanking sequence (PFS) of A, C or U (Abudayyeh et al., 2016). As shown by the Cas12 system, Cas13a proteins can autonomously process their own pre-crRNAs without the involvement of tracrRNA. This crRNA maturation activity is catalysed by a domain called Helical1 and can be harnessed for multiplexed processing (Abudayyeh et al., 2017; East-Seletsky et al., 2016). The sensitivity of the Cas13a system to single and double mismatches was analysed and revealed that a central mismatch sensitive "seed" region is present in the crRNA, opposed to the 5'-seed regions found in type I and II systems (Abudayyeh et al., 2016; Liu et al., 2017a; O'Connell, 2019).

2.4 CRISPR/Cas reagent delivery and expression in plants

To achieve an effective application of CRISPR/Cas in plants, a crucial requirement is the robust delivery and expression of CRISPR/Cas reagents into plant cells. The three primary methods for delivery include *Agrobacterium*-mediated transformation or physical means such as biolistic bombardment or protoplast transfection. They all depend on either plasmids, viruses or ribonucleoproteins (RNPs) to act as mediators by carrying the required sequences (Kuluev et al., 2019).

Generally, the *Agrobacterium*-mediated delivery of CRISPR/Cas components is the most common approach to obtaining transgenic plants. By using either *A. tumefaciens* or *A. rhizogenes* to facilitate the insertion of T-DNA, a stable expression of the transgenes in the plant genome can be achieved. Alternatively, when the recovery of transgenic plants is not required, a transient expression of the transgenes can also be achieved by agroinfiltration (Nester, 2015). The *Agrobacterium* method is popular because it is inexpensive and allows for the multiplexed delivery of binary constructs, however the transformation efficiency is limited to the genotype of the recipient, particularly for most

monocotyledons and some agronomically important dicotyledons (Altpeter et al., 2016; Ran et al., 2017).

Alternatively, biolistic bombardment transfers CRISPR/Cas components through coated particles carrying a DNA vector into explants by applying a high pressure to penetrate the cell wall. The editing efficiency of this method is dependent on optimised conditions of the transformation and integration occurs in random patterns within the plant genome, also leading to multiple copies of the introduced genes (Sandhya et al., 2020). However, the biolistic delivery of a RNP complex consisting of the Cas nuclease and gRNA has been developed for DNA-free genome editing approaches and significantly improves editing efficiency (Kuluev et al., 2019).

Protoplast transformation is an important method mainly carried out by the presence of a polyethylene glycol (PEG) medium or by electroporation. The transfection of the CRISPR/Cas component, either a plasmid or a pre-assembled Cas/sgRNA RNP, into protoplasts and the subsequent regeneration of transgenic or non-transgenic plants, respectively, has allowed for the successful introduction of desired mutations in several plant species such as rice, tobacco and lettuce (Woo et al., 2015; Xie and Yang, 2013). The convenience and speed of protoplast transfection is useful to validate the mutagenesis efficiency of a CRISPR/Cas system and is widely used for the delivery of RNPs (Yue et al., 2020). However, protoplast isolation and whole-plant regeneration from protoplasts remains a challenge for most plant species (Sandhya et al., 2020).

Therefore, the type of method employed to deliver CRISPR/Cas components can affect the efficiency of CRISPR/Cas-based genome editing. Notably, the success of a delivery method is dependent on the tissue type of a plant and its consecutive regeneration.

2.5 CRISPR/Cas-based targeting of RNA

RNA programmable CRISPR/Cas systems have only recently emerged as research tools. Before the discovery of the Cas13 effector protein, two Cas9 variants were reprogramed to target RNA genomes, namely the Cas9 from *Francisella novicida* (FnCas9), and RNA targeting SpCas9 (termed RCas9). Thereafter, the Cas13 nuclease family was revealed and it contains three experimentally characterised subtypes, including Cas13a, Cas13b and Cas13d (Table 2.1). Using transcriptome-wide mRNA sequencing, a recent study identified more off-targets for RNAi approaches than CRISPR/Cas13-mediated RNA knockdown (Abudayyeh et al., 2017). In addition, the efficiency level of CRISPR/Cas-based RNA knockdown is shown to be higher than RNAi and can be precisely controlled, an advantage for many research fields (Wang et al., 2019).

Table 2.1. Classification of the main CRISPR/Cas RNA-targeting systems.

EFFECTOR	CLASS AND TYPE	ORGANISM(S) HARBOURING RESPECTIVE TYPES	SIGNATURE COMPONENTS	REFERENCES
RCas9	Class 2, Type II	*Streptococcus pyogenes*	Cas9 PAMmer sgRNA	O'Connell *et al.,* 2014
FnCas9	Class 2, Type II	*Francisella novicida*	Cas9 sgRNA	Price *et al.,* 2015 Sampson *et al.,* 2013
Cas13a	Class 2, Type VI-A	*Leptotrichia shahii* *Leptotrichia wadei*	Cas13 crRNA	Abudayyeh *et al.,* 2016 Abudayyeh *et al.,* 2017
Cas13b	Class 2, Type VI-B	*Prevotella buccae* *Bergeyella zoohelcum*	Cas13 crRNA	Smargon *et al.,* 2017
Cas13d	Class 2, Type VI-D	*Ruminococcus flavefaciens* *Eubacterium siraeum*	CasRx crRNA	Konermann *et al.,* 2018 Yan *et al.,* 2018

2.5.1 RCas9 variant

The Cas9 effector derived from *Streptococcus pyogenes* (SpCas9) has been extensively utilised for dsDNA genome editing and has shown that it can be easily reprogrammed for efficient cleavage, making it a suitable candidate to be repurposed for ssRNA targeting and manipulation. This was shown by O'Connell *et al* (2014) who demonstrated the binding and cleavage of ssRNA *in vivo* by SpCas9. In contrast to the native dependence SpCas9 has on the PAM sequence, when synthetic PAM sequences (PAMmers) were supplied exogenously, the SpCas9 was successfully redirected to target the ssRNA sequence complementary to the PAMmers (O'Connell et al., 2014). This indication of RNA targeting was further tested by including dsDNA with the ssRNA targets and PAMmers. Interestingly, the SpCas9 and its crRNA targeting counterpart exclusively targeted the ssRNA, avoiding the corresponding DNA *in vitro*. Thereafter denoted as an RNA targeting Cas9 (RCas9), this effector can be used as a programmable RNA binding platform. While RCas9 shows promise for further applications, a concern to consider is the costly synthesis of PAMmers, as well as the chemical modifications required to stabilise them in living cells (Nelles et al., 2016).

2.5.2 FnCas9 variant

Previously shown to mediate DNA cleavage, a Cas9 effector encoded from *Francisella novicida* (FnCas9) was identified and applied for targeted RNA cleavage *in vivo* (Price et al., 2015; Sampson et al., 2013; Zhang et al., 2018b). Discovered in 2013 (Sampson et al., 2013), the enzyme was shown to target bacterial mRNA and target gene expression. This novel feature of FnCas9 led to its use for the

targeting of several eukaryotic viruses such as the human hepatitis C virus (HCV), and cucumber mosaic virus (CMV) and TMV in plants, with different degrees of successful interference (Price et al., 2015; Zhang et al., 2018b). In addition to the crRNA and tracrRNA, the CRISPR/FnCas9 system also requires a small CRISPR/Cas-associated RNA (scaRNA) that hybridises with tracrRNA, forming a duplex that promotes RNA targeting. Unlike the RCas9 system, the RNA targeting action of FnCas9 does not depend on a PAM. While some studies highlight the potential that the CRISPR/FnCas9 system holds for specific RNA targeting, there are still underlying mechanisms of FnCas9 that remain unknown. Due to its dual DNA and RNA targeting ability, like the RCas9 system, FnCas9 will be less likely selected for RNA manipulation in the nucleus (Price et al., 2015).

2.5.3 Cas13a variants

In its native form, Cas13a can be used for targeted RNA cleavage such as down-regulation of a specific transcript. A pioneer study that characterised the functionality of *Leptotrichia shahii* Cas13a (LshCas13a), later confirmed that Cas13a solely cleaves ssRNA (Abudayyeh et al., 2016). It was shown that LshCas13a could provide interference against an MS2 lytic ssRNA phage in *Escherichia coli*. Interestingly, this study also identified that once activation by the target RNA was completed, unspecific cleavage of RNAs other than the target RNA occurred. This suggests LshCas13a elicits programmed cell death or dormancy in the natural system. Fortunately, this type of 'collateral' activity' was not detected in eukaryotic cells (Abudayyeh et al., 2017; Cox et al., 2017).

A screening of various Cas13a proteins identified LwaCas13a from *Leptotrichia wadei* as having the highest interference activity relative to the other Cas13a orthologues, as well as no unspecific RNA degradation upon activation in cells (Abudayyeh et al., 2017). Using a monomeric superfolder GFP (msfGFP) domain to stabilise the protein and a nuclear localisation signal (NLS), the knockdown ability of LwaCas13a was demonstrated in mammalian cells with no evidence of collateral RNA cleavage. Abudayyeh *et al* (2017) also verified the functionality of RNA knockdown by LwaCas13a in plants, with almost all guides exceeding 50% RNA knockdown in rice protoplasts, suggesting that a wide range of organisms can be edited using this system. Although the LshCas13a orthologue requires a biochemical PFS, analogous to the PAM for Cas9, LwaCas13a was shown to be exempt from this restriction in mammalian cells (Abudayyeh et al., 2017; Cox et al., 2017).

By using point mutations to deactivate the two catalytic residues in the HEPN domains of Cas13, a catalytically "dead" Cas13 can be created, namely dCas13. In this way, the RNA-binding ability is retained and the tracking and localisation of endogenous transcripts inside cells is facilitated. Abudayyeh *et al* (2017) used dLwaCas13a fused to fluorescent proteins to image RNA transcripts in

live cells. For applications in plant virology, this approach will allow the direct visualisation of viral replication with high precision.

2.5.4 Cas13b variants

Another recently categorised CRISPR/Cas13 system identified from computational sequence data mining is Cas13b (previously C2c6), assigned to Class 2 and type VI-B (Smargon et al., 2017). Although Cas13b also contains two HEPN domains and actively targets ssRNA, it has a novel protein sequence that differs significantly from Cas13a. In an *E. coli* essential gene screen, RNA cleavage by Cas13b was shown to be dependent on a double-sided PFS, one on each of the 5'- and 3'-ends of the protospacer target sequence (Smargon et al., 2017). Another interesting finding indicated that Cas13b interacts with two novel proteins, Csx27 and Csx28, of which Csx27 can repress RNA targeting, and Csx28 can enhance RNA cleavage (Smargon et al., 2017). A study by Cox *et al* (2017) evaluated a subset of Cas13 enzymes and found that the Cas13b orthologue from a *Prevotella sp.* P5-125 (PspCas13b), exhibited a higher level of knockdown efficiency and specificity than the previously characterised LwaCas13a. Similar to LwaCas13a though, PspCas13b showed no collateral RNase activity or PFS preference in mammalian cells (Cox et al., 2017). This makes PspCas13b a useful addition to the CRISPR/Cas RNA-targeting suite. Similar to what has been shown on a DNA level, Cox *et al* (2017) used catalytically inactive PspCas13b fused together with adenosine deaminase acting on RNA (ADAR) enzymes to demonstrate the programmable replacement of adenosine with inosine, which is functionally equivalent to guanine during translation. This technology, named RNA Editing for Programmable A-to-I Replacement (REPAIR), allows for precise point mutations within a specific site of mRNA.

2.5.5 Cas13d variants

The most recent addition to the Cas13 subtypes is type VI-D, which appears to be more distantly related on a primary sequence level to previous Cas13 effectors (Yan et al., 2018). Cas13d enzymes are about 20-30% smaller than all the previously reported subtypes Cas13a-Cas13c, and similar to Cas13b, the orthologues from *Eubacterium siraeum* (Es) and *Ruminococcus spp.* (Rsp) possess associated WYL-domain-containing accessory proteins (Konermann et al., 2018; Yan et al., 2018; Zhang et al., 2018a). These proteins enhance the activity of Cas13d and may provide a clue for the improvement of its binding and cleavage actions. Similar to other members of the Cas13 superfamily, Cas13d has two HEPN domains responsible for pre-crRNA processing and it is flexible in the sense that it does not depend on the presence of a PFS when a target sequence is selected (Zhang et al., 2019a). When compared with other Cas13a and Cas13b effectors, the strongest target knockdown of ssRNA in both mammalian cell and plant applications was shown by RfxCas13d (CasRx), especially when fused to a cellular localisation signal (Konermann et al., 2018; Mahas et al., 2019; Wessels et al., 2020). In

addition, while a seed region was previously not reported for Cas13d, researchers found a critical seed region for optimal Cas13d knockdown efficiency between nucleotides 15-21 of the gRNA. By performing a set of pooled screens for CRISPR/Cas13d, they identified optimal gRNA design rules for Cas13d and developed a predictive model to select gRNAs with optimal efficiency (Guo et al., 2020; Wessels et al., 2020). With reports of favourable RNA targeting efficiency, this enzyme will enable a wide scope of RNA manipulations in plants. Already, a CRISPR/CasRx activity prediction tool for gRNA target design was recently developed for mammalian cell culture applications (Wessels et al., 2020).

2.6 CRISPR/Cas-based plant virus interference

Plant viruses infect a wide range of plant species and are responsible for substantial losses in the yield and quality of staple crops (Nicaise, 2014; Oerke and Dehne, 2004). The first studies that looked at using the genome editing tool CRISPR/Cas for plant viruses were designed to target DNA viruses. Two broad strategies are available for this application: the first approach targets a region of a DNA virus for viral genome editing; while the second approach targets the host plant factors that are responsible for DNA or RNA virus propagation for plant genome editing. However, the majority of plant viruses have RNA genomes and often plant DNA viruses have an intermediate RNA stage in their life cycle (Roossinck, 2003), making effectors with RNA specificity the systems of choice for this application (Figure 2.5).

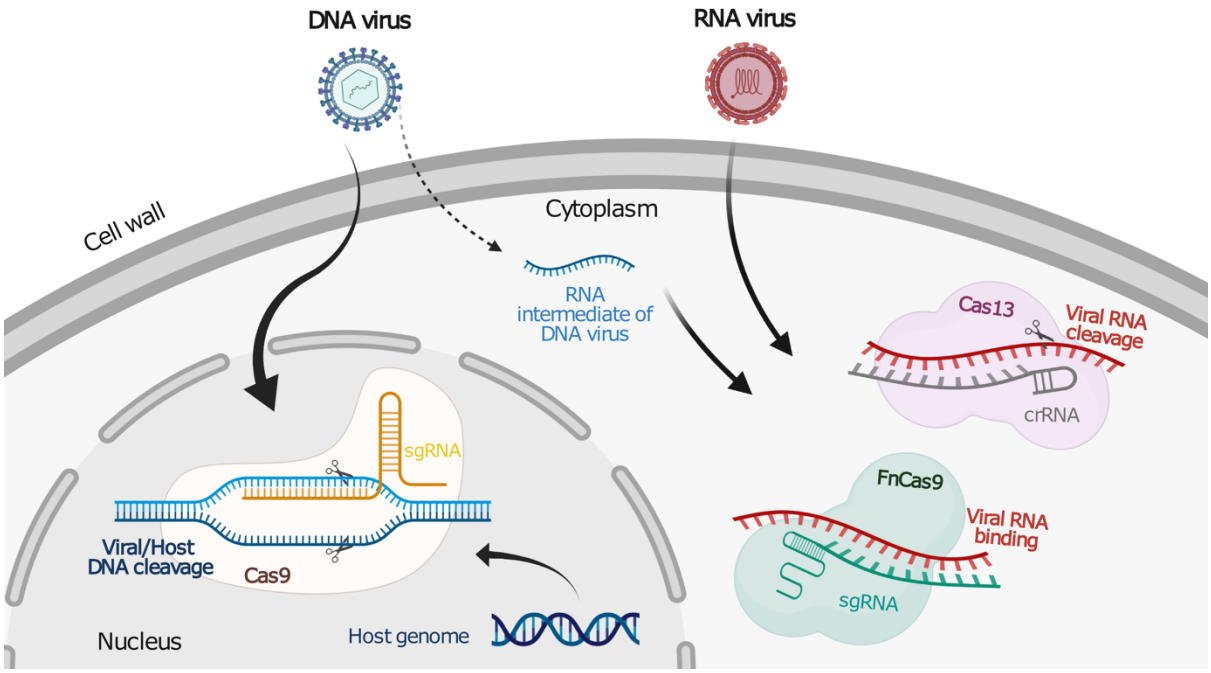

Figure 2.5 Schematic diagram of Class 2 CRISPR/Cas strategies used to target plant viruses. Upon DNA virus entry into the plant cell, the Cas9/sgRNA complex binds to and cleaves DNA target sites. Alternatively, host susceptibility factors can be disrupted by CRISPR/Cas9 to perturb viral infection. For RNA viruses or the RNA transcripts of pathogens with DNA genomes, both FnCas9 and Cas13a proteins guided by their cognate sgRNA or crRNA, respectively, have been proven to target and cleave the virus genome or transcripts. This figure was created using Biorender.

2.6.1 DNA viruses

It has been demonstrated that CRISPR/Cas9-mediated DNA editing can be used as a successful defence mechanism against plant DNA viruses (Ali et al., 2015a). The members of the plant virus family *Geminiviridae* are composed of ssDNA genomes but also contain replicative intermediates of dsDNA, making them suitable candidates for CRISPR/Cas9 targeting. There are three studies that reported the first successful uses of CRISPR/Cas9 to generate geminivirus resistance in the model plants *Nicotiana benthamiana* and *Arabidopsis thaliana* (Table 2.2). They selected target regions within the virus genomes such as the replicase, coat protein or intergenic region to design sgRNAs. As expected, all of these studies showed that the transgenic plants that expressed the CRISPR/Cas9 components and were challenged with the respective virus had reduced virus loads and symptoms (Ali et al., 2015b; Baltes et al., 2015; Ji et al., 2015). In another approach targeting a monopartite geminivirus, Yin *et al* (2019) used transgenic *N. benthamiana* plants expressing Cas9 and sgRNAs which simultaneously targeted two different sequences in the genome of the cotton leaf curl multan virus (CLCuMuV). This led to the plants being completely resistant to CLCuMuV. In addition to the *Geminiviridae* family, strong virus resistance was achieved against the cauliflower mosaic virus (CaMV), a plant pararetrovirus with a dsDNA genome. Here, the expression of multiple sgRNAs targeting the coat

protein region conferred successful resistance in transgenic Arabidopsis plants (Liu et al., 2018). There are some pararetroviruses such as the banana streak virus (BSV) that may integrate its DNA into the nuclear genome of a plant host, forming an endogenous virus (eBSV) that can also induce infections under stress conditions. By generating transgenic banana plants expressing Cas9 and sgRNAs targeting integrated regions of the eBSV genome, Tripathi *et al* (2019) demonstrated the inactivation of the pathogenic virus. When the transgenic plants were challenged under water stress conditions, they were resistant to reactivation of the virus when compared with the non-transgenic control plants.

Recently, some studies have translated CRISPR/Cas-mediated resistance against geminiviruses from model plants to crop plants. For example, Tashkandi *et al* (2018) engineered the CRISPR/Cas9 machinery in tomato plants to target tomato yellow leaf curl virus (TYLCV) genomic sequences, resulting in robust interference of TYLCV in all tomato plants from the T2 to the homozygous T3 generation. Later on, another study showed effective resistance against the wheat dwarf virus (WDV) in the monocot plant barley. The sgRNA-Cas9 construct was developed to introduce mutations at multiple sites within conserved regions of two WDV strains (Kis et al., 2019). In contrast, Mehta *et al* (2019) attempted to engineer resistance to an important geminivirus using CRISPR/Cas9 in the stable food crop cassava. They failed to induce effective resistance against the african cassava mosaic virus (ACMV) in transgenic cassava plants expressing Cas9 and sgRNAs targeting regions of the virus genome. Also, they identified that the use of CRISPR/Cas9 editing led to the emergence of a novel, conserved mutant virus that cannot be cleaved by CRISPR/Cas9 again, across three independent plant lines. This study therefore highlights the risks surrounding transgenic CRISPR/Cas9 plants, given that they may accelerate the evolution of novel virus genomes that can escape engineered resistance if they are not monitored correctly.

Table 2.2. Major applications of CRISPR/Cas technology for DNA and RNA virus resistance in plants.

VIRUS GENOME	CRISPR SYSTEM	VIRUS FAMILY	VIRUS GENUS	VIRUS NAME	PLANT SPECIES	REFERENCES
ssDNA	SpCas9	*Geminiviridae*	*Mastrevirus*	Bean yellow dwarf virus (BeYDV)	*N. benthamiana*	(Baltes et al., 2015)
			Curtovirus	Beet severe curly top virus (BSCTV)	*N. benthamiana* *A. thaliana*	(Ji et al., 2015) (Ali et al., 2015a)
			Begomovirus	Tomato yellow leaf curl virus (TYLCV) Cotton leaf curl Kokhran virus (CLCuKoV) Merremia mosaic virus (MeMV)	*N. benthamiana*	(Ali et al., 2015a, 2016)
			Begomovirus	Cotton leaf curl multan virus (CLCuMuV)	*N. benthamiana*	(Yin et al., 2019)
			Mastrevirus	Wheat dwarf virus (WDV)	Barley (*Hordeum vulgare* L. cv. Golden promise)	(Kis et al., 2019)
			Begomovirus	Tomato yellow leaf curl virus (TYLCV)	*S. lycopersicum* (tomato) *N. benthamiana*	(Tashkandi et al., 2018)
			Begomovirus	African cassava mosaic virus (ACMV)	*M. esculenta* (cassava)	(Mehta et al., 2019)
			Begomovirus	Chilli leaf curl virus (ChiLCV)	*N. benthamiana*	(Roy et al., 2019)
dsDNA		*Caulimoviridae*	*Caulimovirus*	Cauliflower mosaic virus (CMV)	*A. thaliana*	(Liu et al., 2018)
			Badnavirus	Banana streak virus (BSV)	*M. balbisiana* (banana)	(Tripathi et al., 2019)
+ssRNA		*Potyviridae*	*Ipomovirus*	Zucchini yellow mosaic virus (ZYMV) Cucumber vein yellowing virus (CVYV) Papaya ring spot mosaic virus-W (PRSV-W)	*C. sativus* (cucumber)	(Chandrasekaran et al., 2016)

VIRUS GENOME	CRISPR SYSTEM	VIRUS FAMILY	VIRUS GENUS	VIRUS NAME	PLANT SPECIES	REFERENCES
+ssRNA	*SpCas9*	*Potyviridae*	*Ipomovirus*	Turnip mosaic virus (TuMV)	*A. thaliana*	(Pyott et al., 2016)
				Cassava brown streak virus (CBSV)	*M. esculenta* (cassava)	(Gomez et al., 2019)
		Alphaflexiviridae	*Potexvirus*	Potato virus X (PVX)	*S. lycopersicum* (tomato)	(Wang et al., 2018b)
		Virgaviridae	*Tobamovirus*	Tobacco mosaic virus (TMV)		
		Sequiviridae	*Waikavirus*	Rice tungro spherical virus (RTSV)	*O. sativa* (rice)	(Macovei et al., 2018)
	FnCas9	*Virgaviridae*	*Tobamovirus*	Tobacco mosaic virus (TMV)	*N. benthamiana*	(Zhang et al., 2018b)
		Bromoviridae	*Cucumovirus*	Cucumber mosaic virus (CMV)	*N. benthamiana* *A. thaliana*	
	LshCas13a	*Potyviridae*	*Potyvirus*	Turnip mosaic virus (TuMV)	*N. benthamiana* *A. thaliana*	(Aman et al., 2018a, 2018b)
dsRNA	LshCas13a	*Reoviridae*	*Fijivirus*	Southern rice black-streaked dwarf virus (SRBSDV)	*O. sativa* (rice)	(Zhang et al., 2019b)
-ssRNA		*Rhabdoviridae*	*Cytorhabdovirus*	Rice stripe mosaic virus (RSMV)		
+ssRNA		*Virgaviridae*	*Tobamovirus*	Tobacco mosaic virus (TMV)	*N. benthamiana*	
	LshCas13a	*Potyviridae*	*Potyvirus*	Potato virus Y (PVY)	*S. tuberosum* (potato)	(Zhan et al., 2019)
	LshCas13a LwaCas13a BzCas13b PspCas13b CasRx	*Virgaviridae*	*Tobamovirus*	Tobacco mosaic virus (TMV)	*N. benthamiana*	(Mahas et al., 2019)
		Potyviridae	*Potyvirus*	Turnip mosaic virus (TuMV)		
	CasRx	*Potyviridae*	*Potyvirus*	Turnip mosaic virus (TuMV)	*N. benthamiana*	(Cao et al., 2021)
		Virgaviridae	*Tobamovirus*	Tobacco mosaic virus (TMV)		
		Bromoviridae	*Cucumovirus*	Cucumber mosaic virus (CMV)		

2.6.2 RNA viruses

The majority (more than 60%) of plant infecting viruses have RNA genomes and pose a serious threat to agricultural production (ICTV, 2018). The discovery of CRISPR/Cas variants from various bacterial strains such as RCas9, FnCas9 and Cas13a/b/d have led to these being used to target RNA *in vivo* (Abudayyeh et al., 2017; O'Connell et al., 2014; Sampson et al., 2013). The first report of CRISPR/Cas9 engineered plant immunity for an RNA virus was performed by a group that targeted CMV and TMV using FnCas9 and observed a reduction in virus accumulation in both transgenic tobacco and Arabidopsis plants (Table 2.2) (Zhang et al., 2018b). Applications of RNA virus interference by CRISPR/Cas13 in plants have been described in recent literature. Aman *et al* (2018a) first demonstrated the RNA targeting ability of CRISPR/Cas13 as a tool to combat viruses in plants. The study used LshCas13a for engineered interference against a green fluorescent protein (GFP)-expressing turnip mosaic virus (TuMV), a member of the *Potyvirus* genus, in *N. benthamiana*. Leaves of plants stably transformed with a codon-optimised LshCas13a were infiltrated with mixed *Agrobacterium* cultures carrying TuMV-GFP and crRNAs that target different regions of the virus genome. Post-infiltration, a ~50% reduction in GFP signal was detected in the leaves for two of the tested crRNAs targets. These initial results indicated the functional capacity for CRISPR/Cas13 in plants. Not long after, the same group conducted a study with the same objectives but in *A. thaliana* (Aman et al., 2018b). RNA interference against TuMV-GFP virus replication was successful in *A. thaliana* too.

A preliminary study demonstrated that the LshCas13a system can target and degrade viral RNA genomes and confer resistance to an RNA virus in a monocot grain plant (Zhang et al., 2019b). Transgenic rice plants harbouring the CRISPR/Cas13a system were generated, with three crRNAs each targeting the RNA genomes of the southern rice black-streaked dwarf virus (SRBSDV) and the rice stripe mosaic virus (RSMV), respectively. Inhibition of viral infection was confirmed in the transgenic rice plants, indicating that CRISPR/Cas13a can effectively target viral RNA in monocot plants too. Zhan *et al* (2019) verified that the CRISPR/Cas13a system can be engineered to deliver broad-spectrum resistance to transgenic potato plants against multiple potato virus Y (PVY) strains. Confirmed by enzyme-linked immunosorbent assays (ELISA) and quantitative reverse-transcription polymerase chain reaction (RT-qPCR), the transgenic potato plants expressing Cas13/sgRNA showed a significant reduction in PVY accumulation.

Most recently, a study by Mahas *et al* (2019) characterised multiple Cas13 proteins from three different Cas13 subtypes (a, b and d) for their efficiency to target viral RNA in *N. benthamiana*. To improve cellular localisation, each Cas13 orthologue was fused to either an NLS or a nuclear export

signal (NES). Transient and stable overexpression assays were conducted using a TMV-RNA-based overexpression (TRBO-G) system expressing GFP, as well as a GFP-expressing TuMV, as interference targets. The TRBO-GFP construct served as a reporter system that is not capable of systemic movement, while the TuMV-GFP virus was used to test whether the variants could limit systemic spread efficiently (Lindbo, 2007). Overall, while the variants LwaCas13a, PspCas13b and CasRx all showed high interference activities (over ~50% virus reduction), CasRx mediated the most robust interference in both stable and transient assays (Mahas et al., 2019). In addition, it was shown that CasRx can target either one virus or two RNA viruses simultaneously, making CasRx a variant that is potentially amenable to multiplex targeting of RNA plant viruses. Likewise, Cao *et al* (2021) recently expanded on the applicability of CasRx and was able to show a CRISPR/CasRx-mediated RNA interference against an array of RNA viruses. Together, these findings indicate that CasRx is the most efficient Cas13 variant to date for applications of RNA virus interference, and it may offer new possibilities for future transcriptome engineering applications.

2.6.3 Host plant factors

Although all of the aforementioned studies proved the applicability of targeting a viral genome with the Cas/gRNA system, stable transgenic plants had to be generated to overexpress the Cas nuclease to impart durable resistance. This is a potential limitation when it comes to the ethical issues that are raised regarding genetically modified crops, as well as the unwanted off-target mutations that can result from the overexpression of Cas in the plants (Khatodia et al., 2017). To bypass this limitation, a few studies have used the approach that leads to interference with host-encoded genes (Table 2.2). By using this approach, transgene-free genetically edited crops can be obtained if the heritable and homozygous mutations are segregated out of a self-pollinating species. For example, Chandrsekaran *et al* (2016) designed the CRISPR/Cas9 system to induce mutations in the host gene *eIF4E* (eukaryotic translation initiation factor 4E) of cucumber plants, necessary for the maintenance of the potyvirus life cycle. They reported the effective resistance of cucumber plants against three different potyviruses that have RNA genomes, namely the zucchini yellow mosaic virus (ZYMV), cucumber vein yellowing virus (CVYV), and papaya ringspot mosaic virus-W (PRSV-W). After three generations of backcrossing, homozygous non-transgenic cucumber plants showed broad virus resistance. Similarly, by introducing site-specific mutations in the host factor *eIF(iso)4E* locus via CRISPR/Cas9, resistance to the potyvirus TuMV in *A. thaliana* plants was conferred (Pyott et al., 2016). In tomatoes, important genes such as Dicer-like 2 (DCL2) are also involved in the pathways of plant defence systems. By generating loss-of-function DCL2 mutants using the CRISPR/Cas9 system and infecting them with potato virus X (PVX) and TMV, it was suggested that DCL2 is a key component of resistance pathways against RNA viruses as the mutants displayed viral symptoms (Wang et al., 2018a, 2018b). An

investigation by Macovei *et al* (2018) demonstrated novel sources of resistance in rice (*Oryza sativa*) against rice tungro spherical virus (RTSV) through biomimicking of *eIF4G* alleles. Their selected T2 plants were resistant to RSTV and tested negative for the presence of Cas9. In addition to this, they did not exhibit any observed mutations in the off-target sites. More recently, the CRISPR/Cas9-based targeting of two eIF4E isoforms found to interact with the viral genome-linked protein of cassava brown streak virus (CBSV) significantly suppressed the symptoms of the disease in cassava plants (Gomez et al., 2019). Thus, as of yet, it is evident that a fundamental candidate for host gene targeting by CRISPR is the translation initiation factor. In order to advance the practical applications of this CRISPR technology approach for plant virus resistance, there is an urgent demand for the identification of novel virus susceptibility genes from our understanding of plant-virus interactions.

2.7 Conclusion

Modern biotechnology shows potential to overcome the limitations of conventional virus resistance breeding and RNA silencing strategies. Collectively, the CRISPR/Cas systems present much promise as robust, precise and scalable DNA and RNA-targeting platforms and can be efficiently exploited to achieve virus resistance in plants. CRISPR/Cas13 can target specific endogenous RNAs, viral RNAs and RNA intermediates of DNA viruses in plants, and thus increases possibilities for its application in agriculture.

CHAPTER 3: Establishing CRISPR/Cas13a-mediated RNA targeting in *Nicotiana benthamiana*

3.1 INTRODUCTION

Gene editing, or genome editing, refers to a group of technologies used to modify a target DNA sequence in a wide variety of organisms. Site-directed nucleases (SDNs) such as ZFNs (zinc finger nucleases), TALENs (transcription activator-like effectors nucleases) and CRISPR/Cas (clustered regularly interspaced short palindromic repeats/CRISPR-associated proteins) are the primary approaches that have been developed for genome editing. Since the first gene-targeting experiment in *N. tabacum* protoplasts (Paszkowski et al., 1988) and the discovery that an induction of site-specific DNA DSBs can enhance the efficiency of gene targeting (Puchta et al., 1993), scientists have sought to develop these tools for several plant breeding purposes. Although the ZFN and TALEN platforms led to important advances, each has its own limitations and their use in plants has proven to be technically challenging. In comparison, the CRISPR/Cas system became established as a widely adopted, easily manipulated and low-cost genome editing technique for crop improvement applications.

The DNA-targeting CRISPR enzymes Cas9 and Cas12a (formerly Cpf1) have enabled many new avenues for studying and manipulating DNA sequences. Recently, a newly uncovered RNA-targeting CRISPR effector, Cas13, was shown to bind and cleave RNA rather than DNA substrates (Shmakov et al., 2015, 2017). The diverse Cas13 family currently contains four known subtypes, including Cas13a (formerly C2c2), Cas13b, Cas13c, and Cas13d, all shown to programmatically bind and cleave complementary target single-stranded RNA (Abudayyeh et al., 2016; Konermann et al., 2018; Shmakov et al., 2017; Smargon et al., 2017). A conserved feature of the family is the presence of two domains with homology to higher eukaryotes and prokaryotes nucleotide-binding (HEPN) RNase domains, which together form the unique ribonuclease-active site (Anantharaman et al., 2013; East-Seletsky et al., 2016; Shmakov et al., 2015).

Like DNA-targeting CRISPR systems, Cas13 uses a guide RNA to mediate target specificity (Figure 3.1). The Cas13 protein forms a complex with a crRNA that is complementary to the target RNA, and cleavage remote from the recognition site occurs when the complementary crRNA spacer hybridises to the target region (Abudayyeh et al., 2016). In bacteria, the first Cas13 variants that were characterised from *Leptotrichia shahii* (LshCas13a), *Bergeyella zoohelcum* Cas13b (BzoCas13b) and *Prevotella buccae* Cas13b (PspCas13b) required a protospacer flanking site (PFS) for efficient target recognition (Cox et al., 2017; Smargon et al., 2017). However, further investigation of PspCas13b and other Cas13 orthologs in plants and mammalian cells showed

that a PFS did not affect the targeting efficiency (Aman et al., 2018a; Konermann et al., 2018; Mahas et al., 2019). After the recognition and cleavage of a target transcript, the Cas13 enzyme was also shown to degrade any nearby non-complementary transcripts *in vitro*, exhibiting collateral activity. Fortunately, this type of non-specific RNA cleavage activity was only displayed in bacterial cells (Abudayyeh et al., 2016). This feature has since been harnessed to develop a Cas13-based nucleic acid detection tool known as Specific High-Sensitivity Enzymatic Reporter UnLOCKing (SHERLOCK) (Gootenberg et al., 2017).

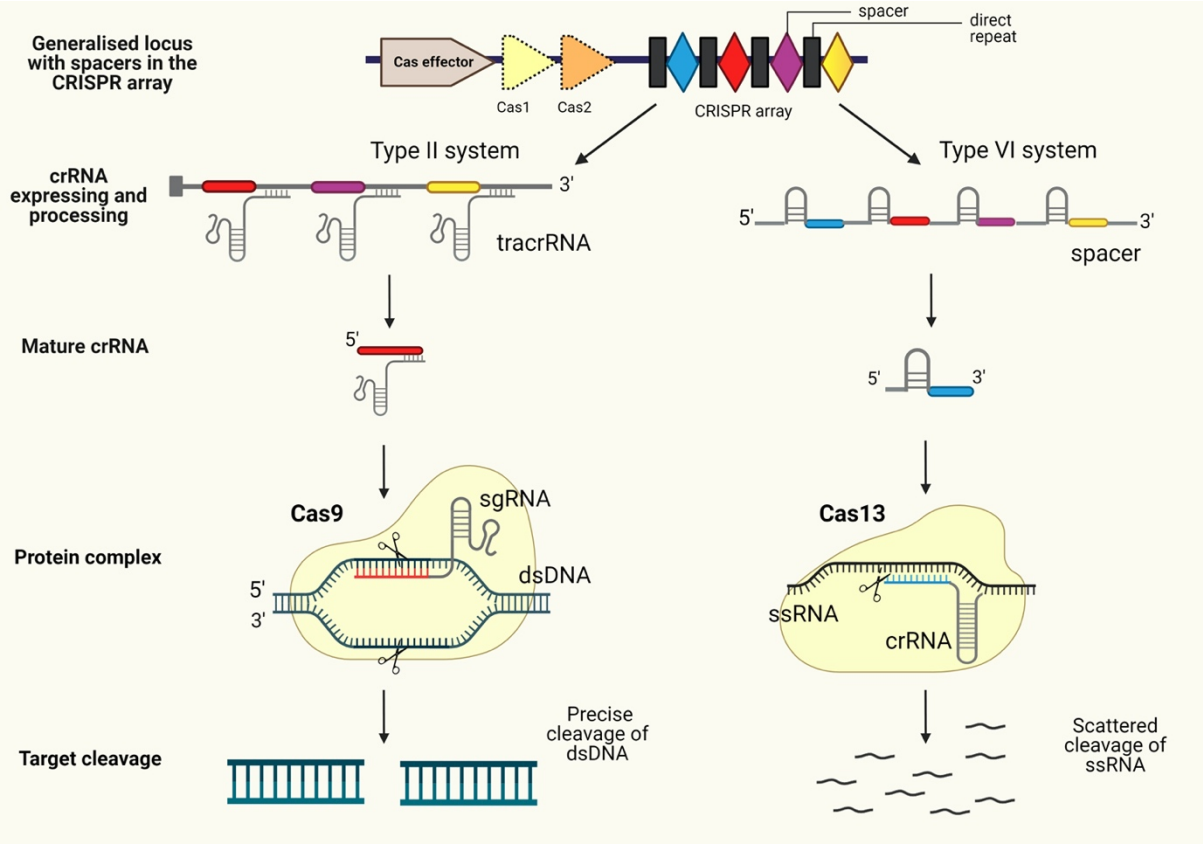

Figure 3.1 A comparison between the general CRISPR immunity steps of the DNA-targeting Type II Cas9 system and the RNA-targeting Type IV Cas13 system. In a complex with a sgRNA, the Cas9 endonuclease binds to dsDNA and mediates a double-strand break. Similarly, Cas13 is guided by a crRNA to target RNA sequences, resulting in cleavage at multiple sites within the single-stranded regions. Adapted from (Engreitz et al., 2019) using Biorender.

Furthermore, these features of the CRISPR/Cas13 platform allowed for RNA-editing applications to be developed. In plants, the heterologous expression of *Leptotrichia wadei* Cas13a (LwaCas13a) resulted in a 50% gene expression knockdown in rice protoplasts. At the same time, a comparative assessment of the widely used approach RNA interference (RNAi), and CRISPR/Cas13-mediated RNA degradation showed that the CRISPR/Cas system downregulated individual transcripts with greater specificity (Abudayyeh et al., 2017). To confer virus resistance, the Cas13a, Cas13b and Cas13d orthologs have since been employed to target viral RNA genomes in both monocot and dicot

plants (Aman et al., 2018a, 2018b; Mahas et al., 2019; Zhan et al., 2019). In the most recent study, the Cas13d effector was shown to be the most effective ortholog at RNA virus targeting, when compared with PspCas13b and LwaCas13a (Mahas et al., 2019). Notably, this group also demonstrated the value of fusing nuclear localisation or export signals (NLS/NES) to different Cas13a variants for virus interference applications. Other CRISPR/Cas13-based applications such as precise RNA base editing and live-cell transcript tracking have been tested in mammalian cells and are highly anticipated for their manipulation in plant research studies.

Since its inception, CRISPR/Cas technology has been successfully applied for the engineering of genomes and transcriptomes across a wide range of eukaryotic species. Recent advancements show great promise for crop improvement applications, as conventional plant breeding strategies are unlikely to meet the demand for the production of crops with higher yields and environmental adaptations. From a local and global standpoint, grapevine is one of the most important fruit harvests that makes a vital contribution to the agricultural sector. Unfortunately, grapevine production is susceptible to abiotic and biotic stresses, generating significant economic losses. Primarily, this study aimed to re-purpose the CRISPR/Cas13a system for an application in grapevine, but due to its recalcitrant nature towards *Agrobacterium*-mediated transformations and prolonged regeneration period, a model plant was used to immediately test the efficiency of the system. Thus, the aim of this chapter is to provide a proof of concept for CRISPR/Cas13a-mediated RNA transcript knockdown in *N. benthamiana*. The well-annotated endogenous gene, lycopene β-cyclase (*LCYB*), was selected as the target transcript of interest and binary LwaCas13a/crRNA constructs were assembled using two design strategies. Transgenic plant lines were regenerated and a preliminary indication of CRISPR/Cas13a-mediated down-regulation of the transcript is presented here.

3.2 MATERIALS AND METHODS

3.2.1 Design of crRNA targets

Two crRNAs targeting the lycopene β-cyclase (*LCYB*) transcript in *Nicotiana benthamiana* (Niben101Scf06266, Sol Genomics) and *Vitis vinifera* (Genbank accession JQ319639.1) were selected using the CRISPR RNA-Targeting Prediction and Visualization Tool (Zhu et al., 2018) http://bioinfolab.miamioh.edu/CRISPR-RT. Target candidates were selected according to their number of putative off-targets in both species, with the parameters being limited to: (a) a maximum of one mismatch site in the seed region (referring to the ~10-nt centre of the crRNA-target duplex); and (b) a maximum of two mismatch sites in the non-seed region. In addition, command-line BLASTN® (BLAST+) was optimised for short sequences and used to identify any putative off-targets that shared

homology with *N. benthamiana* and six *V. vinifera* cultivars: Corvina, Pinot noir (ENTAV), Cabernet, Pinotage, Pinot noir (PN40024) and Tannat.

3.2.2 Generation of crRNA cassettes

The crRNA targets were ordered and synthesised as ssDNA oligonucleotides with *Bbs*I restriction site overhangs (Supplementary Table S1), from IDT (Integrated DNA Technologies, USA). The oligos were annealed in a reaction consisting of: 1.5 µl of the forward oligo (100µM), 1.5 µl of the reverse oligo (100µM), 5 µl of 10x NEB (New England Biolabs, USA) buffer 2.1, and dH_2O to a total volume of 50 µl. The conditions were set as 95°C for 4 minutes, 70°C for 10 minutes and then cooled to room temperature. The annealed oligos were each ligated into a *Bbs*I-digested pjjb308 plasmid (Addgene; plasmid #107699) directly before the gRNA scaffold. The ligation reaction composed of 1 µl of the annealed oligo pair, 0.5 µl of *Bbs*I-digested pjjb308 DNA (20 ng/µl), 2 µl of 10x Ligase Buffer (NEB), 0.05 U/µl T4 Ligase (NEB), and dH_2O to a total volume of 20 µl, and incubated overnight at 4°C. Primers pjjb208_F/R (Table 3.1) were used to confirm the ligation by Sanger sequencing at the Central Analytical Facilities (CAF) (Stellenbosch University, SA). The plasmid map is provided in Supplementary Figure 1.

Table 3.1 Primers used for cloning, Sanger sequencing and gene expression analyses.

Primer name	Sequence (5'-3')	Tm (°C)	Amplicon length (bp)
pjjb308_F	AGGCCCCTGGGAATCTGAAA	58.7	341
pjjb308_R	GGTGACGCAGGTGATGAAAAG	56.5	
TC430	GTTGGATCTCTTCTGCAGCA	55.0	820
M13F	GTAAAACGACGGCCAGT	52.6	
NLS/NES_Fcheck	ACCAACAAAATACGCCCATC	59.7	N/A
NLS/NES_Rcheck	TGTCGGGGATCTTCTCAATC	56.3	
CaMV35s_F	ACGTAAGGGATGACGCACAA	59.7	820
LwaCas13a_R	TGTCGGGGATCTTCTCAATC	54.0	
actin5_F	GTCCCTATACGCCAGT	57.0	216*
actin3_R	ACATCGCGGACAATTT	56.0	488**
Cas13_qPCR-F	ATCAAGCGGATCTTCGAGTACC	56.5	102
Cas13_qPCR-R	GTAGTTGTACTTGCCGCAGTTC	56.1	
LCYB_RT-F	TTTGAGCTTCCTATGTATGACCCT	55.6	101
scaffold_RT-R	CGACTCGGTGCCACTTTTTC	56.6	
LCYB_qPCR F	TTTGGAGCTTGTACCTGAGACC	56.7	143
LCYB_qPCR R	CTTCTGAAACCTGCTGAGCAAC	56.4	
APR_F	CATCAGTGTCGTTGCAGGTATT	55.3	107
APR_R	GCAACTTCTTGGGTTTCCTCAT	55.6	

* PCR on cDNA
** PCR on genomic DNA

3.2.3 Generation of LwaCas13a/crRNA constructs

The pjjb308_crRNA plasmid was included in a one-step Golden Gate assembly reaction comprised of three other plasmids: intermediate module vectors pjjb296 and pMOD_C0000, and the transformation backbone pTRANS_220d (Addgene; plasmids #107691, #91081 and #91114, respectively). To assemble a control plasmid, the pjjb308 plasmid with no crRNA was included for the same aforementioned reaction. The reactions were setup as described by Čermák *et al.* (Čermák et al., 2017) with 75 ng pTRANS_220d, 150 ng pjjb296, 150 ng pMOD_C000, 150 ng pjjb308_crRNA, 0.8 µl *Aar*I oligonucleotide (0.5 µM) (Thermo Scientific, USA), 1 µl *Aar*I enzyme (2 U/µl) (Thermo Scientific, USA), 0.05 U T4 DNA Ligase (NEB), 2 µl 10x T4 DNA ligase buffer, and dH_2O for a total volume of 20 µl. The PCR cycle parameters were set to: 10 x (37°C/5min + 16°C/10min) + 37°C/15min + 80°C/5min + 4°C hold. The final construct was confirmed by Sanger sequencing at CAF (Stellenbosch University, SA) using primers TC430 and M13F (Table 3.1). The final plasmid map is provided in Supplementary Figure 2.

3.2.4 Addition of NLS/NES sequences

The LwaCas13a/crRNA plasmids were linearised with restriction enzymes *BamH*I and *Hind*III-HF to remove the LwaCas13a sequence (New England Biolabs, USA). Using primers designed for Gibson cloning (Supplementary Table S2) and the Phusion DNA polymerase (New England Biolabs, USA), LwaCas13a_NLS/NES fragments were amplified from plasmids pC014 and pC0056 (Addgene plasmids #91902 and #105815, respectively). PCR conditions were set as follows: 98°C /30 sec + 35 × (98°C/10 sec + 67°C/30 sec + 72°C/2:30 min) + 72°C/5 min + 4°C hold. Subsequently, the digested backbone and PCR products of the desired size were purified from a 0.8% (w/v) agarose gel using the Zymoclean Gel DNA Recovery Kit (Zymo Research, USA). The purified vector and insert fragments were mixed and assembled with the NEBuilder Hifi DNA Assembly Kit (New England Bioloabs, USA) according to the manufacturer's protocol. The resulting vectors were confirmed by Sanger sequencing at CAF (Stellenbosch University, SA) using primer pair NLS/NES_check (Table 3.1). Final plasmid maps are provided in Supplementary Figure 3.

3.2.5 Plant transformation and regeneration

The LwaCas13a constructs were individually introduced into *A. tumefaciens* strain EHA105 by electroporation. A single positive colony was inoculated into 5 ml of liquid YEB (10 g/l peptone, 10 g/l yeast extract and 5 g/l NaCl) media containing 50 µg/ml kanamycin and 50 µg/ml rifampicin and incubated on a shaker at 150 rpm overnight at 28°C. The following day 1 ml of culture was inoculated into 50 ml of liquid YEB media containing 50 µg/ml kanamycin, 50 µg/ml rifampicin and 100 µg/ml acetosyringone and incubated overnight at 28°C. The culture was centrifuged at 3000 rpm for 15 minutes and resuspended in MS3 broth (4.4 g/l Murashige and Skoog (MS) medium, 30 g/l sucrose, pH 5.8) containing 100 µg/ml acetosyringone to OD_{600} = 0.8-1.0. Approximately 50 leaf disc explants per construct were dissected from *in vitro* grown *N. benthamiana* plants and used for *Agrobacterium*-mediated transformation using the method described by Clemente (Clemente, 2006). The explants were regenerated on selective media plates (4.4 g/l MS salts, 30 g/l sucrose, 3.3 g/l phytagel, 1 µM BAP, pH 5.8) containing 100 µg/ml kanamycin and 400 µg/ml carbenicillin. The plates were incubated at 25°C with a 16-h light/8-h dark photoperiod cycle, and the leaf discs were sub-cultured every 14 days. When shoots regenerated from the callus, they were excised and placed onto rooting medium (2.2 g/l MS salts, 15 g/l sucrose, 3.3 g/l phytagel, pH 5.8) containing 100 µg/ml kanamycin and 400 µg/ml carbenicillin. Once fully regenerated, putative transgenic lines were maintained on rooting medium and subjected to molecular analysis.

3.2.6 LwaCas13a detection by PCR

Leaf material was harvested from the regenerated plantlets (T0) and briefly homogenised by tissue grinders in liquid nitrogen. Using 200 mg of powdered sample, genomic DNA was extracted using the standard CTAB method (Murray and Thompson, 1980). To identify putative transgenic plants, primers CaMV35s_F and LwaCas13a_R were used (Table 3.1). Standard PCR conditions were set as follows: 95°C/3 min + 35 x (95°C/30 sec + 52°C/30 sec + 72°C/30 sec) + 72°C/5 min + 4°C hold and 50 ng/µl DNA per reaction was used. Once confirmed, each plant was propagated in triplicate and maintained on rooting media. In preparation for RNA extractions, leaf material was sampled and briefly homogenised by tissue grinders in liquid nitrogen.

3.2.7 RNA extraction and cDNA synthesis

Total RNA from 100 mg of ground leaf tissue was extracted with the Spectrum™ Plant Total RNA Kit (Sigma, USA), as per the manufacturer's instructions, and the samples were eluted in 40 µL dH_2O. The RNA integrity and purity was evaluated using agarose gel electrophoresis and spectrophotometry (Nanodrop 2000; Thermo Scientific, USA). One microgram of total RNA was DNase-treated with RQ1 RNase-Free DNase (Promega, USA) according to the manufacturer's instructions. First-strand cDNA was synthesised from the DNase-treated RNA using random hexamer primers (Promega, USA) and Maxima Reverse Transcriptase (Thermo Scientific, USA) in a final volume of 20 µL according to the manufacturer's protocol. To verify the removal of DNA, the resulting cDNA samples were used for a PCR detection of the β-actin gene (GenBank accession JQ256516.1). Primers were designed to generate different products from genomic DNA and cDNA templates (Table 3.1). PCR cycle parameters were set as: 95°C/3 min + 35 x (95°C/30 sec + 54°C/30 sec + 72°C/30 sec) + 72°C/5 min + 4°C hold. The PCR products were resolved on a 2% (w/v) agarose gel and visualised by ethidium bromide dye staining (Thermo Scientific, USA).

3.2.8 Reverse transcription (RT)-PCR: transgene expression assay

Expression of LwaCas13a and the *LCYB* Target 1 crRNA was analysed by RT-PCR. Using cDNA samples and the GoTaq DNA Polymerase (Promega, USA), primers Cas13_qPCR-F and Cas13_qPCR-R were used to amplify LwaCas13a and primers GFP_RT-F and scaffold_RT-R were used to amplify the crRNA and scaffold fragment (Table 3.1). The thermal cycling conditions were set as follows: 95°C /3 min + 35 × (95°C/30 sec + 55°C/30 sec + 72°C/30 sec) + 72°C/5 min + 4°C hold. The PCR products were resolved on a 1.8 % (w/v) agarose gel and visualised by ethidium bromide dye staining (Thermo Scientific, USA).

3.2.9 Quantitative RT-PCR (RT-qPCR) expression analysis

All RT-qPCR reactions were performed in 10 µl final volumes using the PowerUp™ SYBR™ Green Master Mix (Applied Biosystems, USA) with 40 ng cDNA and 1.5 µl per primer (2.5 mM). The reactions were setup in a 96-well plate with three technical replicates for each biological replicate, while the Adenine phosphoribosyltransferase like (*APR*) housekeeping gene was selected as an internal control. The *APR* and *LCYB* primer pairs are listed in Table 3.1. The PCR was performed on a QuantStudio™ 3 Real-Time PCR System (Applied Biosystems, USA) and the comparative C_T ($\Delta\Delta C_T$) method was selected. The standard cycle parameters were set up as follows: 50°C/2 min + 95°C/2 min + 40 x (95°C/15 sec + 60°C/1 min) and the melt curve parameters were set as default by the software. The relative levels of gene expression comparative to reference samples were calculated using the $2^{-\Delta\Delta Ct}$ method (Livak and Schmittgen, 2001) and analysed using the Thermo Fischer Design and Analysis app. Error bars represent 95% confidence intervals.

3.2.10 Measurement of total carotenoid content

Leaf material (~90-100 mg) from *in vitro* plants was harvested and homogenised using liquid nitrogen and tissue grinders, while working with minimal light exposure. Ground tissue samples were extracted with 100% acetone (v/v) and centrifuged briefly (3000 rpm, 5 min) at room temperature. The absorbance of the extract was measured at 470, 647 and 663 nm using a Lambda 25 UV/Vis spectrophotometer (Perkin Elmer, USA). From the measured absorbance, the chlorophyll *a* (C_a), chlorophyll *b* (C_b) and total carotenoid (C_{x+c}) concentrations were calculated on a mg/g of fresh weight (FW) basis using the equations derived by (Lichtenthaler & Buschmann, 2001):

$$\text{Chlorophyll a (µg/ml): } C_a = [(12.25*A_{663}) - (2.79*A_{647})]*\text{dilution factor}$$

$$\text{Chlorophyll b (µg/ml): } C_b = [(21.50*A_{647}) - (5.10*A_{663})]*\text{dilution factor}$$

$$\text{Total carotenoids (µg/ml): } C_{x+c} = [(1000*A_{470} - 1.82*C_a - 85.02*C_b)/198]*\text{dilution factor}$$

3.2.11 Statistical analysis

All statistical analyses were conducted using the Prism GraphPad software Version 8.3.0 (GraphPad Software, USA). A two-tailed unpaired Student's t-test was used to calculate the significance between relative fold expression levels of each transgenic line and the control group. All data are presented as the mean ± standard error of the mean (SEM) of three biological replicates per plant line. Determination of significance was set as $p \leq 0.05$.

3.3 RESULTS

3.3.1 The selection of two *LCYB* targets

The transcript chosen for a proof-of-concept for LwaCas13a-mediated RNA targeting is *LCYB*, a key enzyme of the carotenoid biosynthesis pathway in most plant species (Hirschberg, 2001). By designing crRNA targets conserved across both the *N. benthamiana* and *V. vinifera LCYB* transcripts, it allowed for the assembly of Cas13a constructs that can perform RNA knockdown in both species. Furthermore, the *LCYB* transcript was selected to test if the knockdown of its gene expression could potentially result in a detectable phenotype. For instance, the phytoene desaturase (*PDS*) enzyme, also involved in the carotenoid biosynthetic pathway, is widely used as a common marker gene for RNA interference (RNAi)-induced gene silencing approaches in many plant species, as a knockdown of the transcript results in the inhibition of chlorophyll biosynthesis and subsequently a photobleached phenotype (Kumagai et al., 1995; Naing et al., 2019; Qin et al., 2007).

It has been observed that mismatches in the centre of the crRNA-target duplex are least tolerated and can affect HEPN domain activation, suggesting to the presence of a central seed region for Cas13a and Cas13b (Abudayyeh et al., 2016; Bandaru et al., 2020; East-Seletsky et al., 2016; Liu et al., 2017a; Tambe et al., 2018). Two targets, each 28 nt in length, were designed and assessed for on- and off-target sites within the *N. benthamiana* and *V. vinifera* reference transcriptomes. Using CRISPR-RT set to the pre-determined mismatch limits, no off-targets were found for Target 1, and a total of two putative off-targets were found for Target 2 in the *N. benthamiana* transcriptome. No off-targets were found for Target 1 and 2 in the *V. vinifera* transcriptome. In addition, possible off-targets caused by homology of the targets with the transcriptomes were identified using BLAST+. The results for Target 1 indicated no more than three off-targets in *N. benthamiana* and no more than three off-targets in each of the *V. vinifera* cultivars. For Target 2, BLAST+ identified no more than two off-targets in *N. benthamiana,* and no more than two off-targets in each of the *V. vinifera* cultivars (Figure 3.2 A and B).

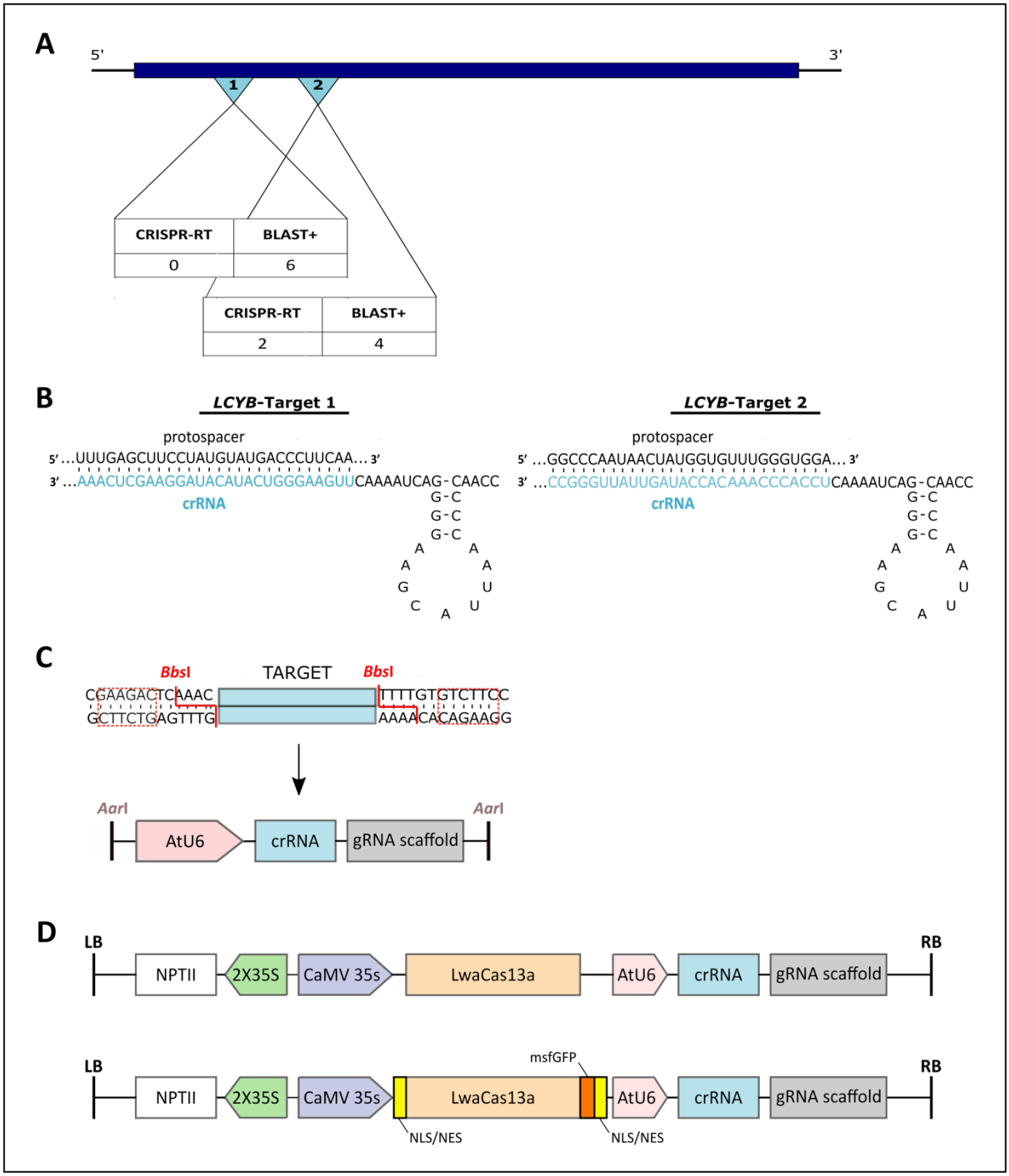

Figure 3.2 Target design and the CRISPR/Cas13 machinery assembled for plant transformations. (**A**) The *LCYB* transcript of *N. benthamiana* and *V. vinifera* with the estimated positions of the selected crRNA targets and their CRISPR-RT and BLAST+ scores across both species. (**B**) The selected RNA targets (28 nucleotides in length) paired with their respective crRNAs. The stem-loop sequence is obtained from Abudayyeh *et al* 2016. (**C**) A schematic representation of the *Bbs*I cut sites adjacent to the target sequence that was followed by ligation into the intermediate vector pjjb308. (**D**) Schematic representation of the T-DNA region of the two assembled LwaCas13a/crRNA constructs with their respective components. The CaMV_35s promoter and the Arabidopsis U6-26 gene promoter (AtU6) are responsible for the expression of LwaCas13a and the crRNA, respectively. For selection purposes, it contains a neomycin phosphotransferase type II gene (NPTII) driven by a 35s promoter. NLS, nuclear localisation sequence; NES, nuclear export signal; msfGFP, monomeric superfolder GFP; LB, left border; RB, right border.

3.3.2 The construction of LwaCas13a expression cassettes

Once the crRNAs were synthesised, they were cloned under the AtU6 promoter for expression and adjacent to a gRNA scaffold in an intermediate vector (Figure 3.2 C). Using the Golden Gate assembly method, these components were then integrated into the T-DNA region of a LwaCas13a expression vector to generate a binary vector for each *LCYB* target (Figure 3.2 D). As a negative control, an identical binary vector without a crRNA was assembled in parallel.

Recently, Mahas *et al* (2019) showed that the different signals, i.e. NLS and NES, could localise Cas13a variants to either nuclear or cytoplasmic subcellular areas, therefore improving activity against the target transcripts. In light of this report, the existing construct LwaCas13a_T1 was modified to investigate if subcellular localisation of the CRISPR modules could improve RNA-targeting efficiency. Henceforth, the Gibson assembly method was used to modify the existing LwaCas13a constructs by replacing the LwaCas13a open reading frame with a LwaCas13a fragment flanked by an NLS/NES sequence on both the N- and C- termini (Figure 3.2 D).

3.3.3 Production of transgenic *N. benthamiana* plants

Two independent transformation experiments of *N. benthamiana* leaf disc explants were conducted with the CRISPR/Cas13a constructs that were assembled. The first transformation, herewith referred to as Experiment A, the constructs LwaCas13a_T1 and LwaCas13a_T2 (T1 and T2 referring to the *LCYB* crRNA targets) and the control LwaCas13a_EMPTY, were used. Through *Agrobacterium*-mediated transformation, a total of twenty LwaCas13a_T1, sixteen LwaCas13a_T2 and eight LwaCas13a_EMPTY independent plants were regenerated on the rooting medium with kanamycin selection (Table 3.2). Transgenic lines were established after PCR identification of exogenous T-DNA insertion, revealing an average transformation rate of 59% for the first experiment (Figure 3.3 A). The plants that were confirmed by PCR for the absence of the Cas13a transgene were excluded from all future molecular analyses. Thereafter, each transgenic plant line was propagated in triplicate to reduce system variation and ensure synchronisation of their growth stages.

Table 3.2 Plant count of the explants, regenerated plantlets and transgenic T0 lines from the *Agrobacterium*-mediated stable transformation experiments of *N. benthamiana*.

EXPERIMENT	Constructs used for *A. tumefaciens* transformation	Total number of leaf discs	Total number of regenerated plantlets	Total number of confirmed transgenic plants
A	LwaCas13a_T1	80	20	10
	LwaCas13a_T2	80	16	8
	LwaCas13a_EMPTY	50	8	8
B	LwaCas13a/NLS-T1	80	12	11
	LwaCas13a/NES-T1	60	9	7
	LwaCas13a/NES-EMPTY	50	8	5

The second *Agrobacterium*-mediated transformation experiment, referred to as Experiment B, was conducted with the LwaCas13a_T1 constructs modified for cellular localisation: LwaCas13/NLS-T1 and LwaCas13a/NES-T1. The LwaCas13/NES-EMPTY plasmid was also included as a negative control. A total of twelve LwaCas13/NLS-T1, nine LwaCas13a/NES-T1 and eight LwaCas13a/NES-EMPTY rooting *N. benthamiana* plants were obtained from the *Agrobacterium*-mediated transformation events (Table 3.2). Among these T0 plants, screening by PCR amplification of the Cas13a transgene revealed eleven LwaCas13a/NLS-T1, seven LwaCas13a/NES-T1 and five LwaCas13a/NES-EMPTY plants to be transgenic (Figure 3.3 B). Each transgenic plant line was propagated in triplicate and maintained on rooting media in a growth chamber.

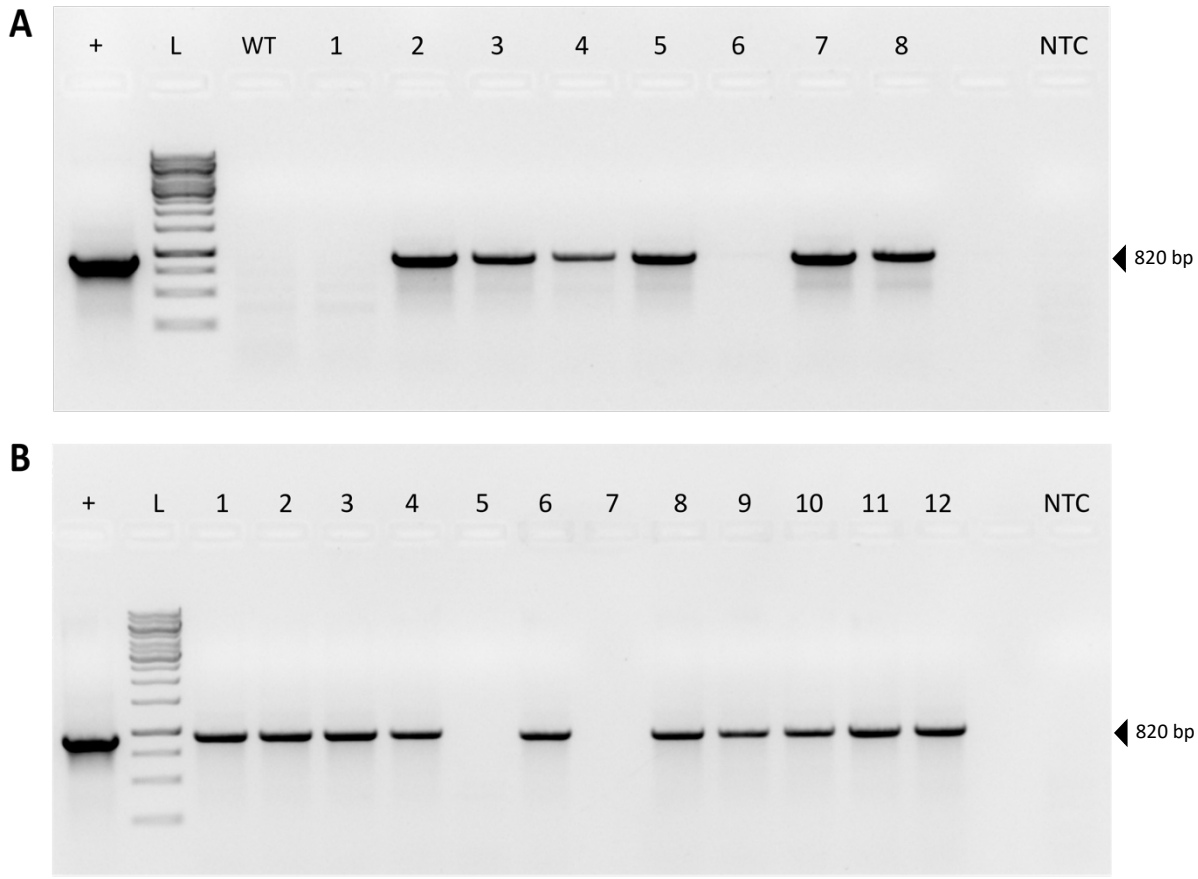

Figure 3.3 PCR screening of T0 transformants using Cas13a-specific primers (~820 bp) at the genomic DNA level. (**A**) Representative 1% (w/v) agarose gel for Experiment A selection of transgenics. Lanes 1-8: independently transformed plants. L: 1kb molecular weight marker (GeneRuler, Thermo Scientific); Positive control (+): LwaCas13a_EMPTY plasmid DNA; WT: wild-type *N. benthamiana* DNA sample; NTC: No template control. (**B**) Representative 1% (w/v) agarose gel for Experiment B selection of transgenics. Lanes 1-12: independently transformed plants. L: 1kb molecular weight marker (GeneRuler, Thermo Scientific); Positive control (+): LwaCas13a/NES-EMPTY plasmid DNA; NTC: No template control.

Across both experiments, no phenotypic differences were observed between the plants transformed with LwaCas13a constructs and the control plants transformed with the LwaCas13a harbouring no crRNA (Figure 3.4). Notably, a proportion of plants from the transgenic lines displayed phenotypic abnormalities such as vitrification and a lack of apical dominance during the regeneration process and post-micropropagation, when compared with wild-type plants.

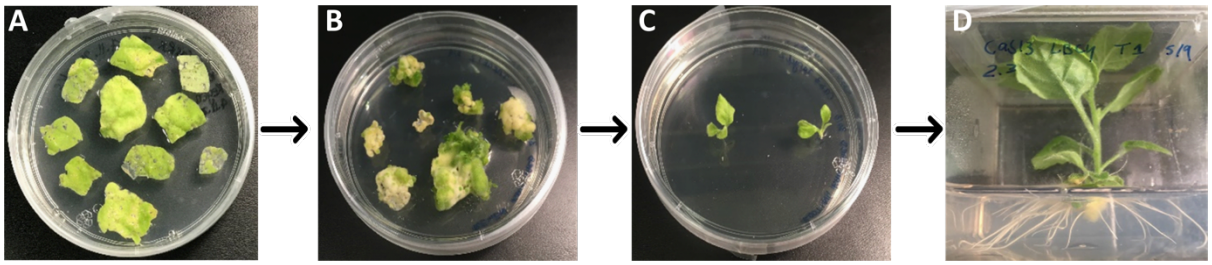

Figure 3.4 Regeneration process of the *N. benthamiana* leaf discs transformed with a binary vector. (**A**) The growth of leaf discs on co-cultivation medium after incubation with *Agrobacterium* (**B)** Calli formation stage with shoots. (**C**) Isolation of shoots onto root induction medium. (**D**) Fully regenerated putative transgenic plant.

3.3.4 Gene expression analyses of transgenic plant lines

3.3.4.1 Experiment A – Comparison of the crRNA targets

The following subsets of transgenic plant lines were selected for gene expression analyses by RT-qPCR: lines 9, 16 and 20 transformed with the LwaCas13a_T1 construct; lines 8, 13 and 14 transformed with the LwaCas13a_T2 construct and plants E1, E2 and E3 transformed with the control plasmid LwaCas13_EMPTY. Three plants per transgenic line were selected and as another negative control, three wild-type *N. benthamiana* samples were included. First, the integrity of the cDNA samples of these selected plants was validated by PCR for the housekeeping gene actin. As shown in Figure 3.5, cDNA synthesis was confirmed to be successful for all samples except for two wild-type *N. benthamiana* samples that were henceforth excluded from further analyses.

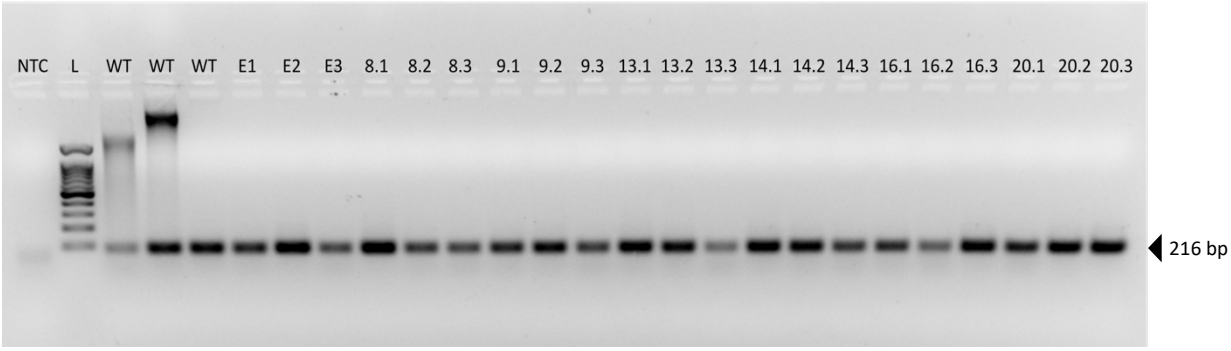

Figure 3.5 Actin PCR on cDNA samples selected for gene expression analyses. The amplified PCR products (~216 bp) were visualised on a 2% (w/v) agarose gel. NTC: No template control; L: 1kb molecular weight marker (GeneRuler, Thermo Scientific); WT: wild-type *N. benthamiana* cDNA.

Thereafter, *LCYB* gene expression was quantified by RT-qPCR and normalised with the housekeeping gene *APR*. In Figure 3.6 A, the expression of *LCYB* is observed in all the transgenic lines and control plants. The control samples E1, E2 and E3 present highly variable levels of expression, with E1 being the only sample expressing a similar level of *LCYB* expression to the wild-type sample. This variability is also true for the samples within each transgenic line and across both the LwaCas13a_T1 and LwaCas13a_T2 transgenic lines. Notably, independent plants from line 9 and line 8 appear to indicate a reduced level of *LCYB* expression, approximately 2-fold lower, compared with the reference sample E1 and the wild-type sample. However, once all plants per line were biologically grouped, no significant difference in *LCYB* expression was observed for any of the transgenic lines when compared with the control group (Figure 3.6 B).

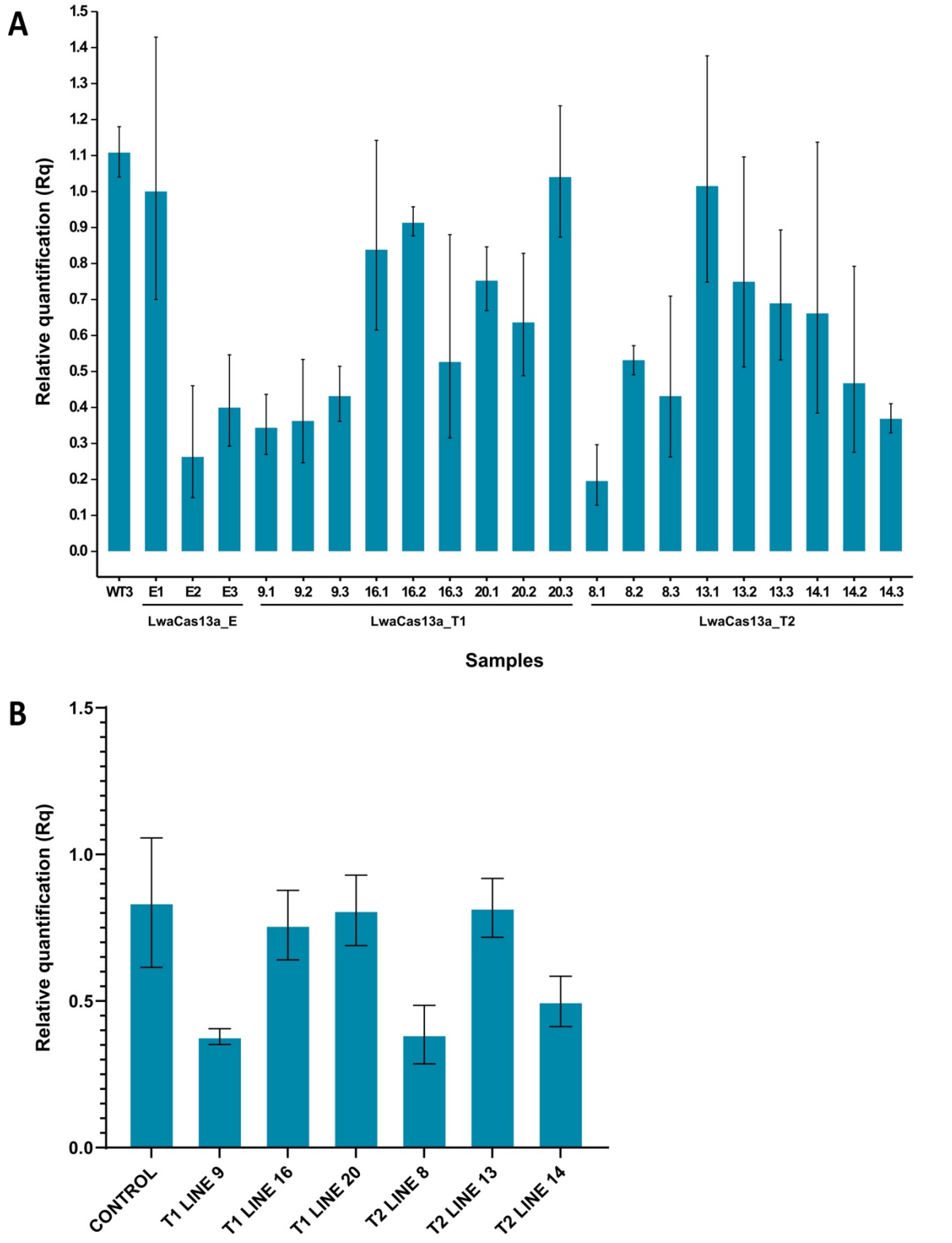

Figure 3.6 RT-qPCR analysis of *LCYB* gene expression in the selected transgenic lines. (**A**) Relative fold expression is normalised to reference sample E1 and the error bars represent 95% confidence intervals of n=3 technical replicates. The samples are grouped according to the constructs they were transformed with: control plasmid LwaCas13a_EMPTY (LwaCas13a_E), LwaCas13a-*LCYB* Target 1 (LwaCas13a_T1) and LwaCas13a-*LCYB* Target 2 (LwaCas13a_T2). (**B**) Data is shown as mean fold expression ± SEM of the transgenics lines (n=3 biological repeats per line). Statistical analysis was performed using the Student's unpaired t-test and significant difference was determined at $p \leq 0.05$ with respect to the control group.

3.3.4.2 Experiment B – Comparison of the localised LwaCas13a_T1 constructs

Ten transgenic lines that were transformed with the LwaCas13a/NLS-T1 construct (NLS1-NLS10), seven transgenic lines that were transformed with the LwaCas13a/NES-T1 construct (NES1-NES7) and five transgenic control lines transformed with LwaCas13a/NES-EMPTY (E1-E5) were selected for quantitative analyses. As a preliminary assessment, one plant per transgenic line was selected.

First, the endogenous actin housekeeping gene was used to verify the integrity of the cDNA samples. The presence of the expected actin cDNA amplification product and the absence of the corresponding genomic DNA product confirmed that the cDNA samples were not contaminated with genomic DNA. Sample E3 did not present cDNA actin amplification (Figure 3.7 A), however the PCR was repeated with a higher concentration of cDNA and was thereafter confirmed (Supplementary Figure 5). Subsequently, the samples were assessed by end-point PCR for LwaCas13a and the *LCYB* Target 1 crRNA expression. The LwaCas13a gene and *LCYB* Target 1 crRNA is shown to be constitutively expressed in most of the samples (Supplementary Figure 4). All NLS and NES samples that did not amplify in these LwaCas13a and the *LCYB* Target 1 crRNA RT-PCRs were re-assessed using higher concentrations of cDNA and were thereafter confirmed to express both components, while samples that failed to amplify in both these subsequent PCRs were therefore excluded from further expression analyses (Supplementary Figure 5).

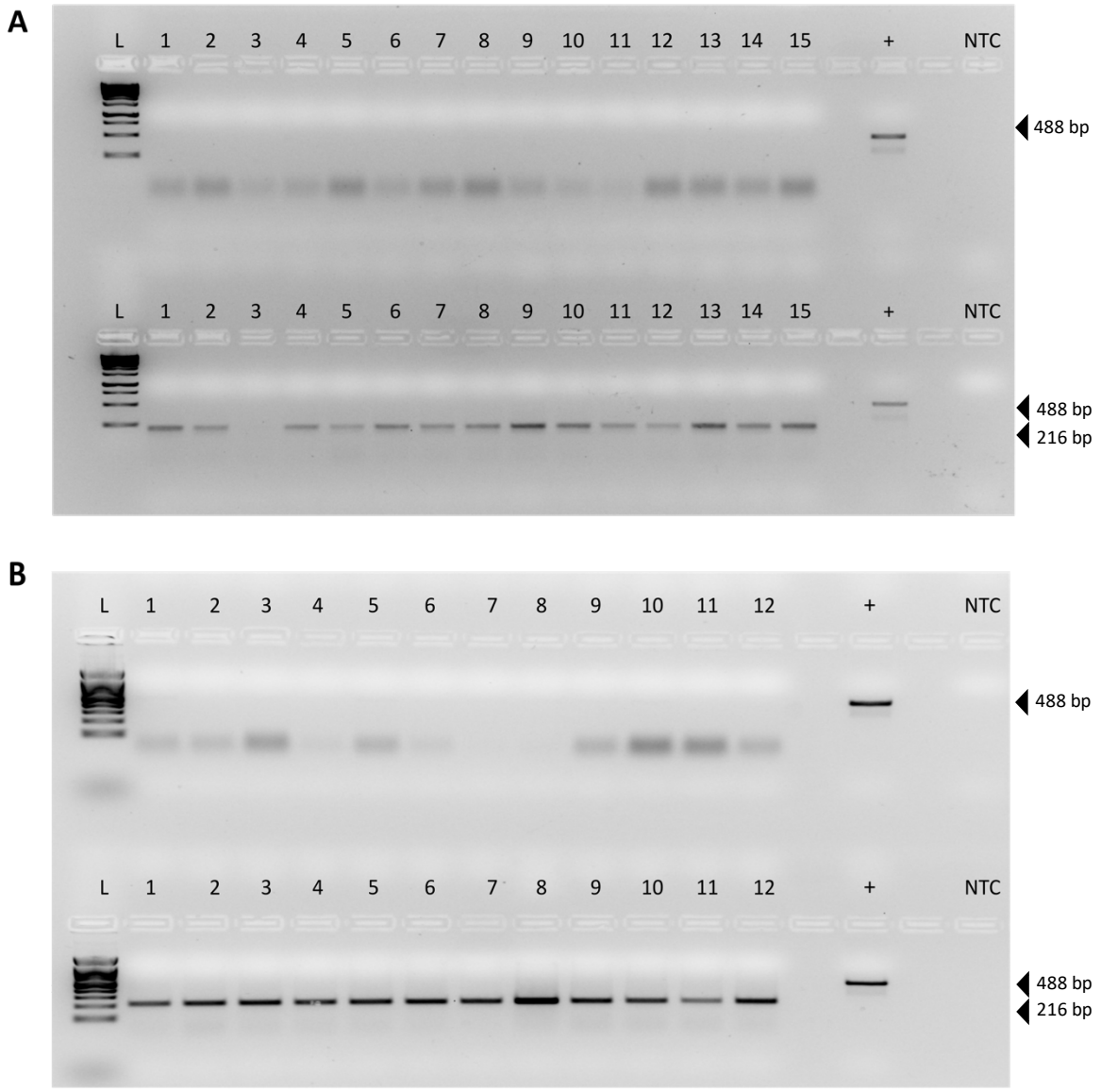

Figure 3.7 Detection of actin in RNA samples (TOP row) and cDNA samples (BOTTOM row), with anticipated PCR products of 216 bp for cDNA and 488 bp for genomic DNA. PCR products are resolved on 1% (w/v) agarose gels. (**A**) Lanes 1- 5: Samples E1-E5; Lanes 6-15: Samples NLS1-NLS10. L: 1kb molecular weight marker (GeneRuler, Thermo Scientific); Positive control: wild-type *N. benthamiana* DNA sample; NTC: No template control. (**B**) Lanes 1- 5: samples E1-E3; Lanes 6-15: samples NES1-NES7. L: 100bp molecular weight marker (Cleaver Scientific, USA); Positive control: wild-type *N. benthamiana* DNA sample; NTC: No template control.

To determine the transcriptional regulation of the gene encoding *LCYB*, a RT-qPCR analysis was performed on the selected transgenic lines and normalised with the endogenous control gene *APR*. As shown in Figure 3.8 A and B, all of the selected samples expressed *LCYB*, with variation in the transcript's abundance seen across both the NLS and NES lines. In particular, the results show a potential reduction in *LCYB* expression, equal to or more than a ~1.7-fold reduction, for independent plants NLS1, NLS4 and NES1, when compared with their respective reference control samples.

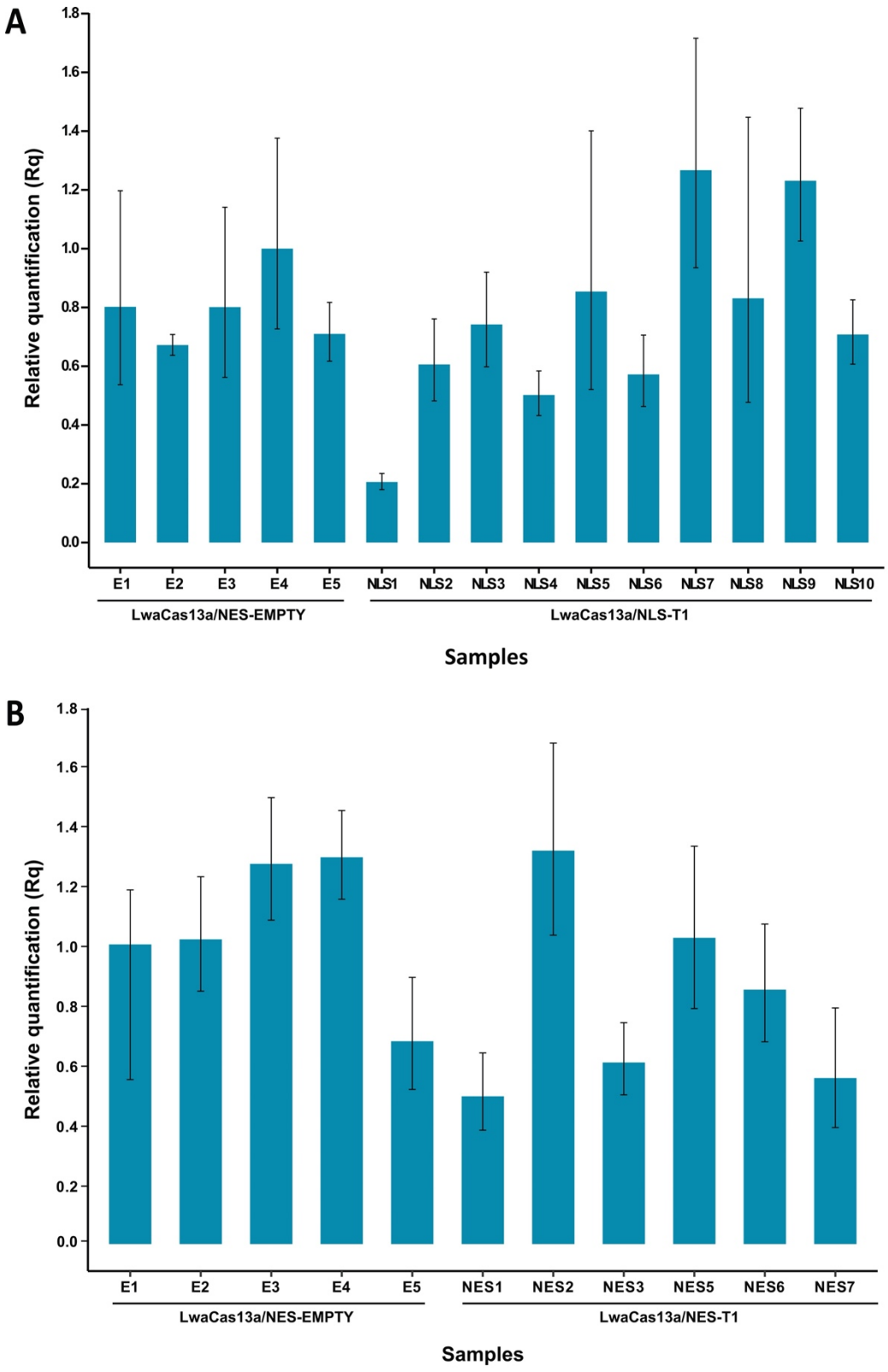

Figure 3.8 RT-qPCR analysis of *LCYB* gene expression. The error bars represent 95% confidence intervals of n=3 technical replicates. (**A**) Samples are grouped according to the constructs they were transformed with: control plasmid (LwaCas13a/NES-EMPTY) and LwaCas13a_NLS *LCYB* Target 1 (LwaCas13a/NLS-T1). Expression is normalised to reference sample E4. (**B**) Samples are grouped according to the constructs they were transformed with: control plasmid (LwaCas13a/NES-EMPTY) and LwaCas13a_NES *LCYB* Target 1 (LwaCas13a/NES-T1). Expression is normalised to reference sample E1.

Based on these preliminary results, two more plants from each of these three transgenic plant lines were selected for the same RT-qPCR analysis to statistically elucidate if this reduction in expression is consistent across each transgenic line. Prior to quantifying the expression of *LCYB*, the quality of the cDNA samples was verified by a standard PCR for actin and the constitutive expression of the LwaCas13a gene and *LCYB* T1 crRNA were confirmed by RT-PCR (Supplementary Figures 6 and 7). Once these samples passed these preliminary tests, RT-qPCR *LCYB* expression analysis was performed on plant lines NLS1, NLS4 and NES1, with three biological replicates per line. Three transgenic control plants, which were transformed with the LwaCas13a_NES EMPTY construct, were included to form a control group. The results suggest that the transcript encoding *LCYB* is significantly downregulated in line NES1 as the relative expression is ~>2 fold lower when compared with the control group (Figure 3.9 A). No significant changes in *LCYB* expression were observed for the two NLS lines 1 and 4.

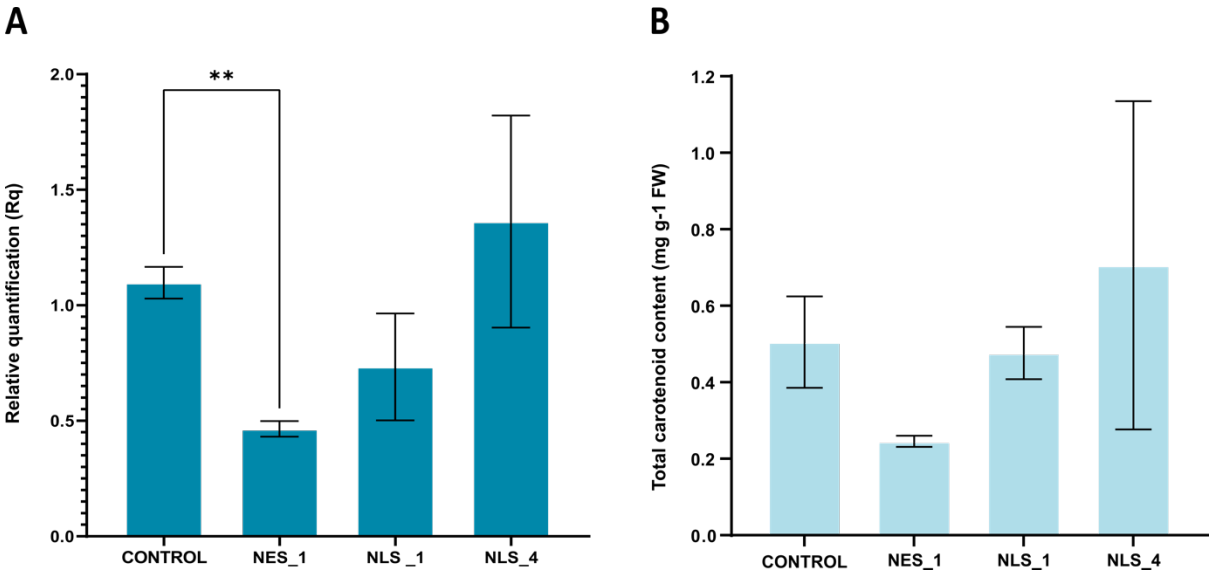

Figure 3.9 Assessment of CRISPR/Cas13a-mediated targeting of the *LCYB* transcript in selected transgenic lines. (**A**) RT-qPCR analysis of *LCY*B gene expression in the transgenic lines. The mean fold expression of the LwaCas13a_NLS and LwaCas13_NES transgenics lines (n=3 biological repeats per line) is compared with that of the control group. Statistical analysis was performed using the Student's unpaired t-test ($p < 0.05$) and the error bars represent ±SEM. ** = $p \leq 0.01$ (**B**) Total carotenoid content in selected transgenic lines. Data is representative of mean C_{x+c} values (n=2) and the error bars represent ±SEM.

3.3.5 Preliminary indication of total carotenoid content

In order to obtain a measurement of the main photosynthetic pigments present in the transgenic lines, measurements from UV/vis absorption spectra were used to provide a preliminary quantification. Shown in Figure 3.9 B, the mean carotenoid content levels are representative of two transgenic plants per line. The levels of carotenoid content in the transgenic lines appear to correlate with the same trend in results obtained from the RT-qPCR analysis of NES line 1, as it is evident a lower level of total

carotenoid content is recorded for NES line 1, while lines NLS 1 and 4 do not show a decrease in total carotenoid content when compared with the control group.

3.4 DISCUSSION

The ability to modulate gene activity is critical for our understanding of biological functions and molecular breeding prospects. New CRISPR technologies, more importantly those specific to targeting/editing RNA genomes, show potential to extend diverse innovations into plant research. For example, recent applications of CRISPR/Cas13a/FnCas9 to engineer resistance against economically important plant RNA viruses has opened new opportunities for the development of broad-spectrum viral immunity in plants (Aman et al., 2018a; Zhan et al., 2019; Zhang et al., 2018b, 2019b). Less explored as of yet, the *in vivo* cleavage of endogenous mRNA transcripts in plants is another unprecedented application of CRISPR/Cas13a, which could be harnessed for site-specific transcriptional/post-transcriptional gene regulation (Abudayyeh et al., 2017; Mahas et al., 2018).

Carotenoids are products of the isoprenoid biosynthetic pathway in plants. After the formation of lycopene, the pathway bifurcates to produce α- and β- carotenes and their derivatives through the activity of two lycopene cyclases: lycopene ε- and β- cyclase (LCYE and LCYB) (Nisar et al., 2015; Sun et al., 2020). The enzyme activities of *LCYE* and *LCYB* in relation to one another therefore play a major role in controlling carotenoid composition. Indeed, transgenic manipulations of *LCYE* and *LCYB* expression in tobacco, sweet potato, tomato, banana, *B. napus* and wheat altered the metabolic flux of carotenes and xanthophylls (Apel and Bock, 2009; Kaur et al., 2020; Kim et al., 2014; Shi et al., 2014; Yu et al., 2008; Zeng et al., 2015). Generally, plant species share similar and highly functional domains of *LCYB* (Cunningham and Gantt, 1998; Cunningham et al., 1996). As the genome of *N. benthamiana* is allotetraploid, it has two homologous copies per functional gene. This means that there are two copies of the *LCYB* gene in *N. benthamiana*, *LCYB*-1 and *LCYB*-2. The expression of *LCYB-1* has been shown to be significantly higher in leaf tissue than any other organ of the plant, indicating that its role in photosynthesis and other biological processes lies predominantly in the leaves (Shi et al., 2014).

Recently, our research group developed a CRISPR/Cas9 system for the targeted gene knockout of *LCYB* in *N. benthamiana* and grapevine. Mutations of this gene by Cas9 in *N. benthamiana* produced a lethal knockout phenotype in a portion of the transgenic T0 progeny and molecular analyses confirmed a significant reduction in *LCYB* expression, accordingly. Based on this, the *LCYB* transcript was chosen as the target of interest for this study to investigate the CRISPR/Ca13a-mediated cleavage of the cellular RNA in *N. benthamiana*, instead of DNA. Discussed here are the results from the experiments that were conducted, followed by suggestions for future research.

First, two targets both positioned at the 5'-end of the transcript were selected, based on the low off-target scores they obtained according to the target design strategies. Binary Cas13a vectors containing each crRNA were assembled and used for stable *Agrobacterium*-mediated transformations (Table 3.2). Interestingly, the regenerated transgenic plants were phenotypically indistinguishable from the wild-type plants, apart from a portion of plants that showed a retardation in growth. However, this could be a result of the efficiency of the plant regeneration protocol, such as the *in vitro* growth conditions or the antibiotic and phytohormone concentrations in the selection medium (Bidabadi and Mohan Jain, 2020; Hazarika, 2006). Subsequently, gene expression levels of *LCYB* were evaluated by RT-qPCR and initially a select number of independent plants from the transgenic lines presented a potentially significant reduction of *LCYB* expression when compared with the control. However, this observation did not translate to a statistically significant difference in *LCYB* expression once the transgenic lines were each compared with the control group (Figure 3.6). This discrepancy could be attributed to the variation in gene expression observed across the control samples, which in turn affected the mean relative expression of the control group.

In eukaryotic cells, mRNAs mature in the nucleus and are also exported to the cytoplasm for their translation to proteins. Therefore, Experiment B was conceptualised to determine if the localisation of the assembled LwaCas13a constructs to either the nuclear or cytoplasmic cellular compartments would affect the RNA cleavage efficiency of our Cas13a binary constructs. It has been primarily demonstrated in mammalian cell-based applications that the fusion of a nuclear localisation signal to the Cas13 protein results in moderately greater efficiencies of endogenous RNA knockdown, rather than nuclear export signals (Abudayyeh et al., 2017; Konermann et al., 2018; Wessels et al., 2020). Based on this research, the LwaCas13a/NLS plant lines were hypothesised to demonstrate a higher level of *LCYB* transcript knockdown efficiency than the LwaCas13a/NES plant lines. Using Gibson assembly, both NLS and NES fusions were made to the existing LwaCas13a_T1 construct and used for *Agrobacterium*-mediated transformations of *N. benthamiana*. The preliminary gene expression analyses by RT-qPCR indicated a reduction that equated to two-fold or lower in *LCYB* transcript levels in the independent transgenic plants NES1, NLS1 and NLS4, each transformed with the LwaCas13a/NES and LwaCas13a/NLS constructs, respectively. These transgenic plants were therefore propagated in triplicate and the results from the gene expression analysis by RT-qPCR on these plant lines confirmed a significant two-fold reduction in the level of *LCYB* expression in NES line 1, while the two NLS plant lines 1 and 4 did not differ significantly from the control group. The result for NES line 1 is in accordance with two studies that demonstrated the inhibition of *LCYB* expression in RNAi tobacco plants, which both presented silencing efficiencies ranging from 50%–70% in their RNAi

transgenic lines (Kössler et al., 2021; Shi et al., 2015). Similarly, a post-transcriptional silencing strategy in wheat reported a reduction in *LCY*B expression between 70% and 84% (Zeng et al., 2015).

To determine whether the regulation of the *LCYB* transcript levels in the selected NES and NLS transgenic lines controlled the differential accumulation of total carotenoid content in the leaf-tissues, a preliminary measurement was obtained (Figure 3.9). The transgenic line NES 1, which presented the most significant reduction in *LCYB* gene expression, showed a reduced level of total carotenoid content. Although the observed reduction is not statistically significant and is considered a preliminary result due to the low number of biological replicates, it can be speculated that a suppression in *LCYB* gene expression was responsible for an overall decrease in carotenoid accumulation in this line. This is consistent with studies that used various strategies to modulate the levels of either of the two cyclases, *LCYB* or *LCYE*, to control carotenoid content (Diretto et al., 2006; Moreno et al., 2013; Yu et al., 2008; Zeng et al., 2015). It is important to note however that carotenoids such as lycopene and α-carotene or lutein are direct substrates or products, respectively, of *LCYB*, and often because *LCYB* works synergistically with other genes to control carotenoid biosynthesis, the accumulation of these downstream and upstream carotenoids is often reported (Bai et al., 2009; Moreno et al., 2013). This can possibly be explained by a flux in the metabolic pathway that is compensated for by the activity of other enzymes that are not affected by the reduced expression of *LCYB*. To further investigate the feedback mechanism in the regulation of the carotenoid pathway, a robust method that allows for detailed carotenoid separation and quantification, such as high-performance liquid chromatography (HPLC), would be essential.

Therefore, when comparing the RNA targeting abilities of the nuclear-localised and the cytoplasmic-localised variants (LwaCas13/NLS and LwaCas13a/NES) based on the RT-qPCR results, the NES-variant appears to have induced a better down-regulation of *LCYB* transcript accumulation. This finding is however limited in sample size and in order to obtain a better statistical representation, more transgenic lines per construct would need to be analysed. To further ascertain if the varying levels of *LCYB* expression correlate with carotenoid accumulation levels, the carotenoid and chlorophyll content should be quantitatively estimated using more biological replicates and more transgenic lines per construct. Nevertheless, the preliminary RT-qPCR analyses did show a decrease in *LCYB* expression in a subset of the NLS transgenic plants, suggesting that subcellular localisation may actually be independent from the catalytic activity of the Cas13a construct. For LwaCas13a, this result is consistent with a previous study in *Drosophila* (Huynh et al., 2020).

RNAi-induced silencing studies have often used enzymes that catalyse carotenoid biosynthesis, such as PDS, as common target genes to provide an easily detectable phenotype for the monitoring of RNAi effectivity, where an inverse correlation between target mRNA levels and the severity of RNAi

phenotypes are reported (Wang et al., 2005). Indeed, this type of marker has also been used for the perceptible affirmation of genome editing in several plant species, as established by our research group in *N. benthamiana* whereby CRISPR/Cas9-mediated precise targeting of the *LCY*B gene resulted in a clear photobleached phenotype. Interestingly, the Cas13a transgenic lines from both Experiment A and B of this study predominantly showed a wild-type phenotype. One possibility to explain this observation could be that the reduction in mRNA abundance of *LCYB* was not significant enough to translate to result in a detectable phenotype, suggesting a potential threshold for *LCYB* expression levels. Furthermore, reduced *LCYB* expression in RNAi tobacco lines is reported to negatively affect a multitude of factors, such as plant physiology and development, primary and secondary metabolism, photosynthetic efficiency, and ultimately plant biomass (Kössler et al., 2021). As some Cas13a transgenic lines were visibly retarded in growth, a detailed analysis of these aforementioned factors would provide a stronger conclusion for the origin of the phenotype.

The observation that few transgenic plant lines from both Experiment A and B produced lower levels of *LCYB* expression may be explained by several factors. The first being the accessibility of the target due to secondary structures. As RNA acquires secondary structure inside cells, the double-stranded regions are inaccessible to the crRNA and Cas13-mediated cleavage occurs extensively at single-stranded regions. *In vitro*, Cas13 has been shown to selectively cleave near exposed regions of the target RNA (Abudayyeh et al., 2016; East-Seletsky et al., 2017), thereby limiting the *in vivo* cleavage efficiency to predicted secondary structures. In bacteria and mammalian cells, spacers located on the transcript with low secondary structure resulted in a greater knockdown of the target RNA (Abudayyeh et al., 2017; Smargon et al., 2017). These associations are an indication that targeting regions with substantial base pairing may reduce the efficiency of RNA knockdown. Therefore, there is still some uncertainty around guide RNA design for the Cas13 family of nucleases and it is extremely important to consider the secondary structure of target transcripts (Bandaru et al., 2020; Wessels et al., 2020). It can be postulated that the fact that secondary structure was not accounted for during crRNA target design may have contributed to the low editing efficiency by Cas13a in this study. When designing crRNAs, computational tools such as RNAfold (http://rna.tbi.univie.ac.at/cgi-bin/RNAWebSuite/RNAfold.cgi) can provide folding structure predictions to narrow the target region spaces. Moreover, the web tool CHOPCHOP now includes support for CRISPR/Cas13a-based gRNA target design, by implementing searches for off-targets on complete transcriptomes and calculating the predicted secondary structures in the transcript at a specific gRNA target site using RNAfold (http://chopchop.cbu.uib.no/; Labun *et al.*, 2019). After optimising target design, different modalities of crRNAs can be assayed to enhance specific targeting.

Beyond target design, another aspect to consider is how Cas13 subtypes can differ in functionality and/or activity in different model systems. For plant applications, LwaCas13a is the only variant to have been tested for a targeted knockdown of endogenous RNA (Abudayyeh et al., 2017). Alternatively, LwaCas13a, PspCas13, and RfxCas13d have all been demonstrated to achieve robust knockdown across numerous genes in mammalian cells (Abudayyeh et al., 2017; Cox et al., 2017; Konermann et al., 2018). Although RfxCas13d is currently the most robust variant for RNA virus interference in plants (Mahas et al., 2019), it remains to be tested for its ability to target an endogenous mRNA transcript. Furthermore, due to the ability of Cas13 to process its own pre-crRNA (East-Seletsky et al., 2016), a multiplexed delivery of crRNAs can provide additive effects on gene knockdown as several mRNAs involved in a single pathway can be simultaneously targeted.

The occurrence of chimeric transgenic plants has been reported in many herbaceous and woody species, including tobacco (Schmülling and Schell, 1993), potato (Rakosy-Tican et al., 2007), soybean (Christou, 1990), apple (Malnoy et al., 2010) and grapevine (Costa et al., 2019). The phenomenon of a transgenic chimera is proposed to form during shoot organogenesis, where a shoot emerges from a group of transformed or untransformed cells. Additionally, chimeras and “escapes” (or non-transgenics) may result from the ineffectiveness of a selective agent in the regeneration medium or the protection of transformed cells that surround non-transgenic cells, during the early stages of regeneration (Ding et al., 2020; Faize et al., 2010). As a result, regenerated plants would possess chimeras of the introduced CRISPR components, for example. Although chimerism is more common in plant species that give a recalcitrant response to genetic transformation and *in vitro* regeneration, it is important that transgenes remain stably expressed in any plant transformation experiment for the downstream molecular analyses (Gelvin, 2017). To eliminate this possibility, future expansions could look to modifying the concentration of kanamycin in selection media during the shoot and root regeneration stages and to conduct molecular analyses on T1 generation plants. By optimising the transformation and regeneration protocol, this would also rectify and reduce the occurrence of abnormal phenotypes of putative transgenic plants. Furthermore, the use of secondary embryogenesis, a phenomenon wher

eby new somatic embryos are induced through somatic embryos, is favoured for some plant transformations because if single transformed cells are cultured for a sufficient length of time, then all the cells (and plants) derived from that single cell will contain identical genetic material.

CHAPTER 4: RNA virus inhibition in *Nicotiana benthamiana* using a CRISPR/Cas13a system

4.1 INTRODUCTION

The majority of known plant viruses possess single-stranded positive-sense RNA genomes. Examples of economically important families from this group of viruses include *Potyviridae, Closteroviridae* and *Bromoviridae* (Matthews, 1998). They are renowned for their ability to evolve quickly and generate high genetic variability, a result of their rapid replication and high mutation rates (Chare and Holmes, 2006; Rubio et al., 2020). These highly diverse phytopathogens cause severe losses in agricultural crops and pose a threat to global food security (Sastry and A. Zitter, 2014). Their ability to develop evading mechanisms against host defences means they are often non-responsive to prophylactic measures and a broad-spectrum and durable mode of resistance is therefore required.

In the context of CRISPR/Cas discoveries, the class 2 type II CRISPR/Cas9 system of *Streptococcus pyogenes* was the first prokaryotic immune system to be harnessed for its ability to target genomic DNA (Jinek et al., 2012). The impressive genome editing applications that followed thus forth encouraged researchers to exploit the CRISPR/Cas9 technology for antiviral defence strategies against eukaryotic viruses. In plants, effective viral interference strategies against a range of single-stranded DNA viruses, predominantly from the *Geminiviridae* family, have been demonstrated (Ali et al., 2015a, 2016; Baltes et al., 2015; Tripathi et al., 2019; Yin et al., 2019). Nevertheless, this left a research gap for the targeting of pathogens with RNA genomes using CRISPR/Cas technology, especially considering that RNA viruses are the most common form of plant viruses and several plant DNA viruses contain an RNA intermediate during a stage of their replication cycle**.**

Thanks to numerous studies, systems capable of selective recognition and/or cleavage of RNA molecules have been discovered. Class II type VI CRISPR/Cas systems are RNA-guided and are currently the only CRISPR/Cas effectors known to solely target single-stranded RNA (Abudayyeh et al., 2016; Smargon et al., 2017). All type VI loci include a single effector protein called Cas13, formerly known as C2c2, that utilises a crRNA guide to achieve RNA interference. A distinct feature of the Cas13 effector is the presence of two higher eukaryotic and prokaryotic nucleotide-binding domains (HEPN) that drive the RNase activity needed for RNA degradation (Liu et al., 2017b). A separate nuclease activity in Cas13 is responsible for catalysing the processing of precursor crRNA into mature crRNA (East-Seletsky et al., 2016). Based on the phylogeny of the Cas13 effector-complexes, the Type IV family consists of four known subtypes (A, B, C, and D) (Konermann et al., 2018; Shmakov et al., 2017; Smargon et al., 2017).

LshCas13a was the first Cas13 orthologue to be characterised and harnessed for programmable RNA-targeting activities, which expanded the application of CRISPR/Cas systems from DNA to RNA-based cleavage in plants (Abudayyeh et al., 2017). For instance, LshCas13a with a crRNA targeting viral RNA sequences of the turnip mosaic virus (TuMV) exhibited rapid and effective RNA interference in both *N. benthamiana* and *A. thaliana* plants (Aman et al., 2018a, 2018b). Similarly, effective resistance to rice stripe mosaic virus (RSMV) and southern rice black-streaked dwarf virus (SRBSDV) in rice plants transformed with a CRISPR/Cas13a system specifically targeting genomic RNA was also shown (Zhang et al., 2019b). Transgenic potato plants expressing LshCas13a/crRNA constructs targeting multiple strains of potato virus Y (PVY) confirmed the effectiveness of the system in interfering with viral infection (Zhan et al., 2019). The latest protein of Cas13 to be characterised and classified into the type VI-D effector is Cas13d (CasRx) (Konermann et al., 2018). Recently, researchers found that Cas13d showed greater interference activity over other Cas13 variants, LwaCas13a and PspCas13b, when it was used in transient assays to interfere with a TMV and TuMV GFP-expressing virus in *N. benthamiana* plants (Mahas et al., 2019).

Using transient assays in *N. benthamiana*, this study therefore aims to elucidate the viral interference activity of the CRISPR/Cas13a platform. To this end, a viral amplicon-based system expressing the GFP gene to serve as a reporter construct was acquired, and a LwaCas13a/crRNA binary vector was assembled to target the GFP reporter gene. The resulting GFP signal intensity allowed virus propagation to be tracked visually and the levels of GFP expression were molecularly quantified to measure the effectivity of the CRISPR/Cas13a system in reducing viral RNA levels.

4.2 MATERIALS AND METHODS

4.2.1 Selection and synthesis of the crRNA target

To assess the interference activity of LwaCas13a against a plant-infecting virus, we obtained the TRBO-GFP infectious clone (Lindbo, 2007) (Addgene; plasmid #80083) to use as a reporter system in a transient assay. Previously demonstrated by Mahas *et al*, Cas13 orthologues with a crRNA targeting the GFP coding sequence of the TRBO-GFP genome mediated effective virus interference (Mahas et al., 2019). Based on the success of their results, we adopted their GFP target for our study.

The crRNA target sequences were ordered and synthesised as ssDNA oligonucleotides with *Bbs*I restriction site overhangs. The oligos were annealed in a reaction consisting of: 1.5 µl of the forward oligo (100 µM), 1.5 µl of the reverse oligo (100 µM), 5 µl of 10x NEB (New England Biolabs, USA) buffer 2.1, and dH_2O to a total volume of 50 µl. The conditions were set as 95°C for 4 minutes, 70°C for 10 minutes and then cooled to room temperature. The annealed oligo was ligated into the *Bbs*I-digested

pjjb308 plasmid (Addgene; plasmid #107699) directly before the gRNA scaffold. The ligation reaction composed of 1 µl of the annealed oligo pair, 0.5 µl of *Bbs*I-digested pjjb30b (20 ng/µl), 2 µl of 10x Ligase Buffer (NEB), 0.05 U/µl T4 Ligase (NEB), and dH_2O to a total volume of 20 µl, and incubated overnight at 4°C. Primers pjjb208_F/R (Table 4.1) were used to confirm the ligation using Sanger sequencing at CAF (Stellenbosch University, SA) and the plasmid was renamed pjjb308_GFP.

Table 4.1 Primers used for cloning, Sanger sequencing and gene expression analysis.

Primer name	Sequence (5'-3')	Tm (°C)	Amplicon length (bp)
pjjb308_F	AGGCCCCTGGGAATCTGAAA	58.7	341
pjjb308_R	GGTGACGCAGGTGATGAAAAG	56.5	
TC430	GTTGGATCTCTTCTGCAGCA	55.0	820
M13F	GTAAAACGACGGCCAGT	52.6	
NLS/NES_Fcheck	ACCAACAAAATACGCCCATC	59.7	N/A
NLS/NES_Rcheck	TGTCGGGGATCTTCTCAATC	56.3	
ubi3bent_F	GCCGACTACAACATCCAGAAGG	57.6	142
ubi3bent_R	TGCAACACAGCGAGCTTAACC	58.3	
TRB0-GFP qPCR-F	CCAGACAACCATTACCTGTCG	55.5	121
TRB0-GFP qPCR-R	GCTCATCCATGCCATGTGTA	55.2	
APR_F	CATCAGTGTCGTTGCAGGTATT	55.3	107
APR_R	GCAACTTCTTGGGTTTCCTCAT	55.6	
Cas13_qPCR-F	ATCAAGCGGATCTTCGAGTACC	56.5	102
Cas13_qPCR-R	GTAGTTGTACTTGCCGCAGTTC	56.1	
GFP_RT-F	AACAGGTAGTTTTCCAGTAGTGCA	56.2	101
scaffold_RT-R	CGACTCGGTGCCACTTTTTC	56.6	

4.2.2 Construction of LwaCas13a/crRNA plasmids

The pjjb308_GFP plasmid was included in a one-step Golden Gate assembly reaction comprised of three other plasmids: intermediate module vectors pjjb296 and pMOD_C0000, and the transformation backbone pTRANS_220d (Addgene; plasmids #107691, #91081 and #91114, respectively). To assemble a control plasmid, the pjjb308 plasmid with no crRNA was included for the same aforementioned reaction. The reactions were setup as described by Čermák *et al* (2017) with 75 ng/µl pTRANS_220d, 150 ng/µl pjjb296, 150 ng/µl pMOD_C000, 150 ng/µl pjjb308_GFP/EMPTY, 0.8 µl *Aar*I oligonucleotide (0.5 µM) (Thermo Scientific, USA), 1 µl *Aar*I enzyme (2 U/µl) (Thermo Scientific, USA), 0.05 U T4 DNA Ligase (NEB), 2 µl 10x T4 DNA ligase buffer, and dH_2O for a total volume of 20 µl. The PCR cycle was set to: 10 x (37°C/5 min + 16°C/10 min) + 37°C/15 min + 80°C/5 min + 4°C hold and

the final plasmids were confirmed by Sanger sequencing at CAF (Stellenbosch University, SA) using primers TC430 and M13F (Table 4.1). The final plasmid map is provided in Supplementary Figure 2.

Subsequently, the modified plasmids were renamed LwaCas13a_GFP and LwaCas13_EMPTY and linearised with restriction enzymes *BamH*I and *Hind*III-HF to remove the LwaCas13a sequence (New England Biolabs, USA). Using primers designed for Gibson cloning and Phusion DNA polymerase (New England Biolabs, USA), the LwaCas13a_NES fragment was amplified from the plasmid pC0056 (Addgene plasmid #105815). PCR conditions were set as follows: 98°C/30 sec + 35 × (98°C/10 sec + 67°C/30 sec + 72°C/2:30 min) + 72°C/5 min + 4°C hold. The digested backbone and PCR products of the desired size were purified from a 0.8% (w/v) agarose gel using the Zymoclean Gel DNA Recovery Kit (Zymo Research, USA). The purified vector and insert were mixed and assembled with the NEBuilder Hifi DNA Assembly Kit (New England Bioloabs, USA) according to the manufacturer's protocol. The resulting vectors were confirmed by Sanger sequencing using primer pair NLS/NES_check (Table 4.1) and named LwaCas13a_NES/GFP and LwaCas13_NES. The final plasmid map is provided in Supplementary Figure 3.

4.2.3 Agro-infiltration of *N. benthamiana* plant material

The constructs LwaCas13a_NES/GFP and LwaCas13a_NES were individually electroporated into *A. tumefaciens* strain EHA105, while the infectious clone TRBO-GFP (Lindbo, 2007) (Addgene; plasmid #80083) was electroporated into *A. tumefaciens* strain GV3101. Single colonies were grown overnight (28°C, 250 rpm shaker) in 10 ml LB media containing 50 µg/ml kanamycin and 50 µg/ml rifampicin, and subsequently centrifuged at 4000 rpm for 15 minutes at room temperature. The cultures were re-suspended with infiltration buffer (10 mM MES [pH 5.6], 10 mM MgCl2, and 200 µM acetosyringone) to a final OD_{600} of 0.5-1.0 for constructs LwaCas13a_NES GFP and LwaCas13a_NES EMPTY and 0.007 for TRBO-GFP. The cultures were incubated for 4 hours in the dark at room temperature and thereafter mixed at a 1:1 ratio. Four-week-old wild-type *N. benthamiana* plants grown under long-day conditions (16-h light, 8-h dark at 25°C) were used for infiltration of the underside of three leaves per plant with a 5 ml needleless syringe.

4.2.4 GFP imaging

The infiltrated plants were kept in a growth chamber (16-h light, 8-h dark at 25°C) and GFP expression was observed and photographed at three/four days post-infiltration using a hand-held UV light. To quantify the GFP signal intensity in the images from the half-leaf infiltrations, the mean pixel values of the 32-bit greyscale-converted images were analysed using the ImageJ software (http://imagej.nih.gov/ij/). For each leaf, the GFP signal intensity was calculated as the corrected total cell fluorescence (CTCF) using the formula: CTCF = integrated density – (selected area × mean

fluorescence of background readings). The CTCF values were averaged from the biological replicates and normalised to the average CTCF values of the control samples.

4.2.5 RNA extraction and cDNA synthesis

The infiltrated leaf material from each plant was harvested and pooled together before being frozen in liquid nitrogen. The frozen tissue was ground to a fine powder in liquid nitrogen with a sterile mortar and pestle and stored as 100-200 mg aliquots at -80°C. Total RNA from the ground leaf tissue was extracted with the Spectrum™ Plant Total RNA Kit (Sigma, USA), as per the manufacturer's instructions, and the samples were eluted in 40 µL dH_2O. The RNA integrity and purity was evaluated using agarose gel electrophoresis and spectrophotometry (Nanodrop 2000; Thermo Scientific, USA). One microgram of total RNA was DNase-treated with RQ1 RNase-Free DNase (Promega, USA) according to the manufacturer's instructions. First-strand cDNA was synthesised from the DNase-treated RNA using random hexamer primers (Promega, USA) and Maxima Reverse Transcriptase (Thermo Scientific, USA) in a final volume of 20 µL according to the manufacturer's protocol. The integrity of the resulting cDNA was assessed by end-point PCR using the primer set *Ubi3* (Table 4.1) for the housekeeping gene ubiquitin (Genbank accession AY912494.1). PCR cycle parameters were set as: 95°C/3 min + 35 x (95°C/30 sec + 55°C/30 sec + 72°C/30 sec) + 72°C /5 min + 4°C hold. The PCR products were resolved on a 2% (w/v) agarose gel and visualised by ethidium bromide dye staining (Thermo Scientific, USA).

4.2.6 Reverse transcription (RT)-PCR: transgene expression assay

Expression of LwaCas13a and the GFP-targeting crRNA was analysed by RT-PCR. Primers Cas13_qPCR-F and Cas13_qPCR-R were used to amplify LwaCas13a and primers GFP_RT-F and scaffold_RT-R were used to amplify the crRNA and scaffold fragment (Table 4.1). The thermal cycling conditions were set as follows: 95°C /3 min + 35 × (95°C/30 sec + 55°C/30 sec + 72°C/30 sec) + 72°C/5 min + 4°C hold. The PCR products were resolved on a 1.8% (w/v) agarose gel and visualised by ethidium bromide dye staining (Thermo Scientific, USA).

4.2.7 Quantitative RT-PCR (RT-qPCR) expression analysis

All RT-qPCR reactions were performed in 10 µl final volumes using the PowerUp™ SYBR™ Green Master Mix (Applied Biosystems, USA) with 40 ng cDNA and 1.5 µl per primer (2.5 mM). The reactions were setup in a 96-well plate with three technical replicates for each biological replicate, while the Adenine phosphoribosyltransferase like (*APR*) housekeeping gene was selected as an internal control. The qPCR primer pairs are listed in Table 4.1. The PCR was performed on a QuantStudio™ 3 Real-Time PCR System (Applied Biosystems, USA) and the comparative CT (ΔΔ CT) method was selected. The

standard cycle parameters were set up as follows: 50°C/2 min + 95°C/2 min + 40 x (95°C/15 sec + 60°C/1 min) and the melt curve parameters were set as default by the software. The relative levels of gene expression, compared with reference samples, were calculated using the $2^{-\Delta\Delta Ct}$ method (Livak and Schmittgen, 2001) and analysed using the Thermo Fischer Design and Analysis app. Error bars represent 95% confidence intervals.

4.2.8 Statistical analysis

For statistical analyses of relative gene expression and GFP fluorescence intensity, the two-tailed unpaired Student's t-test was computed using the Prism GraphPad software Version 8.3.0 (GraphPad Software, USA) to compare each test group to the respective control group. All data are represented as the mean ± standard error of the mean (SEM) of a minimum of five biological replicates per plant line. Determination of significance was set as $p \leq 0.05$.

4.3 RESULTS

4.3.1 Assembly of the LwaCas13a construct and infiltration setup

In order to assess the interference activity of a Cas13a construct against a plant-infecting RNA virus, a transient experimental setup with a visual reporter system was selected (Figure 4.1 A). The selected reporter system, TMV RNA-based overexpression system (TRBO-GFP), is a tobacco mosaic virus infectious clone that has been modified by replacing the coat protein-encoding sequence with a GFP-encoding sequence so that it cannot move systemically in an infected plant, but it can express the GFP protein and continue to replicate efficiently as usual (Lindbo, 2007). In order to visualise the inhibition of viral infection, a crRNA targeting the GFP coding sequence of the TRBO-GFP genome was adopted from Mahas *et al*, as they demonstrated successful CRISPR/Cas13a-mediated interference with the crRNA both phenotypically and molecularly (Mahas et al., 2019). The GFP target sequence is shown in Figure 4.1 B.

Given that TMV is a positive-sense single-stranded RNA virus, replication and assembly occurs in the cytoplasm of host plant cells (Lindbo, 2007; Liu and Nelson, 2013). In accordance, the selected crRNA was assembled into a binary vector harbouring the LwaCas13a gene fused with a NES tag (Figure 4.1 C). The LwaCas13a_NES/GFP construct and TRBO-GFP infectious clone was co-delivered into wild-type *N. benthamiana* leaves via *Agro*-infiltration. As a control, a LwaCas13a_NES construct that does not harbour any crRNA was included. For both experiments, the plants co-infiltrated with TRBO-GFP and the control LwaCas13a_NES were labelled 1.1-1.5, while the plants co-infiltrated with TRBO-GFP and LwaCas13a_NES/GFP were labelled 2.1-2.5.

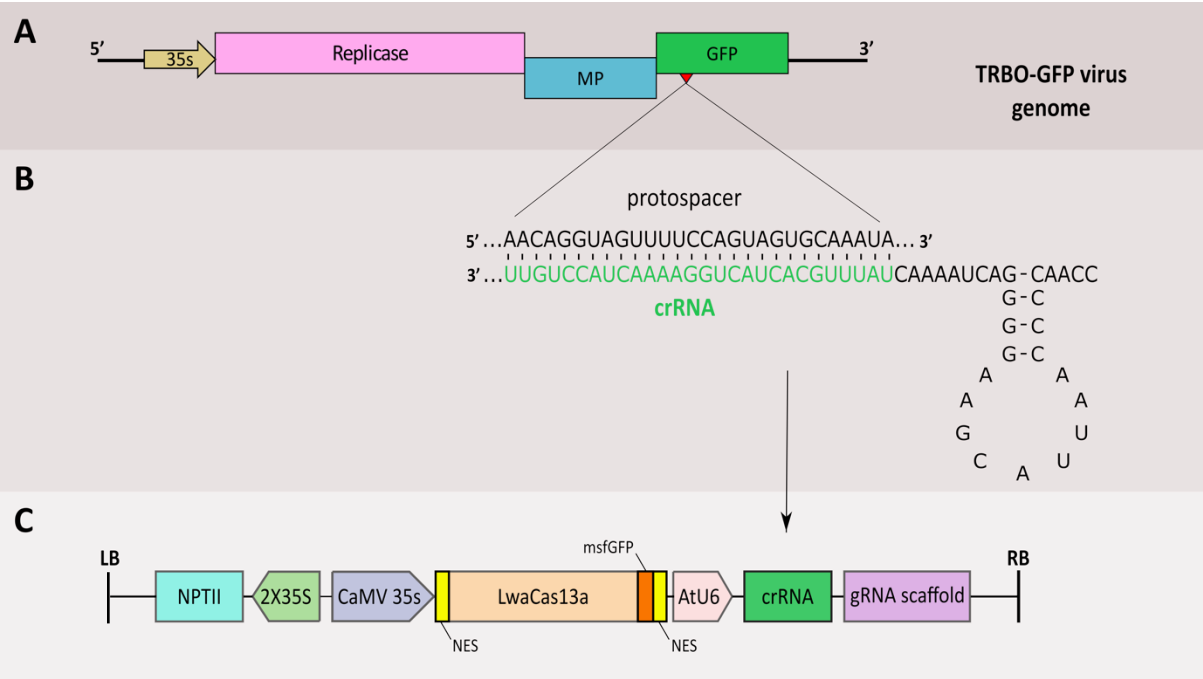

Figure 4.1 Schematic representation of the selected crRNA and the construct it was assembled into. (**A**) The TRBO-GFP virus genome represented by the main ORFs of the T-DNA region. 35S, CaMV duplicated 35s promoter; Replicase, TMV 126K/183K ORF; MP, movement protein; GFP, green fluorescent protein. (**B**) The protospacer sequence and the corresponding crRNA of the selected target candidate. The approximate position of the target is shown by the red arrow on the TRBO-GFP virus genome. The stem-loop sequence is obtained from Abudayyeh *et al* (2016). (**C**) The crRNA was cloned under the Arabidopsis U6-26 (AtU6) promoter in the T-DNA region of the final LwaCas13a binary vector. The CaMV_35s promoter is responsible for the expression of LwaCas13a. NLS, nuclear localisation sequence; NES, nuclear export signal; msfGFP, monomeric superfolder GFP. LB, left border; RB, right border.

4.3.2 Phenotypic and molecular analysis: experiment 1

After three days post-infiltration, the green fluorescence was observed in the inoculated leaves with a UV light. Notably, the GFP fluorescence in some of the leaves inoculated with LwaCas13a_NES/GFP was moderately weaker than those of the control plants (Figure 4.2).

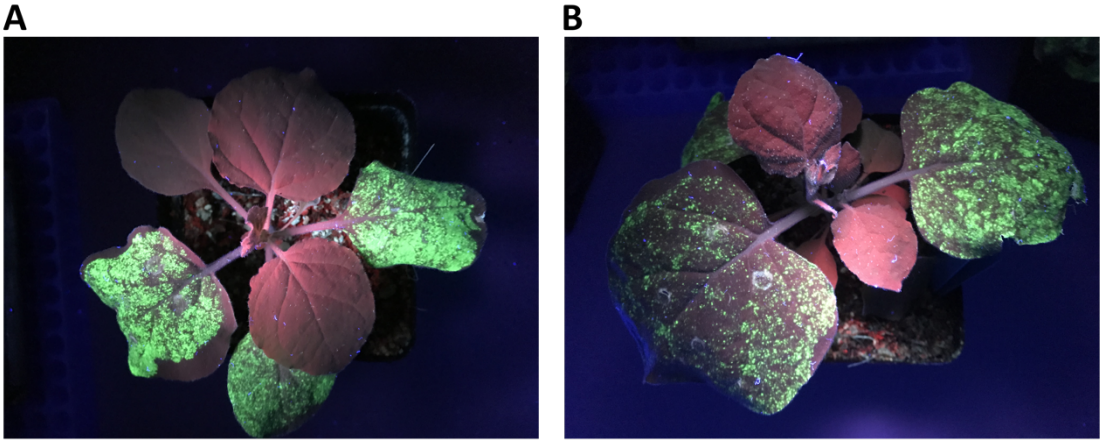

Figure 4.2 GFP fluorescence of a wild-type *N. benthamiana* plant transiently expressing (**A**) TRBO-GFP & LwaCas13a_NES and (**B**) TRB0-GFP & LwaCas13a_NES/GFP. Images were taken three days post-infiltration.

The infiltrated leaves were collected for RNA extractions and successful cDNA synthesis was confirmed by a *ubiquitin* PCR (Supplementary Figure 8). In order to ascertain whether LwaCas13a and the GFP-targeting crRNA were expressed in the leaves after infiltration, an RT-PCR was conducted. As expected, the expression of LwaCas13a was confirmed in all samples while the expression of the crRNA was confirmed in the plants that were infiltrated with LwaCas13a_NES/GFP (Figure 4. 3).

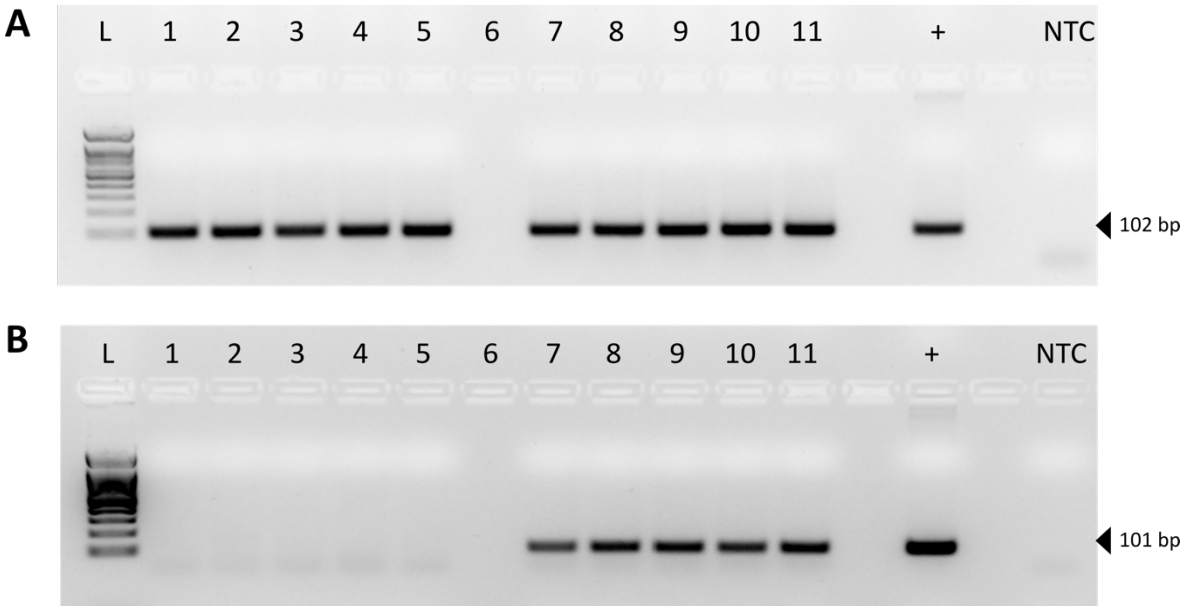

Figure 4.3 RT-PCR analysis to confirm the expression of LwaCas13a (**A**) and the GFP-targeting crRNA (**B**). PCR products are resolved on a 2% (w/v) agarose gel. Lanes 1- 5: samples 1.1-1.5; Lanes 7-11: samples 2.1-2.5. L: 1kb molecular weight marker (GeneRuler, Thermo Scientific); Positive control: LwaCas13a_NES/GFP target plasmid DNA; NTC: No template control.

To accurately assess if this observation (Figure 4.2) was a result of interference against TRBO-GFP, the level of GFP expression in the leaves was quantified using RT-qPCR and normalised with the housekeeping gene *APR*. The results in Figure 4.4 A depict the control samples (labelled 1.1-1.5) that were co-infiltrated with TRBO-GFP and LwaCas13_NES EMPTY and test samples 2.1-2.5 that were co-infiltrated with TRBO-GFP and LwaCas13a_NES/GFP. For samples 2.3, 2.4 and 2.5, the data from the RT-qPCR is partially consistent with the level of GFP signal observed under UV in that they all show a ~2-fold reduction in GFP expression when compared with the reference control sample 1.3. The results also indicate that the level of GFP expression varies significantly between the control samples as samples 1.1 and 1.4 exhibit a much lower expression abundance than samples 1.2, 1.3 and 1.5. However, when samples 1.1-1.5 and 2.1-2.5 are grouped together as biological replicates, no significant reduction in GFP expression is observed when the test group is compared with the control group (Figure 4.4 B).

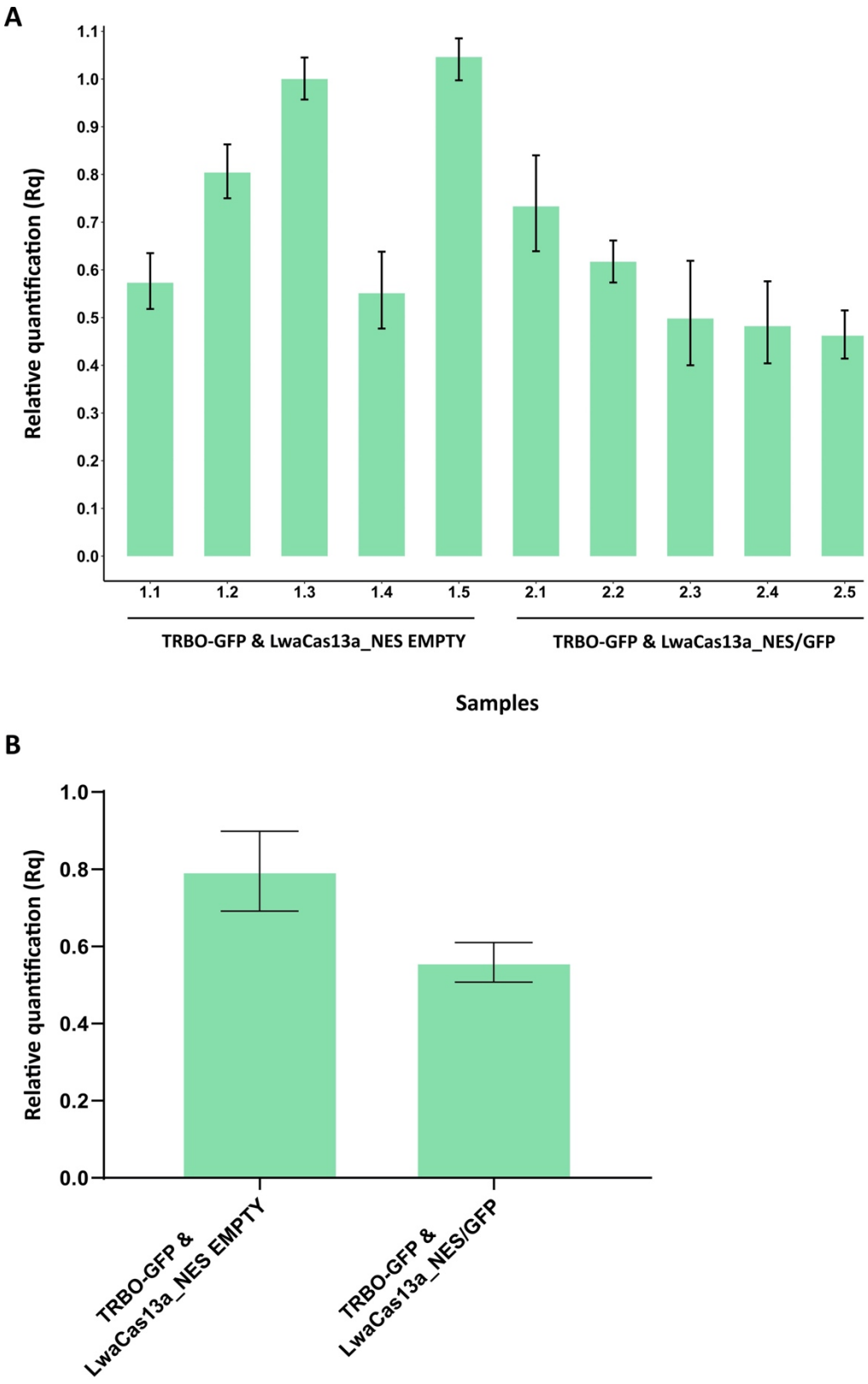

Figure 4.4 GFP expression of TRBO-GFP assessed using RT-qPCR. (**A**) Relative fold expression is normalised to reference sample 1.3 and the error bars represent 95% confidence intervals for n=3 technical replicates. (**B**) Relative quantification values grouped biologically. Data is shown as the mean relative gene expression ± SEM of the biological replicates (n=5). Statistical analysis was performed using the Student's unpaired t-test and significant difference was determined at $p \leq 0.05$ with respect to the control group.

4.3.3 Phenotypic and molecular analysis: experiment 2

According to (Lindbo, 2007), the TRBO-GFP vector expresses GFP in *N. benthamiana* leaves infiltrated with *A. tumefaciens* cells up to a dilution of 1:300 from an OD_{600} reading of 1.0. This means that even very dilute suspensions of the *A. tumefaciens* culture containing TRBO-GFP can be efficiently inoculated in plants and ensure complete infection. Given the results of the first experiment, a second assay was conducted but with slight modifications to two procedures in the methodology. The LwaCas13a_NES constructs were resuspended to higher densities in an effort to provide a more optimal agrobacterial concentration. Once the constructs were co-infiltrated with TRBO-GFP into the *N. benthamiana* leaves, only the area of infiltration that fluoresced under UV light post-infiltration was collected for molecular analyses. This sought to eliminate the non-infiltrated leaf tissue from the analyses, considering that both the LwaCas13_NES constructs and TRBO-GFP do not move systemically. After three days post-infiltration, no GFP fluorescence was observed in any of the plants under the UV light. When visualised four days post-infiltration, the level of GFP fluorescence differed slightly between the two sets of infiltrated plants, with a potential reduction of GFP fluorescence observed in the plants infiltrated with the LwaCas13a_NES/GFP construct (Figure 4.5).

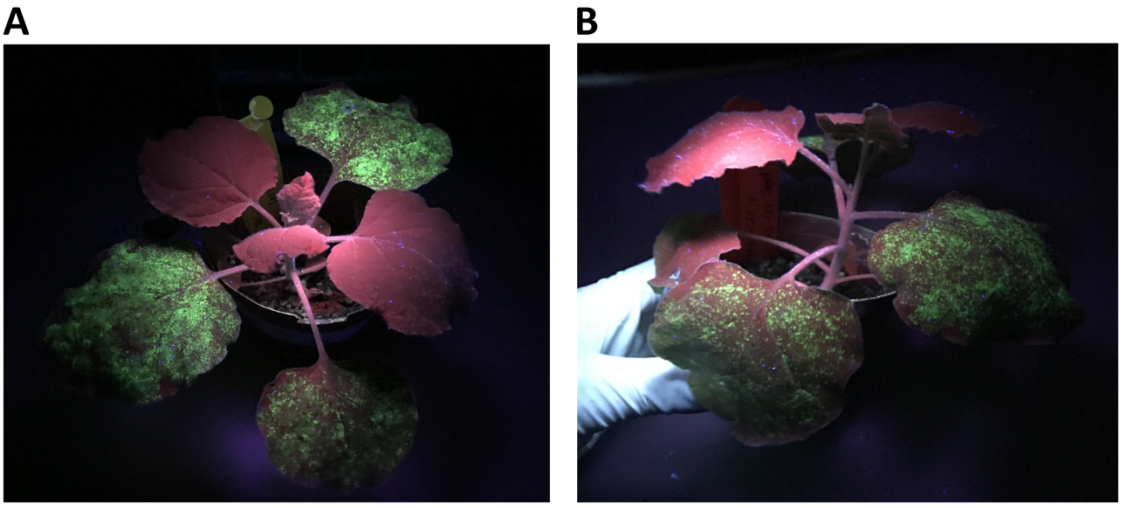

Figure 4.5 GFP fluorescence of wild-type *N. benthamiana* plants transiently expressing (**A**) TRBO-GFP & LwaCas13a_NES and (**B**) TRB0-GFP & LwaCas13a_NES GFP. Images were taken four days post-infiltration.

The infiltrated leaf samples were collected for cDNA synthesis from total RNA extractions and following a cDNA integrity assessment (Supplementary Figure 8), the expression of LwaCas13a and the GFP-targeting crRNA was verified using RT-PCR. Shown in Figure 4.6, the PCR results indicate that these two important transgenes from the constructs are indeed transiently expressed post-infiltration.

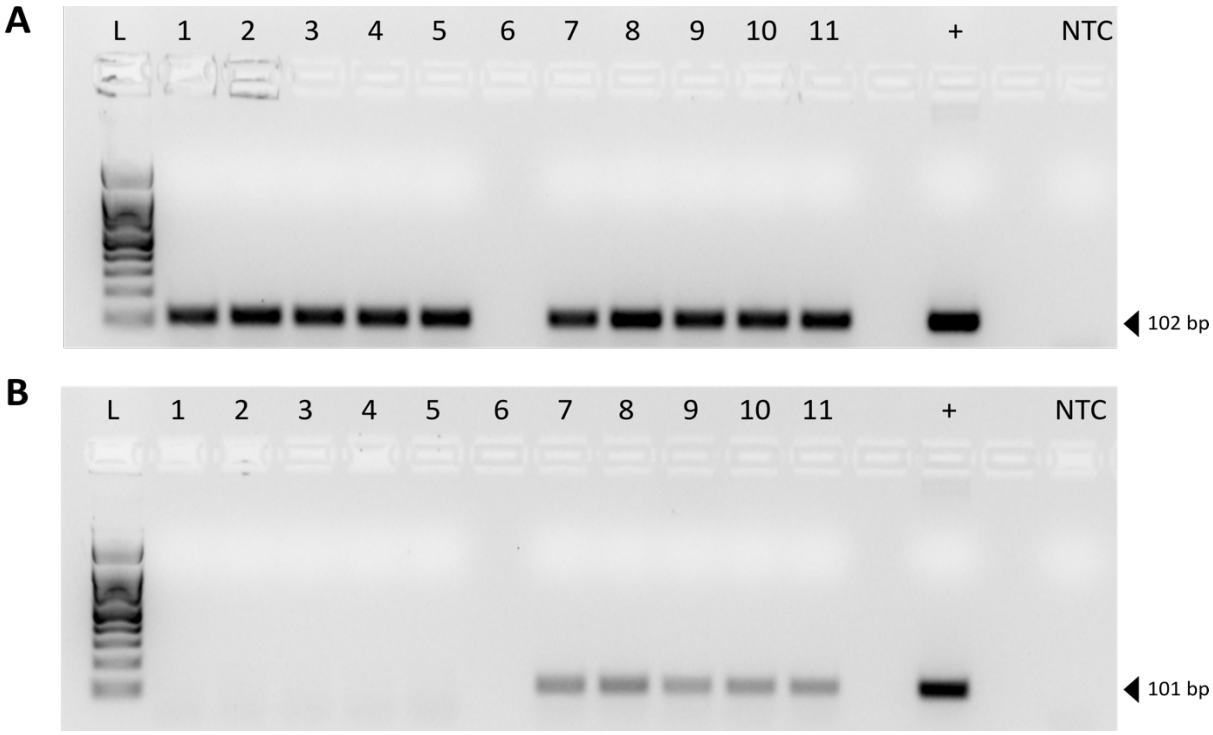

Figure 4.6 RT-PCR analysis to confirm the expression of LwaCas13a (**A**) and the GFP-targeting crRNA (**B**). PCR products are resolved on a 2% (w/v) agarose gel. Lanes 1- 5: samples 1.1-1.5; Lanes 7-11: samples 2.1-2.5. L: 1kb molecular weight marker (GeneRuler, Thermo Scientific); Positive control: LwaCas13a_NES/GFP target plasmid DNA; NTC: No template control.

Subsequently, the level of GFP expression was analysed using RT-qPCR. In Figure 4.7 A, the results show that sample 2.3 may present successful virus interference as it shows a ~2.5-fold reduction in GFP expression when compared with the reference sample 1.4. However, the remaining samples do not indicate a reduction in GFP expression post-infiltration as distinct as sample 2.3. Similar to the previous experiment, the level of GFP expression varies significantly between the control samples, with 1.1-1.3 showing lower levels of GFP expression than 1.4 and 1.5. As a result, test samples 2.1-2.5 that were grouped together biologically do not present any reduction in GFP expression when compared with the control group (Figure 4.7 B).

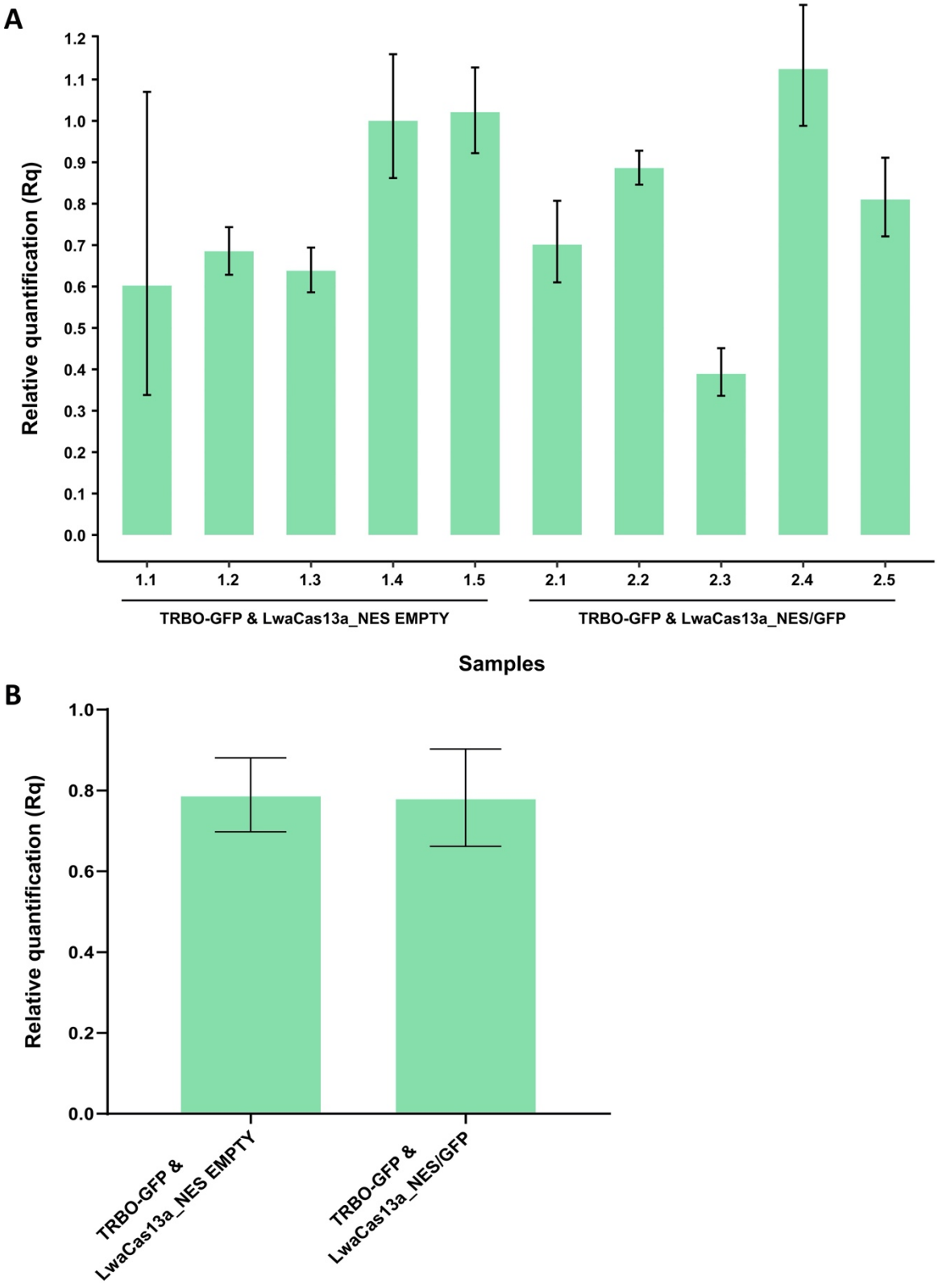

Figure 4.7 GFP expression of TRBO-GFP assessed using RT-qPCR. (**A**) Relative fold expression is normalised to reference sample 1.4 and the error bars represent 95% confidence intervals for n=3 technical replicates. (**B**) Relative quantification values grouped biologically. Data is shown as the mean relative gene expression ± SEM of the biological replicates (n=5).

4.3.4 Evaluation of Cas13a and crRNA expression in selected samples

To investigate potential expression patterns, a selected number of samples from both experiments 1 and 2 that demonstrated varying degrees of GFP expression, were selected for an RT-qPCR analysis that would assess whether the levels of expression of Cas13a and the GFP-targeting crRNA were related to the differing levels of GFP expression that were observed from the previous RT-qPCRs (Figure 4.4 A & Figure 4.7 A). The results show that no apparent relationship exists between GFP expression and the levels of either Cas13a and/or crRNA expression per sample (Figure 4.8). A potential trend can be seen across samples 2.4, 2.5 and 2.6, where plants with lower levels of GFP expression, appear to express the crRNA at a marginally higher level than it does Cas13a. This may attest to the fact that the expression of Cas13a and the crRNA are driven by separate transcriptional regulatory units. When using higher cell densities for the *Agrobacterium*-mediated infiltration, samples 2.6 and 2.7 showed higher levels of Cas13a and crRNA expression compared with the reference sample 2.1.

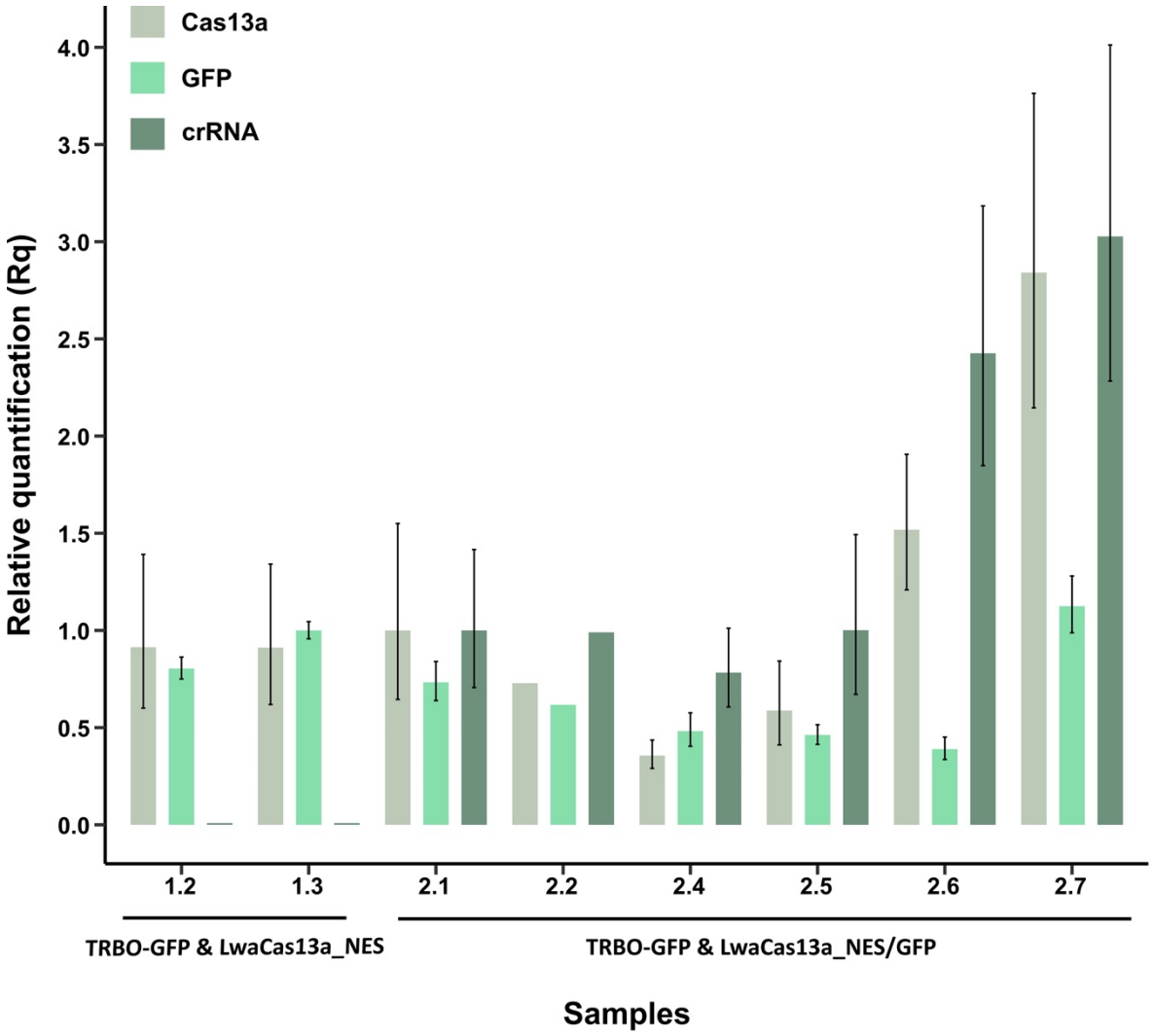

Figure 4.8. RT-qPCR measurement of Cas13a, crRNA and GFP expression. The error bars represent 95% confidence intervals of n=3 technical replicates. Expression is normalised to reference sample 2.1. Samples 1.2,1.3, 2.1-2.5 are from experiment 1 and samples 2.6 and 2.7 are renamed samples 2.3 and 2.4 from experiment 2.

4.3.5 Half-leaf infiltrations

As a means to reduce variation between leaves and quantify GFP signal intensity, a half-leaf *Agro*-infiltration experiment was conducted. The left halves of *N. benthamiana* leaves were co-infiltrated with TRBO-GFP and the control LwaCas13a_NES EMPTY, while the right halves were co-infiltrated with TRBO-GFP and LwaCas13a_NES GFP. At four days post-infiltration, the leaves that showed GFP fluorescence under a hand-held UV light were photographed (Figure 4.9 A). A quantitative evaluation of the GFP signal intensity of these leaf images was conducted (Figure 4.9 B) and by averaging and normalising the values to the control group, an approximate 50% reduction in GFP signal of the leaf-halves infiltrated with the LwaCas13_NES GFP construct was observed (Figure 4.9 C).

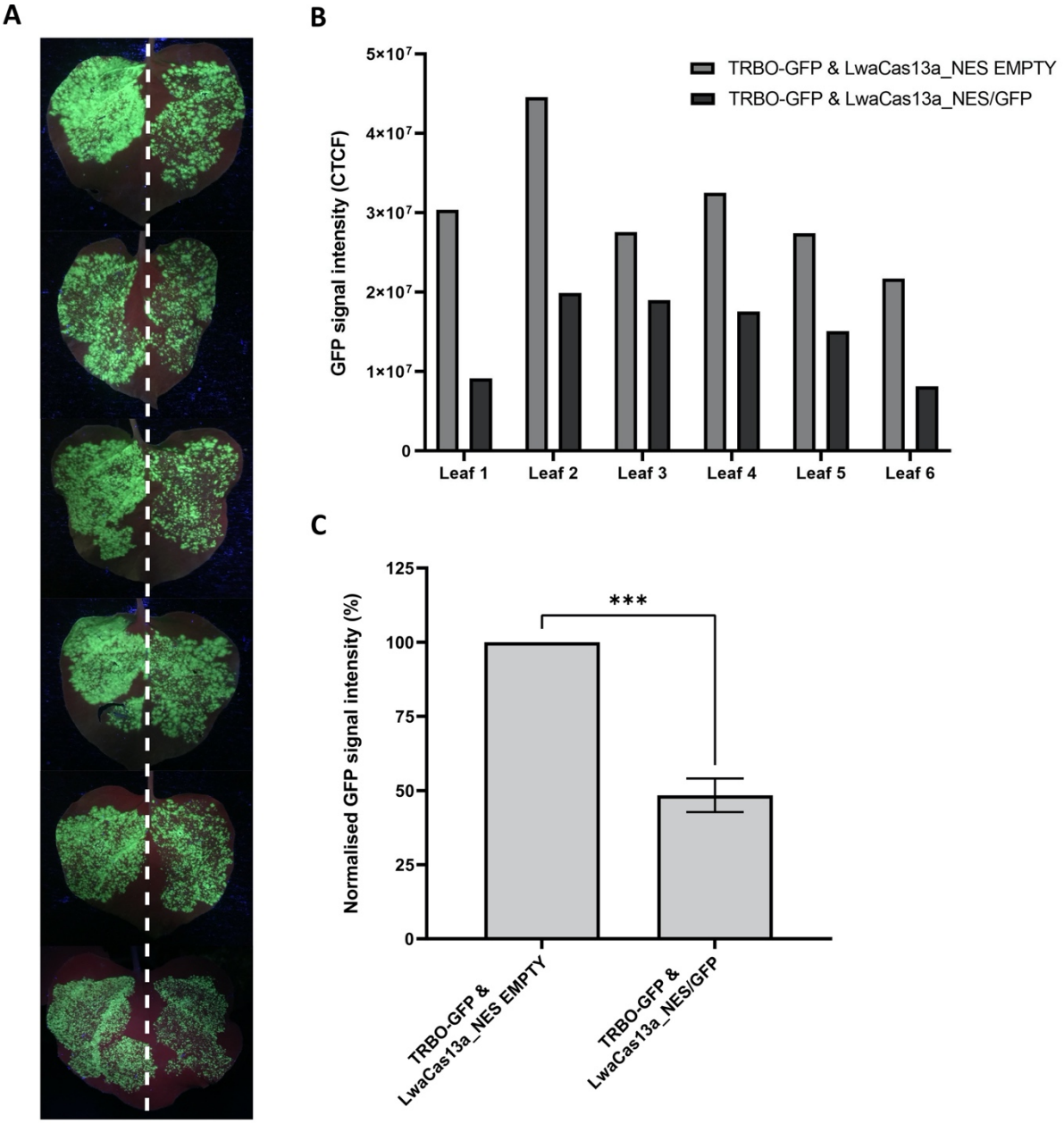

Figure 4.9 GFP fluorescence monitoring of LwaCas13a-mediated virus interference of TRBO-GFP. (**A**) GFP visualisation of the six infiltrated leaves. Left half: TRBO-GFP & LwaCas13a_NES EMPTY (control). Right half: TRBO-GFP & LwaCas13a_NES GFP. Images were taken under UV illumination four days post-infiltration. (**B**) GFP fluorescence intensity quantification of the six infiltrated leaf images. The GFP signal intensity data is shown as CTCF values. (**C**) GFP fluorescence intensity quantification of the infiltrated leaf images. The GFP signal intensity data is shown as a percentile graph and normalised to the average of the control's CTCF values (TRBO-GFP & LwaCas13a_NES EMPTY). Error bars represent $\pm$SEM (n=6) and *** = $p \leq 0.001$ calculated using the unpaired Student's t-test.

4.4 DISCUSSION

In a study by the Mahas group, the researchers comprehensively compared the RNA virus interference efficiency of different Cas13 variants, since prior to their study, LshCas13a was the only Cas13 variant used for RNA virus interference applications in plants (Mahas et al., 2019). Their targets were ssRNA viruses modified to express the GFP reporter gene, the TMV-RNA based overexpression system (TRBO-GFP) and the TuMV-GFP virus. Different crRNAs designed to target different regions of the GFP transcript and other protein-coding sequences of the target viruses were both transiently and systemically expressed in *N. benthamiana* plants using a tobacco rattle virus (TRV)-based viral vector system. Their results indicated that the CasRx variant was the most robust in conferring virus interference against each virus, followed by the LwaCas13a and the PspCas13b, in transient assays, as well as in transgenic plants constitutively expressing the different Cas13 variants. They also highlighted the necessity to fuse either NLS or NES tags to the Cas13 variants, depending on where the effector is required to be localised to, for the targeted cleavage to occur. Based on the findings of Mahas *et al*, the current study adopted the TRBO-GFP reporter system as the interference target and assembled a single binary vector harbouring the LwaCas13a protein flanked by NES sequences and a GFP-targeting crRNA. The construct was therefore used for transient assays in *N. benthamiana* plants, wherein the construct and the TRBO-GFP clone were co-infiltrated.

The results of the first assay, experiment 1, showed that a negligible reduction in the level of GFP expression were observed in three plants (2.3-2.5) infiltrated with the GFP-targeting Cas13a construct when compared with the control group. However, this did not reflect as a statistically significant overall reduction in GFP expression when the two biological groups of the experiment were compared (Figure 4.4). This outcome is contrary to the study by Aman *et al,* where transgenic *N. benthamiana* lines stably expressing LshCas13a, which were co-infiltrated with infectious GFP-expressing TuMV and a TRV-system expressing crRNAs designed to target TuMV-GFP, showed up to a ~50% reduction in GFP signal (Aman et al., 2018a). As the experiment could not confirm a complete viral interference mediated by the CRISPR/Cas13a system, it was repeated with minor modifications. For the second assay, experiment 2, the initial RT-qPCR data suggested that effective viral interference against the TRBO-GFP clone by CRISPR/Cas13a occurred in sample 2.3, as it showed more than a two-fold reduction in GFP expression when compared with the control reference sample. This is however not observed in the rest of the samples, as they presented similar and/or higher levels of GFP expression and consequently no difference in the level of GFP expression between the control group and test group was noted (Figure 4.7). Subsequently, a selected number of samples that showed varying levels of GFP expression from the RT-qPCR analysis of both experiments 1 and 2 were used for the expression analysis of the crRNA, and Cas13a and GFP transcripts. The RT-qPCR was inconclusive as the expression

levels of the three transcripts varied across all the samples and there was no particular relationship between them that could be deduced (Figure 4.8).

Interestingly, the molecular analyses of GFP expression from both experiments did not corroborate the preliminary phenotypic observations. These observations were quantified by the half-leaf infiltration experiment, where a significant two-fold reduction in GFP signal intensity was recorded in the area of the leaves infiltrated with the GFP-targeting Cas13a construct, consistent with the result obtained by the Aman group (Aman et al., 2018a). A possible explanation for this contrariety could be ascribed to the position of the primers designed for RT-qPCR expression analysis of the GFP gene. The GFP-qPCR primers are located at the 5' end of the GFP sequence and the amplicon they produce does span the GFP target sequence selected for the crRNA. This may have an implication in the validation of CRISPR/Cas13a-mediated cleavage of mRNA, as the GFP-qPCR primer set may be persistent in quantifying the cleaved mRNA fragments that are not degraded and overestimate the amount of functional mRNA that is present in the sample (Holmes et al., 2010; Maier et al., 2009). In this case, a clear loss in GFP protein is not reflected in the quantification of mRNA (Yepes-Molina et al., 2020). To eliminate this possible discrepancy, a western blot detection of the corresponding active/mature GFP protein may be more ideal to verify gene knockdown. Indeed, several studies have depended on Western blot analysis either alone, or in conjunction with RT-qPCR analysis, to detect and quantify a virus-expressed GFP protein in transient assays (Aman et al., 2018b; Mahas et al., 2019; Tian et al., 2014; Yu et al., 2020).

The variation in GFP expression levels between individual samples observed from the RT-qPCR results is prominent. A possible explanation for this result may be the difference in levels of transient expression between the TRBO-GFP infectious clone and the Cas13a/crRNA construct in a single leaf (Cody et al., 2017; Li et al., 2013). Furthermore, the physiological state of a *N. benthamiana* test plant is important and within-leaf variation due to differences in sampling spots is reported to affect quantitative assays (Bashandy et al., 2015). This possibility may therefore provide support for the half-leaf agroinfiltration method, as a means to obtain reproducible transient expression data with smaller variations. To investigate further, a RT-qPCR analysis of GFP expression for the half-leaf infiltration experiment is required.

The transgenic *N. benthamiana* line 16C contains a single copy of a transgene encoding GFP, known as mGFP5, meaning the plants accumulate high levels of GFP and their leaves and stems fluoresce green under UV illumination. Given that the crRNA target from this study is position-matched with mGFP5 transcript in the 16C line, meaning the transcript is also a target candidate for the crRNA, the LwaCas13a/crRNA construct was used for infiltration experiments of 16C plants, to visually assess the

RNA-targeting activity of the LwaCas13a vector. While this experiment would be a representation of Cas13-mediated cleavage of an endogenous transcript and not viral RNA, the primary objective was to demonstrate the functionality of the LwaCas13a/crRNA construct. However, these preliminary assessments were inconclusive as the only changes in the phenotype of the 16C plants observed post-infiltration, were signs of necrosis in the infiltrated areas (Supplementary Figure 9). For future expansions, it may be necessary to develop a viral expression vector that is capable of delivering the Cas13a nuclease and crRNA to the 16C plants systemically and enable a high-level expression.

Plant viruses have been used as vectors for a variety of different purposes for some time. Recent developments in genome editing technologies have provoked the use of viral vectors to deliver important genome editing components to a plant cell (Shan-E-Ali Zaidi and Mansoor, 2017). Among these viruses are TRV (Ali et al., 2015b; Ghoshal et al., 2020), TMV (Cody et al., 2017), pea early-browning virus (PEBV) (Ali et al., 2018), and beet necrotic yellow vein virus (BNYVV) (Jiang et al., 2019), which have all been shown to be efficient vectors in delivering small CRISPR/Cas reagents to *N. benthamiana*, *A. thaliana* and *Beta macrocarpa* plants. Virus-mediated gRNA delivery provides a number of advantages compared with the conventional promoter-driven expression of gRNAs, as the rapid replication and systemic spread of the virus ensures effective amplification of the gRNA, while its small genome size allows for multiplexing and simple cloning strategies (Ali et al., 2015c). Using a TRV-based system, the delivery of crRNAs conferring specificity against RNA viruses has been employed for systemic and transient expression in plants, whereby the crRNA is cloned under a PEBV promoter in the TRV-RNA2 genome (Aman et al., 2018a, 2018b; Cao et al., 2021; Mahas et al., 2019).

Single-stranded DNA viruses, typically geminiviruses, have also been modified to carry heterologous coding sequences for increased protein expression in plants (Gil-Humanes et al., 2017; Yin et al., 2015). Interestingly, a recent study found that a geminiviral replicon-based expression vector was more efficient at LwaCas13a-mediated RNA targeting than a regular binary vector in *N. benthamiana*. The study reported a higher accumulation of LwaCas13a and crRNA transcripts in leaves infiltrated with their replicon-based expression vector (Yu et al., 2020). It can therefore be hypothesised that the use of a viral vector for the separate delivery of the crRNA and/or Cas13a components could ensure a more effective expression of the CRISPR/Cas modules and provide a more robust interference of viral RNA. Alternatively, the establishment of transgenic plant lines constitutively expressing the Cas and gRNA components also ensure higher levels of expression than transient assays and have been correlated with a greater viral genome inhibition efficiency (Ji et al., 2015).

Studies that have established resistance against plant viruses generally target conserved regions of the virus genome, namely the coat protein (CP), movement protein (MP) and the replicase gene (Rep), as each of these are involved in crucial stages of virus replication (Mushtaq et al., 2020). In a Cas13

application, four viral genomic regions of TuMV-GFP were targeted: one in the coat protein (CP), one in the helper component proteinase silencing suppressor (HC-Pro) and two in the GFP region. Interestingly, the crRNAs targeting the HC-Pro and GFP sequences were more efficient in mediating interference with TuMV-GFP than the crRNA targeting the CP (Aman et al., 2018a). It is however unknown whether this is a phenomenon specific to TuMV and/or related to the viral vector-based system used to deliver the crRNAs in this study. Given that the coat protein of the TRBO-GFP expression vector was replaced with the GFP gene, viable crRNA(s) could be designed to target various regions of the replicase gene or movement protein (Figure 4.1 A). A suggestion for a future study could be to test if the CRISPR/Cas13a-based targeting of the TRBO-GFP vector differs between crRNAs specific to different target regions of the virus genome. Furthermore, crRNAs designed to target these different viral regions could be used for a multiplexing approach that ensures a higher success of fully attenuating the plant virus. One could also determine whether the GFP-targeting crRNA is effective for the CRISPR/Cas13a-based interference of other viral or transcriptomic targets of interest, given that the GFP target is a match. For example, the LwaCas13a_NES/GFP construct could be used in transient assays that investigate the interference activity against a different infectious clone that harbours a GFP gene.

CHAPTER 5: GENERAL DISCUSSIONS AND CONCLUSION

5.1 Summary of findings

Since it was first characterised, the CRISPR/Cas13 system has been optimised and established in plants for many applications. As its unique and sole function is to cleave an RNA target, CRISPR/Cas13 has been programmed to act as a defence mechanism against RNA viruses. Indeed, this is the most prevalent type of application of CRISPR/Cas13 reported in plants to date (Zhu et al., 2020). Therefore, the purpose of this study was to demonstrate both the CRISPR/Cas13a-mediated down-regulation of an endogenous transcript and the inhibition of an RNA virus in a model plant.

The first research chapter (Chapter 3) of this thesis sought to establish a proof-of-concept for the CRISPR/Cas13a-mediated knockdown of the *LCYB* transcript in the experimental plant *N. benthamiana*. At the time of the assembly of the expression constructs for this study, literature reported the LwaCas13a variant as the most effective Cas13 for robust ribonuclease activity and a plant codon-optimised version was available. To date, the endogenous mRNA targeting activity of CRISPR/Cas13a in plants has only been applied in the context of a transient protoplast transfection assay (Abudayyeh et al., 2017). In contrast, stable transformations of *N. benthamiana* for the constitutive expression of the LwaCas13a gene and the crRNA were established in this study. An evaluation of the *LCYB* expression levels of the resultant transgenic Cas13a lines resulted in no significant down-regulation of the *LCYB* transcript; such down-regulation would be an indicator of successful RNA targeting. Fortunately, a comprehensive comparison of an array of Cas13 variants that concomitantly accounted for subcellular localisation of the variants for optimal activity was provided by Mahas *et al*, giving further insight into the functionality of CRISPR/Cas13 systems (Mahas et al., 2019). For this reason, NLS and NES fusions were made to the existing open reading frame of the LwaCas13a coding sequence, in an effort to control localisation. Relative gene expression analyses of a subset of the NLS and NES transgenic lines revealed some measure of successful *LCYB* silencing in one NES line.

The second research chapter (Chapter 4) of this thesis sought to investigate the inhibition activity of the CRISPR/Cas13a system against a viral RNA genome. An efficient reporter system, TRBO-GFP, was selected as a target, since the expression of the GFP gene provided a visual detection of successful viral attenuation, which could be complemented by molecular confirmation. A series of transient assays in *N. benthamiana* were conducted by co-infiltrating TRBO-GFP and the assembled vector harbouring LwaCas13a-NES and the GFP-targeting crRNA. Although a significant reduction in GFP signal intensity was visually observed and, in a separate experiment, quantified post-infiltration, the molecular analyses used to quantify GFP expression did not corroborate these observations.

Although no comparative assessments were conducted between the CRISPR/Cas13a system and RNAi-based tools for the downregulation of an endogenous transcript, the results from Chapter 3 did not present higher levels of target RNA degradation efficiency than existing RNAi studies. Conversely, the results from Chapter 4 suggest that the interference activity of the CRISPR/Cas13a system against viral transcripts is effective in achieving a knockdown efficiency equal to that of existing RNAi-based and CRISPR/Cas13-based antiviral strategies. Together, these findings offer a preliminary step in validating the CRISPR/Cas13a system for the targeting of both an endogenous mRNA transcript and an exogenous viral RNA genome in plants.

5.2 Future considerations

The newly added Cas13d subtype shares many commonalities with some of the Cas13 subtypes LwaCas13a and PspCas13b, such as the lack of PFS requirements and the innate ability to process pre-crRNAs. Interestingly, Cas13d effectors also show minimal sequence identity with previous Cas13 subtypes proteins, making them approximately 26% smaller than other effectors (Yan et al., 2018). The small size of Cas13d is advantageous as it can facilitate flexible packaging into a cargo-limited delivery viral-vector, as demonstrated with an adeno-associated virus (AAV) for a therapeutic approach in mammalian cells (He et al., 2020; Konermann et al., 2018). Notably, the high RNase activity of the RfxCas13d (CasRx) orthologue was shown to provide specificity and robust activity in both mammalian cells and plants, when compared with other Cas13 proteins, like LwaCas13a and PspCas13b (Konermann et al., 2018; Mahas et al., 2019). For viral interference applications, these reports are encouraging for future multiplex strategies that can simultaneously target either (1) multiple species of viruses within the same family to provide broad virus protection or (2) multiple regions of a single virus genome to evade the possibility of evolutionary resistance to the CRISPR/Cas system from occurring. Interesting, while finalising this thesis, a recent study showed that single polyvalent gRNAs (pgRNAs), designed for one spacer to be able to target multiple viral target sequences, in complex with the CasRx effector can effectively supress virus spread and gene expression *in planta*, better than those with a monovalent gRNA counterpart (Bagchi et al., 2021). This observation of enhanced antiviral suppression is related to improvements reported by CRISPR antiviral treatments with multiple gRNAs, and future studies could now also use multiple pgRNAs to further increase the number of target sites. The impressive catalytic activity and high specificity of CasRx therefore enables diverse RNA manipulations in plants and it appears that it will continue to be favoured for viral RNA genome degradation.

Harnessing plant viruses to act as delivery vectors is a promising approach to obtaining CRISPR/Cas-edited plants without the challenges that accompany transgene delivery. As viruses undergo

replication and move around *in planta,* they present several advantages as they can replicate to a high copy number and spread systemically within a plant, ensuring high expression levels of the CRISPR/Cas components that they harbour and overall improved genome editing efficiency (Varanda et al., 2021). Virus genomes are also easy to manipulate and allow for multiplexed targeting when expressing multiple sgRNAs. Although the viral interference study of Chapter 4 was based on methods the Mahas group executed to successfully demonstrate viral interference of TRBO-GFP mediated by CRISPR/Cas13 (Mahas et al., 2019), one of the principal differences between the two experiments was the method used to deliver the CRISPR/Cas components. The Mahas group opted to deliver the crRNAs using a TRV-based vector and thus ensured that the crRNA expression was systemically maintained at a higher level. It can therefore be hypothesised that the use of a plant expression vector in this study may not have provided the level of Cas13a/crRNA expression required for effective Cas13 activity. Until recently, the cargo capacity of several viral vectors limited them to sgRNA delivery, rather than an entire CRISPR/Cas system, and were often used in conjunction with a plant constitutively expressing Cas or co-infiltrated with a plasmid expressing Cas. This obstacle has been overcome by some studies that have reported the combined delivery of the Cas and sgRNA using positive- and negative-strand RNA viruses (Ariga et al., 2020; Ma et al., 2020). Alternatively, a virus belonging to the monopartite geminivirus family was also successfully developed into a virus-based expression vector for the delivery of an entire CRISPR/Cas system, more specifically a LwaCas13a protein and two crRNAs. This study was also able to show that their viral-based RNA targeting vector was more efficient than a regular expression vector (Yu et al., 2020). The use of the more robust and smaller CasRx protein in such a virus-based RNA targeting vector could probably be even more efficient in future viral interference applications.

One of the biggest concerns regarding genome editing by CRISPR/Cas is the occurrence of off-target mutations. Off-target editing is a critical factor for the CRISPR/Cas13 system, although it has been shown to produce significantly lower off-target effects compared with the existing RNA-targeting method RNAi (Abudayyeh et al., 2017; Cox et al., 2017). It is suspected that minimal off-target modifications to a host plant's transcriptome occur when the RNA cleavage activity of the CRISPR/Cas13 system is engineered for the specific targeting of RNA viruses or RNA intermediates of DNA viruses. In all CRISPR/Cas systems, off-targets generally occur due to the tolerance of gRNA sequence mismatches (Tsai and Joung, 2016). This evidently emphasises the need for effective design rules for the generation of efficient gRNAs. At present, the extent to which CRISPR/Cas13-based RNA editing can give rise to transcriptomic irregularities is not completely understood and further research into this is required.

To provide a visualisation of RNA transcripts, the catalytically inactive versions of Cas13 (dCas13) tagged with a fluorescent protein can be used to image the localisation and mobility of target RNAs. This could be a powerful tool for plant research as it can provide opportunities to monitor the effect of growth stages or stress on endogenous RNA mobility for example, or transport a target of interest to a specific cellular location (Abudayyeh et al., 2017; Mahas et al., 2018). Beyond endogenous RNA imaging, this application can also be used as a tool to investigate viral replication, localisation and evolution, allowing researchers to attenuate viral replication with better precision. Furthermore, the precise editing of RNA nucleotides with dCas13 fused to specific RNA deaminases is also anticipated for its application in plants to enable site-specific editing of an RNA molecule (Abudayyeh et al., 2019; Cox et al., 2017).

If the viral RNA targeting activity of Cas13 is intended for heritable purposes, the permanent expression of the CRISPR/Cas13a components would be required, which can only be achieved through the generation of transgenic plants. This is also true for all CRISPR/Cas9-based antiviral approaches that mediate durable resistance to DNA virus genomes (Taliansky et al., 2021). Due to the regulations of genetically modified organisms (GMOs), the practical applications of this technology that require transgenic plants may therefore be challenged by these regulatory constraints (Kalinina et al., 2020; Khatodia et al., 2017). Although not a limitation to this study, it is warranted as a limitation for the development of commercial crop varieties. However, by opting for RNA targeting over DNA targeting in plants, it is possible to confer a temporary or reversible modulation of gene expression, rather than knockout mutagenesis which can often be lethal or have pleiotropic effects (Zhu et al., 2020). Without permanently editing the genome, CRISPR/Cas13 allows researchers to investigate gene function more systemically and could rather be harnessed as a “treatment” application for the transient inhibition of viruses in important crops. Therefore, the temporary nature of RNA editing overcomes major limitations relating to DNA targeting and its broad application in plant virology could potentially help overcome GMO regulatory hurdles.

5.4 Conclusion

CRISPR/Cas research is advancing at an unprecedented pace and it has revolutionised plant breeding since its first application. While molecular breeding has played a pivotal role in controlling and preventing disease-causing plant viruses, CRISPR/Cas can accelerate the generation of virus-resistant crop varieties. This study developed an RNA knockdown and virus inhibition technique based on the CRISPR/Cas13a system from *L. wadei,* and provided preliminary evidence for the repression of an endogenous carotenoid gene and a moderate reduction in the viral accumulation of a reporter system, respectively, in *N. benthamiana.* Support is also provided for future expansions to prioritise robust

crRNA design strategies, optimised CRISPR/Cas delivery methods and explore the high specificity and efficiency associated with the latest Cas13 effector, CasRx, in plants. Additionally, the effective and versatile RNA-targeting activity of the CRISPR/Cas13 system is highlighted, specifically for the engineering of antiviral defence strategies required for economically important crops such as grapevine.

REFERENCES

Abudayyeh, O.O., Gootenberg, J.S., Konermann, S., Joung, J., Slaymaker, I.M., Cox, D.B.T., Shmakov, S., Makarova, K.S., Semenova, E., Minakhin, L., et al. (2016). C2c2 is a single-component programmable RNA-guided RNA-targeting CRISPR effector. *Science*. 353, aaf5573.

Abudayyeh, O.O., Gootenberg, J.S., Essletzbichler, P., Han, S., Joung, J., Belanto, J.J., Verdine, V., Cox, D.B.T., Kellner, M.J., Regev, A., et al. (2017). RNA targeting with CRISPR-Cas13. *Nature*. 550, 280–284.

Abudayyeh, O.O., Gootenberg, J.S., Franklin, B., Koob, J., Kellner, M.J., Ladha, A., Joung, J., Kirchgatterer, P., Cox, D.B.T., and Zhang, F. (2019). A cytosine deaminase for programmable single-base RNA editing. *Science*. 365, 382–386.

Agrawal, N., Dasaradhi, P.V.N., Mohmmed, A., Malhotra, P., Bhatnagar, R.K., and Mukherjee, S.K. (2003). RNA Interference: Biology, Mechanism, and Applications. *Microbiology and Molecular Biology Reviews*. 67, 657–685.

Ali, Z., Abul-faraj, A., Idris, A., Ali, S., Tashkandi, M., and Mahfouz, M.M. (2015a). CRISPR/Cas9-mediated viral interference in plants. *Genome Biology*. 16, 1–11.

Ali, Z., Abul-Faraj, A., Li, L., Ghosh, N., Piatek, M., Mahjoub, A., Aouida, M., Piatek, A., Baltes, N.J., Voytas, D.F., et al. (2015b). Efficient Virus-Mediated Genome Editing in Plants Using the CRISPR/Cas9 System. *Molecular Plant*. 8, 1288–1291.

Ali, Z., Abul-faraj, A., Piatek, M., and Mahfouz, M.M. (2015c). Activity and specificity of TRV-mediated gene editing in plants. *Plant Signaling & Behavior*. 10, e1044191.

Ali, Z., Ali, S., Tashkandi, M., Zaidi, S.S.-A., and Mahfouz, M.M. (2016). CRISPR/Cas9-Mediated Immunity to Geminiviruses: Differential Interference and Evasion. *Scientific Reports*. 6, 26912.

Ali, Z., Eid, A., Ali, S., and Mahfouz, M.M. (2018). Pea early-browning virus-mediated genome editing via the CRISPR/Cas9 system in Nicotiana benthamiana and Arabidopsis. *Virus Research*. 244, 333–337.

Altpeter, F., Springer, N.M., Bartley, L.E., Blechl, A., Brutnell, T.P., Citovsky, V., Conrad, L., Gelvin, S.B., Jackson, D., Kausch, A.P., et al. (2016). Advancing Crop Transformation in the Era of Genome Editing. *The Plant Cell*. 28, 1510–1520.

Aman, R., Ali, Z., Butt, H., Mahas, A., Aljedaani, F., Khan, M.Z., Ding, S., and Mahfouz, M. (2018a). RNA virus interference via CRISPR/Cas13a system in plants. *Genome Biology*. 19, 1.

Aman, R., Mahas, A., Butt, H., Aljedaani, F., and Mahfouz, M. (2018b). Engineering RNA Virus Interference via the CRISPR/Cas13 Machinery in Arabidopsis. *Viruses*. 10, 732.

Anantharaman, V., Makarova, K.S., Burroughs, A.M., Koonin, E. V., and Aravind, L. (2013). Comprehensive analysis of the HEPN superfamily: identification of novel roles in intra-genomic conflicts, defense, pathogenesis and RNA processing. *Biology Direct*. 8, 15.

Anderson, P.K., Cunningham, A.A., Patel, N.G., Morales, F.J., Epstein, P.R., and Daszak, P. (2004). Emerging infectious diseases of plants: Pathogen pollution, climate change and agrotechnology drivers. *Trends in Ecology and Evolution*. 19, 535–544.

Apel, W., and Bock, R. (2009). Enhancement of carotenoid biosynthesis in transplastomic tomatoes by induced lycopene-to-provitamin a conversion. *Plant Physiology*. 151, 59–66.

Ariga, H., Toki, S., and Ishibashi, K. (2020). Potato virus X vector-mediated DNA-free genome editing in plants. *Plant and Cell Physiology*. 61, 1946–1953.

Awasthi, S., Chauhan, R., and Narayan, R.P. (2016). Plant Viruses: History and Taxonomy. In Plant Viruses: Evolution and Management, R.. Gaur, ed. (Singapore: Springer), pp. 1–17.

Bagchi, R., Tinker-kulberg, R., Supakar, T., and Chamberlain, S. (2021). Polyvalent Guide RNAs for CRISPR Antivirals. *BioRxiv*.

Bai, L., Kim, E.H., Dellapenna, D., and Brutnell, T.P. (2009). Novel lycopene epsilon cyclase activities in maize revealed through perturbation of carotenoid biosynthesis. *Plant Journal*. 59, 588–599.

Baltes, N.J., Hummel, A.W., Konecna, E., Cegan, R., Bruns, A.N., Bisaro, D.M., and Voytas, D.F. (2015). Conferring resistance to geminiviruses with the CRISPR-Cas prokaryotic immune system. *Nature Plants*. 1, 4–7.

Bandaru, S., Tsuji, M.H., Shimizu, Y., Usami, K., Lee, S., Takei, N.K., Yoshitome, K., Nishimura, Y., Otsuki, T., and Ito, T. (2020). Structure-based design of gRNA for Cas13. *Scientific Reports*. 10, 1–12.

Barrangou, R., and Marraffini, L.A. (2014). CRISPR-cas systems: Prokaryotes upgrade to adaptive immunity. *Molecular Cell*. 54, 234–244.

Barrangou, R., Fremaux, C., Deveau, H., Richards, M., Boyaval, P., Moineau, S., Romero, D. a, and Horvath, P. (2007). CRISPR provides acquired resistance against viruses in prokaryotes. *Science*. 315, 1709–1712.

Bashandy, H., Jalkanen, S., and Teeri, T.H. (2015). Within leaf variation is the largest source of variation in agroinfiltration of Nicotiana benthamiana. *Plant Methods*. 11, 1–7.

Basso, M.F., Fajardo, T.V.M., and Salderelli, P. (2017). Grapevine Virus Diseases: Economic impact and current advances in viral prospection and management. *Revista Brasileira de Fruticultura*. 39, 1.

Bau, H.J., Cheng, Y.H., Yu, T.A., Yang, J.S., and Yeh, S.D. (2003). Broad-spectrum resistance to different geographic strains of Papaya ringspot virus in coat protein gene transgenic papaya. *Phytopathology*. 93, 112–120.

Baulcombe, D. (2004). RNA silencing in plants. *Nature*. 431, 356–363.

Baulcombe, D.C. (1996). Mechanisms of pathogen-derived resistance to viruses in transgenic plants. *Plant Cell*. 8, 1833–1844.

Belhaj, K., Chaparro-Garcia, A., Kamoun, S., and Nekrasov, V. (2013). Plant genome editing made easy: targeted mutagenesis in model and crop plants using the CRISPR/Cas system. *Plant Methods*. 9, 39.

Bhushan K. (2018). CRISPR/Cas13a targeting of RNA virus in plants. *Plant Cell Reports*. 12, 1707–1712.

Bidabadi, S.S., and Mohan Jain, S. (2020). Cellular, molecular, and physiological aspects of in vitro plant regeneration. *Plants*. 9, 10–13.

Boch, J., Scholze, H., Schornack, S., Landgraf, A., Hahn, S., Kay, S., Lahaye, T., Nickstadt, A., and Bonas, U. (2009). Breaking the code of DNA binding specificity of TAL-type III effectors. *Science*. 326, 1509–1512.

Boualem, A., Dogimont, C., and Bendahmane, A. (2016). The battle for survival between viruses and their host plants. *Current Opinion in Virology*. 17, 32–38.

Bragard, C., Caciagli, P., Lemaire, O., Lopez-Moya, J.J., MacFarlane, S., Peters, D., Susi, P., and Torrance, L. (2013). Status and Prospects of Plant Virus Control Through Interference with Vector Transmission. *Annual Review of Phytopathology*. 51, 177–201.

Brouns, S.J.J., Jore, M.M., Lundgren, M., Westra, E.R., Slijkhuis, R.J.., Snijders, A., Dickman, M.J., Makarova, K.S., Koonin, E. V., and van der (2008). Small CRISPR RNAs Guide Antiviral Defense in Prokaryotes. *Science*. 321, 960–965.

Burmistrz, M., Krakowski, K., and Krawczyk-Balska, A. (2020). RNA-Targeting CRISPR–Cas Systems and Their Applications. *International Journal of Molecular Sciences*. 21, 1122.

Cai, C.Q., Doyon, Y., Ainley, W.M., Miller, J.C., DeKelver, R.C., Moehle, E.A., Rock, J.M., Lee, Y.L., Garrison, R., Schulenberg, L., et al. (2009). Targeted transgene integration in plant cells using designed zinc finger nucleases. *Plant Molecular Biology*. 69, 699–709.

Cao, Y., Zhou, H., Zhou, X., and Li, F. (2021). Conferring Resistance to Plant RNA Viruses with the CRISPR/CasRx System. *Virologica Sinica*. 3–7.

Casacuberta, J.M., Devos, Y., du Jardin, P., Ramon, M., Vaucheret, H., and Nogué, F. (2015). Biotechnological uses of RNAi in plants: Risk assessment considerations. *Trends in Biotechnology*. 33, 145–147.

Čermák, T., Curtin, S.J., Gil-Humanes, J., Čegan, R., Kono, T.J.Y., Konečná, E., Belanto, J.J., Starker, C.G., Mathre, J.W., Greenstein, R.L., et al. (2017). A multipurpose toolkit to enable advanced genome engineering in plants. *Plant Cell*. 29, 1196–1217.

Chandrasekaran, J., Brumin, M., Wolf, D., Leibman, D., Klap, C., Pearlsman, M., Sherman, A., Arazi, T., and Gal-On, A. (2016). Development of broad virus resistance in non-transgenic cucumber using CRISPR/Cas9 technology. *Molecular Plant Pathology*. 17, 1140–1153.

Chare, E.R., and Holmes, E.C. (2006). A phylogenetic survey of recombination frequency in plant RNA viruses. *Archives of Virology*. 151, 933–946.

Christian, M., Cermak, T., Doyle, E.L., Schmidt, C., Zhang, F., Hummel, A., Bogdanove, A.J., and Voytas, D.F. (2010). Targeting DNA double-strand breaks with TAL effector nucleases. *Genetics*. 186, 756–761.

Christou, P. (1990). Morphological description of transgenic soybean chimeras created by the delivery, integration and expression of foreign DNA using electric discharge particle acceleration. *Annals of Botany*. 66, 379–386.

Clemente, T. (2006). *Nicotiana* (*Nicotiana tobaccum, Nicotiana benthamiana*). In Agrobacterium Protocols, (New Jersey: Humana Press), pp. 143–154.

Cody, W.B., Scholthof, H.B., and Mirkov, T.E. (2017). Multiplexed gene editing and protein overexpression using a tobacco mosaic virus viral vector. *Plant Physiology*. 175, 23–35.

Costa, L.D., Malnoy, M., Lecourieux, D., Deluc, L., Ouaked-Lecourieux, F., Thomas, M.R., and Torregrosa, L. (2019). The state-of-the-art of grapevine biotechnology and new breeding technologies (NBTS). *Oeno One*. 53, 205–228.

Cox, D.B.T., Gootenberg, J.S., Abudayyeh, O.O., Franklin, B., Kellner, M.J., Joung, J., and Zhang, F. (2017). RNA editing with CRISPR-Cas13. *Science*. 358, 1019–1027.

Cunningham, F.X., and Gantt, E. (1998). Genes and Enzymes of Carotenoid Biosynthesis in Plants. *Annual Review of Plant Physiology and Plant Molecular Biology*. 49, 557–583.

Cunningham, F.X., Pogson, B., Sun, Z., McDonald, K.A., DellaPenna, D., and Gantt, E. (1996). Functional analysis of the beta and epsilon lycopene cyclase enzymes of Arabidopsis reveals a mechanism for control of cyclic carotenoid formation. *The Plant Cell*. 8, 1613–1626.

Curtin, S.J., Zhang, F., Sander, J.D., Haun, W.J., Starker, C., Baltes, N.J., Reyon, D., Dahlborg, E.J., Goodwin, M.J., Coffman, A.P., et al. (2011). Targeted mutagenesis of duplicated genes in soybean with zinc-finger nucleases. *Plant Physiology*. 156, 466–473.

Ding, L., Chen, Y., Ma, Y., Wang, H., and Wei, J. (2020). Effective reduction in chimeric mutants of poplar trees produced by CRISPR/Cas9 through a second round of shoot regeneration. *Plant Biotechnology Reports*. 14, 549–558.

Diretto, G., Tavazza, R., Welsch, R., Pizzichini, D., Mourgues, F., Papacchioli, V., Beyer, P., and Giuliano, G. (2006). Metabolic engineering of potato tuber carotenoids through tuber-specific silencing of lycopene epsilon cyclase. *BMC Plant Biology*. 6.

Duensing, N., Sprink, T., Parrott, W.A., Fedorova, M., Lema, M.A., Wolt, J.D., and Bartsch, D. (2018). Novel Features and Considerations for ERA and Regulation of Crops Produced by Genome Editing. *Frontiers in Bioengineering and Biotechnology*. 6, 1–16.

East-Seletsky, A., O'Connell, M.R., Knight, S.C., Burstein, D., Cate, J.H.D., Tjian, R., and Doudna, J.A. (2016). Two distinct RNase activities of CRISPR-C2c2 enable guide-RNA processing and RNA detection. *Nature*. 538, 270–273.

East-Seletsky, A., O'Connell, M.R., Burstein, D., Knott, G.J., and Doudna, J.A. (2017). RNA Targeting by Functionally Orthogonal Type VI-A CRISPR-Cas Enzymes. *Molecular Cell*. 66, 373–383.

Engreitz, J., Abudayyeh, O., Gootenberg, J., and Zhang, F. (2019). CRISPR tools for systematic studies of RNA regulation. *Cold Spring Harbor Perspectives in Biology*. 11, a035386.

Faize, M., Faize, L., and Burgos, L. (2010). Using quantitative real-time PCR to detect chimeras in transgenic tobacco and apricot and to monitor their dissociation. *BMC Biotechnology*. 10, 53.

Fereres, A., and Raccah, B. (2015). Plant Virus Transmission by Insects. In Encyclopedia of Life Sciences (ELS), (Chichester, UK: John Wiley & Sons, Ltd), pp. 1–12.

Fire, A., Xu, S., Montgomery, M.K., Kostas, S.A., Driver, S.E., and Mello, C.C. (1998). Potent and specific genetic interference by double-stranded RNA in caenorhabditis elegans. *Nature*. 391, 806–811.

Fitch, M.M.M., Manshardt, R.M., Gonsalves, D., Slightom, J.L., and Sanford, J.C. (1992). Virus Resistant Papaya Plants Derived from Tissues Bombarded with the Coat Protein Gene of Papaya Ringspot Virus. *Nature Biotechnology*. 10, 1466–1472.

Fonfara, I., Richter, H., BratoviÄ, M., Le Rhun, A., and Charpentier, E. (2016). The CRISPR-associated DNA-cleaving enzyme Cpf1 also processes precursor CRISPR RNA. *Nature*. 532, 517–521.

Fuentes, A., Ramos, P.L., Fiallo, E., Callard, D., Sánchez, Y., Peral, R., Rodríguez, R., and Pujol, M. (2006).

Intron-hairpin RNA derived from replication associated protein C1 gene confers immunity to tomato yellow leaf curl virus infection in transgenic tomato plants. *Transgenic Research*. 15, 291–304.

Gaj, T., Gersbach, C.A., and Barbas, C.F. (2013). ZFN, TALEN, and CRISPR/Cas-based methods for genome engineering. *Trends in Biotechnology*. 31, 397–405.

Gaudet, J., VanderElst, I., and Spence, A.M. (1996). Post-transcriptional regulation of sex determination in Caenorhabditis elegans: Widespread expression of the sex-determining gene fem-1 in both sexes. *Molecular Biology of the Cell*. 7, 1107–1121.

Gelvin, S.B. (2017). Integration of Agrobacterium T-DNA into the Plant Genome. *Annual Review of Genetics*. 51, 195–217.

Ghoshal, B., Vong, B., Picard, C., and Feng, S. (2020). A viral guide RNA delivery system for CRISPR-based transcriptional activation and 2 heritable targeted DNA demethylation in Arabidopsis thaliana. 494, 463–467.

Gil-Humanes, J., Wang, Y., Liang, Z., Shan, Q., Ozuna, C. V., Sánchez-León, S., Baltes, N.J., Starker, C., Barro, F., Gao, C., et al. (2017). High-efficiency gene targeting in hexaploid wheat using DNA replicons and CRISPR/Cas9. *The Plant Journal*. 89, 1251–1262.

Gomez, M.A., Lin, Z.D., Moll, T., Chauhan, R.D., Hayden, L., Renninger, K., Beyene, G., Taylor, N.J., Carrington, J.C., Staskawicz, B.J., et al. (2019). Simultaneous CRISPR/Cas9-mediated editing of cassava eIF4E isoforms nCBP-1 and nCBP-2 reduces cassava brown streak disease symptom severity and incidence. *Plant Biotechnology Journal*. 17, 421–434.

Gootenberg, J.S., Abudayyeh, O.O., Lee, J.W., Essletzbichler, P., Dy, A.J., Joung, J., Verdine, V., Donghia, N., Daringer, N.M., Freije, C.A., et al. (2017). Nucleic acid detection with CRISPR-Cas13a/C2c2. *Science*. 356, 438–442.

Guo, Q., Liu, Q., A. Smith, N., Liang, G., and Wang, M.-B. (2016). RNA Silencing in Plants: Mechanisms, Technologies and Applications in Horticultural Crops. *Current Genomics*. 17, 476–489.

Guo, X., Wessels, H.-H., Méndez-Mancilla, A., Haro, D., and Sanjana, N.E. (2020). Transcriptome-wide Cas13 guide RNA design for model organisms and viral RNA pathogens. *BioRxiv*.

Gupta, R.M., and Musunuru, K. (2014). Expanding the genetic editing tool kit: ZFNs, TALENs, and CRISPR-Cas9. *Journal of Clinical Investigation*. 124, 4154–4161.

Hannon, G.J. (2002). RNA interference. *Nature*. 418, 244–251.

Hazarika, B.N. (2006). Morpho-physiological disorders in in vitro culture of plants. *Scientia Horticulturae*. 108, 105–120.

He, B., Peng, W., Huang, J., Zhang, H., Zhou, Y., Yang, X., Liu, J., Li, Z., Xu, C., Xue, M., et al. (2020). Modulation of metabolic functions through Cas13d-mediated gene knockdown in liver. *Protein and Cell*. 11, 518–524.

Hirschberg, J. (2001). Carotenoid biosynthesis in flowering plants. *Current Opinion in Plant Biology*. 4, 210–218.

Holmes, K., Williams, C.M., Chapman, E.A., and Cross, M.J. (2010). Detection of siRNA induced mRNA silencing by RT-qPCR: Considerations for experimental design. *BMC Research Notes*. 3, 1–5.

Huynh, N., Depner, N., Larson, R., and King-Jones, K. (2020). A versatile toolkit for CRISPR-Cas13-based RNA manipulation in Drosophila. *Genome Biology*. 21, 279.

Jeon, Y., Choi, Y.H., Jang, Y., Yu, J., Goo, J., Lee, G., Jeong, Y.K., Lee, S.H., Kim, I.-S., Kim, J.-S., et al. (2018). Direct observation of DNA target searching and cleavage by CRISPR-Cas12a. *Nature Communications*. 9, 2777.

Ji, X., Zhang, H., Zhang, Y., Wang, Y., and Gao, C. (2015). Establishing a CRISPR–Cas-like immune system conferring DNA virus resistance in plants. *Nature Plants*. 1, 1–4.

Jiang, N., Zhang, C., Liu, J., Guo, Z., Zhang, Z., Han, C., and Wang, Y. (2019). Development of Beet necrotic yellow vein virus -based vectors for multiple-gene expression and guide RNA delivery in plant genome editing. *Plant Biotechnology Journal*. 17, 1302–1315.

Jinek, M., Chylinski, K., Fonfara, I., Hauer, M., Doudna, J.A., and Charpentier, E. (2012). A Programmable Dual-RNA-Guided DNA Endonuclease in Adaptive Bacterial Immunity. *Science*. 337, 816–821.

Kalinina, N.O., Khromov, A., Love, A.J., and Taliansky, M.E. (2020). CRISPR Applications in Plant Virology: Virus Resistance and Beyond. *Phytopathology*. 110, 18–28.

Kang, B.-C., Yeam, I., and Jahn, M.M. (2005). Genetics of Plant Virus Resistance. *Annual Review of Phytopathology*. 43, 581–621.

Kaur, N., Alok, A., Shivani, Kumar, P., Kaur, N., Awasthi, P., Chaturvedi, S., Pandey, P., Pandey, A., Pandey, A.K., et al. (2020). CRISPR/Cas9 directed editing of lycopene epsilon-cyclase modulates metabolic flux for β-carotene biosynthesis in banana fruit. *Metabolic Engineering*. 59, 76–86.

Khatodia, S., Bhatotia, K., and Tuteja, N. (2017). Development of CRISPR/Cas9 mediated virus resistance in agriculturally important crops. *Bioengineered*. 8, 274–279.

Kim, S.H., Jeong, J.C., Park, S., Bae, J.Y., Ahn, M.J., Lee, H.S., and Kwak, S.S. (2014). Down-regulation of sweetpotato lycopene β-cyclase gene enhances tolerance to abiotic stress in transgenic calli. *Molecular Biology Reports*. 41, 8137–8148.

Kim, Y.G., Cha, J., and Chandrasegaran, S. (1996). Hybrid restriction enzymes: Zinc finger fusions to Fok I cleavage domain. *Proceedings of the National Academy of Sciences of the United States of America*. 93, 1156–1160.

Kis, A., Hamar, É., Tholt, G., Bán, R., and Havelda, Z. (2019). Creating highly efficient resistance against wheat dwarf virus in barley by employing CRISPR/Cas9 system. *Plant Biotechnology Journal*. 17, 1004–1006.

Knott, G.J., and Doudna, J.A. (2018). CRISPR-Cas guides the future of genetic engineering. *Science*. 361, 866–869.

Konermann, S., Lotfy, P., Brideau, N.J., Oki, J., Shokhirev, M.N., and Hsu, P.D. (2018). Transcriptome Engineering with RNA-Targeting Type VI-D CRISPR Effectors. *Cell*. 173, 665–676.

Koonin, E. V, Makarova, K.S., and Zhang, F. (2017). Diversity, classification and evolution of CRISPR-Cas systems. *Current Opinion in Microbiology*. 37, 67–78.

Kössler, S., Armarego-Marriott, T., Tarkowská, D., Turečková, V., Agrawal, S., Mi, J., de Souza, L.P.,

Schöttler, M.A., Schadach, A., Fröhlich, A., et al. (2021). Lycopene β-cyclase expression influences plant physiology, development, and metabolism in tobacco plants. *Journal of Experimental Botany*. 72, 2544–2569.

Kuluev, B.R., Gumerova, G.R., Mikhaylova, E. V., Gerashchenkov, G.A., Rozhnova, N.A., Vershinina, Z.R., Khyazev, A. V., Matniyazov, R.T., Baymiev, A.K., Baymiev, A.K., et al. (2019). Delivery of CRISPR/Cas Components into Higher Plant Cells for Genome Editing. *Russian Journal of Plant Physiology*. 66, 694–706.

Kumagai, M.H., Donson, J., Della-Cioppa, G., Harvey, D., Hanley, K., and Grill, L.K. (1995). Cytoplasmic inhibition of carotenoid biosynthesis with virus-derived RNA. *Proceedings of the National Academy of Sciences of the United States of America*. 92, 1679–1683.

Kung, Y.J., You, B.J., Raja, J.A.J., Chen, K.C., Huang, C.H., Bau, H.J., Yang, C.F., Huang, C.H., Chang, C.P., and Yeh, S.D. (2015). Nucleotide sequence-homology-independent breakdown of transgenic resistance by more virulent virus strains and a potential solution. *Scientific Reports*. 5, 1–10.

Labun, K., Montague, T.G., Krause, M., Torres Cleuren, Y.N., Tjeldnes, H., and Valen, E. (2019). CHOPCHOP v3: expanding the CRISPR web toolbox beyond genome editing. *Nucleic Acids Research*. 47, W171–W174.

Lefeuvre, P., Martin, D.P., Elena, S.F., Shepherd, D.N., Roumagnac, P., and Varsani, A. (2019). Evolution and ecology of plant viruses. *Nature Reviews Microbiology*. 17, 632–644.

Li, J.-F., Norville, J.E., Aach, J., McCormack, M., Zhang, D., Bush, J., Church, G.M., and Sheen, J. (2013). Multiplex and homologous recombination–mediated genome editing in Arabidopsis and Nicotiana benthamiana using guide RNA and Cas9. *Nature Biotechnology*. 31, 688–691.

Lichtenthaler, H.K., and Buschmann, C. (2001). Chlorophylls and Carotenoids: Measurement and Characterization by UV-VIS Spectroscopy. *Current Protocols in Food Analytical Chemistry*. 1, F4.3.1-F4.3.8.

Lindbo, J.A. (2007). TRBO: A high-efficiency tobacco mosaic virus RNA-based overexpression vector. *Plant Physiology*. 145, 1232–1240.

Liu, C., and Nelson, R.S. (2013). The cell biology of tobacco mosaic virus replication and movement. *Frontiers in Plant Science*. 4, 1–10.

Liu, H., Soyars, C.L., Li, J., Fei, Q., He, G., Peterson, B.A., Meyers, B.C., Nimchuk, Z.L., and Wang, X. (2018). CRISPR/Cas9-mediated resistance to cauliflower mosaic virus. *Plant Direct*. 2, e00047.

Liu, L., Li, X., Ma, J., Li, Z., You, L., Wang, J., Wang, M., Zhang, X., and Wang, Y. (2017a). The Molecular Architecture for RNA-Guided RNA Cleavage by Cas13a. *Cell*. 170, 714-726.e10.

Liu, L., Li, X., Wang, J., Wang, M., Chen, P., Yin, M., Li, J., Sheng, G., and Wang, Y. (2017b). Two Distant Catalytic Sites Are Responsible for C2c2 RNase Activities. *Cell*. 168, 121–134.

Livak, K.J., and Schmittgen, T.D. (2001). Analysis of relative gene expression data using real-time quantitative PCR and the 2-ΔΔCT method. *Methods*. 25, 402–408.

Lomonossoff, G.P. (1995). Pathogen-Derived Resistance to Plant Viruses. *Annual Review of Phytopathology*. 33, 323–343.

Louime, C., Vasanthaiah, H.K., Basha, S.M., and Lu, J. (2010). Perspective of biotic and abiotic stress research in grapevines (Vitis sp.). *International Journal of Fruit Science*. 10, 79–86.

Ma, X., Zhang, X., Liu, H., and Li, Z. (2020). Highly efficient DNA-free plant genome editing using virally delivered CRISPR–Cas9. *Nature Plants*. 6, 773–779.

Macovei, A., Sevilla, N.R., Cantos, C., Jonson, G.B., Slamet-Loedin, I., Čermák, T., Voytas, D.F., Choi, I.R., and Chadha-Mohanty, P. (2018). Novel alleles of rice eIF4G generated by CRISPR/Cas9-targeted mutagenesis confer resistance to Rice tungro spherical virus. *Plant Biotechnology Journal*. 16, 1918–1927.

Mahas, A., and Mahfouz, M. (2018). Engineering virus resistance via CRISPR–Cas systems. *Current Opinion in Virology*. 32, 1–8.

Mahas, A., Neal Stewart, C., and Mahfouz, M.M. (2018). Harnessing CRISPR/Cas systems for programmable transcriptional and post-transcriptional regulation. *Biotechnology Advances*. 36, 295–310.

Mahas, A., Aman, R., and Mahfouz, M. (2019). CRISPR-Cas13d mediates robust RNA virus interference in plants. *Genome Biology*. 20, 1–16.

Maier, T., Güell, M., and Serrano, L. (2009). Correlation of mRNA and protein in complex biological samples. *FEBS Letters*. 583, 3966–3973.

Makarova, K.S., Haft, D.H., Barrangou, R., Brouns, S.J.J., Charpentier, E., Horvath, P., Moineau, S., Mojica, F.J.M., Wolf, Y.I., Yakunin, A.F., et al. (2011). Evolution and classification of the CRISPR-Cas systems. *Nature Reviews Microbiology*. 9, 467–477.

Makarova, K.S., Wolf, Y.I., Alkhnbashi, O.S., Costa, F., Shah, S.A., Saunders, S.J., Barrangou, R., Brouns, S.J.J., Charpentier, E., Haft, D.H., et al. (2015). An updated evolutionary classification of CRISPR-Cas systems. *Nature Reviews Microbiology*. 13, 722–736.

Maliogka, V.I., Martelli, G.P., Fuchs, M., and Katis, N.I. (2015). Control of viruses infecting grapevine. In Advances in Virus Research, G. Loebenstein, and N.I. Katis, eds. (Academic Press), pp. 175–227.

Malnoy, M., Boresjza-Wysocka, E.E., Norelli, J.L., Flaishman, M.A., Gidoni, D., and Aldwinckle, H.S. (2010). Genetic transformation of apple (Malus x domestica) without use of a selectable marker gene. *Tree Genetics and Genomes*. 6, 423–433.

Manghwar, H., Li, B., Ding, X., Hussain, A., Lindsey, K., Zhang, X., and Jin, S. (2020). CRISPR/Cas Systems in Genome Editing: Methodologies and Tools for sgRNA Design, Off-Target Evaluation, and Strategies to Mitigate Off-Target Effects. *Advanced Science.* 7, 1-16.

Martelli, G.P. (2019). Virus Diseases of Grapevine. In Encyclopedia of Life Sciences (ELS), (Chichester, UK: John Wiley & Sons, Ltd), pp. 1–13.

Matthews, R.E.F. (1998). Classification as a Framework for Diagnosis. In Diagnosis of Plant Virus Diseases, (Boca Raton: CRC Press), pp. 59–64.

Mehta, D., Stürchler, A., Anjanappa, R.B., Zaidi, S.S.E.A., Hirsch-Hoffmann, M., Gruissem, W., and Vanderschuren, H. (2019). Linking CRISPR-Cas9 interference in cassava to the evolution of editing-resistant geminiviruses. *Genome Biology*. 20, 1–10.

Missiou, A., Kalantidis, K., Boutla, A., Tzortzakaki, S., Tabler, M., and Tsagris, M. (2004). Generation of

transgenic potato plants highly resistant to potato virus Y (PVY) through RNA silencing. *Molecular Breeding*. 14, 185–197.

Mitter, N., Sulistyowati, E., Graham, M.W., and Dietzgen, R.G. (2001). Suppression of gene silencing: a threat to virus-resistant transgenic plants? *Trends in Plant Science*. 6, 246–247.

Mitter, N., Worrall, E.A., Robinson, K.E., Li, P., Jain, R.G., Taochy, C., Fletcher, S.J., Carroll, B.J., Lu, G.Q., and Xu, Z.P. (2017). Clay nanosheets for topical delivery of RNAi for sustained protection against plant viruses. *Nature Plants*. 3, 16207.

Moreno, J.C., Pizarro, L., Fuentes, P., Handford, M., Cifuentes, V., and Stange, C. (2013). Levels of Lycopene β-Cyclase 1 Modulate Carotenoid Gene Expression and Accumulation in Daucus carota. *PLoS ONE*. 8, e58144.

Murray, M.G., and Thompson, W.F. (1980). Rapid isolation of high molecular weight plant DNA. *Nucleic Acids Research*. 8, 4321–4326.

Mushtaq, M., Bhat, J.A., Mir, Z.A., Sakina, A., Ali, S., Singh, A.K., Tyagi, A., Salgotra, R.K., Dar, A.A., and Bhat, R. (2018). CRISPR/Cas approach: A new way of looking at plant-abiotic interactions. *Journal of Plant Physiology*. 224–225, 156–162.

Mushtaq, M., Mukhtar, S., Sakina, A., Dar, A.A., Bhat, R., Deshmukh, R., Molla, K., Kundoo, A.A., and Dar, M.S. (2020). Tweaking genome-editing approaches for virus interference in crop plants. *Plant Physiology and Biochemistry*. 147, 242–250.

Naidu, R., Rowhani, A., Fuchs, M., Golino, D., and Martelli, G.P. (2014). Grapevine Leafroll: A Complex Viral Disease Affecting a High-Value Fruit Crop. *Plant Disease*. 98, 1172–1185.

Naing, A.H., Kyu, S.Y., Pe, P.P.W., Park, K. Il, Lee, J.M., Lim, K.B., and Kim, C.K. (2019). Silencing of the phytoene desaturase (PDS) gene affects the expression of fruit-ripening genes in tomatoes. *Plant Methods*. 15, 1–11.

Napoli, C., Lemieux, C., and Jorgensen, R. (1990). Introduction of a chimeric chalcone synthase gene into petunia results in reversible co-suppression of homologous genes in trans. *Plant Cell*. 2, 279–289.

Nelles, D.A., Fang, M.Y., O'Connell, M.R., Xu, J.L., Markmiller, S.J., Doudna, J.A., and Yeo, G.W. (2016). Programmable RNA Tracking in Live Cells with CRISPR/Cas9. *Cell*. 165, 488–496.

Nester, E.W. (2015). Agrobacterium: Nature's Genetic Engineer. *Frontiers in Plant Science*. 5, 1–16.

Nicaise, V. (2014). Crop immunity against viruses: outcomes and future challenges. *Frontiers in Plant Science*. 5, 1–18.

Nisar, N., Li, L., Lu, S., Khin, N.C., and Pogson, B.J. (2015). Carotenoid metabolism in plants. *Molecular Plant*. 8, 68–82.

O'Connell, M.R. (2019). Molecular Mechanisms of RNA Targeting by Cas13-containing Type VI CRISPR–Cas Systems. *Journal of Molecular Biology*. 431, 66–87.

O'Connell, M.R., Oakes, B.L., Sternberg, S.H., East-Seletsky, A., Kaplan, M., and Doudna, J.A. (2014). Programmable RNA recognition and cleavage by CRISPR/Cas9. *Nature*. 516, 263–266.

Oerke, E.C., and Dehne, H.W. (2004). Safeguarding production - Losses in major crops and the role of

crop protection. *Crop Protection*. 23, 275–285.

OIV (2018). OIV Statistical Report on World Vitiviniculture. *International Organisation of Vine and Wine*. 1, 1–16.

Oost, J. Van Der, Westra, E.R., Jackson, R.N., and Wiedenheft, B. (2014). Unravelling the structural and mechanistic basis of CRISPR – Cas systems. *Nature Publishing Group*. 12, 479–492.

van der Oost, J., Jore, M.M., Westra, E.R., Lundgren, M., and Brouns, S.J.J. (2009). CRISPR-based adaptive and heritable immunity in prokaryotes. *Trends in Biochemical Sciences*. 34, 401–407.

Pacher, M., and Puchta, H. (2017). From classical mutagenesis to nuclease-based breeding – directing natural DNA repair for a natural end-product. *Plant Journal*. 90, 819–833.

Paszkowski, J., Baur, M., Bogucki, A., and Potrykus, I. (1988). Gene targeting in plants. *The EMBO Journal*. 7, 4021–4026.

Petrov, N.M., Stoyanova, M.I., and Gaur, R.K. (2019). Post-transcriptional Gene Silencing as a Tool for Controlling Viruses in Plants. In Plant Biotechnology: Progress in Genomic Era, S.M. Khurana, and R.K. Gaur, eds. (Singapore: Springer), pp. 527–542.

Price, A.A., Sampson, T.R., Ratner, H.K., Grakoui, A., and Weiss, D.S. (2015). Cas9-mediated targeting of viral RNA in eukaryotic cells. *Proceedings of the National Academy of Sciences*. 112, 6164–6169.

Puchta, H., Dujon, B., and Hohn, B. (1993). Homologous recombination in plant cells is enhanced by in vivo induction of double strand breaks into DNA by a site-specific endonuclease. *Nucleic Acids Research*. 21, 5034–5040.

Pyott, D.E., Sheehan, E., and Molnar, A. (2016). Engineering of CRISPR/Cas9-mediated potyvirus resistance in transgene-free Arabidopsis plants. *Molecular Plant Pathology*. 17, 1276–1288.

Qin, G., Gu, H., Ma, L., Peng, Y., Deng, X.W., Chen, Z., and Qu, L.J. (2007). Disruption of phytoene desaturase gene results in albino and dwarf phenotypes in Arabidopsis by impairing chlorophyll, carotenoid, and gibberellin biosynthesis. *Cell Research*. 17, 471–482.

Rakosy-Tican, E., Aurori, C.M., Dijkstra, C., Thieme, R., Aurori, A., and Davey, M.R. (2007). The usefulness of the gfp reporter gene for monitoring Agrobacterium- mediated transformation of potato dihaploid and tetraploid genotypes. *Plant Cell Reports*. 26, 661–671.

Ran, F.A., Hsu, P.D., Wright, J., Agarwala, V., Scott, D.A., and Zhang, F. (2013). Genome engineering using the CRISPR-Cas9 system. *Nature Protocols*. 8, 2281–2308.

Ran, Y., Liang, Z., and Gao, C. (2017). Current and future editing reagent delivery systems for plant genome editing. *Science China Life Sciences*. 60, 490–505.

Reynolds, A.. (2017). The Grapevine, Viticulture, and Winemaking: A Brief Introduction. In Grapevine Viruses: Molecular Biology, Diagnostics and Management, B. Meng, G.P. Martelli, D.A. Golino, and M. Fuchs, eds. (Cham: Springer), pp. 3–29.

Romano, N., and Macino, G. (1992). Quelling: transient inactivation of gene expression in Neurospora crassa by transformation with homologous sequences. *Molecular Microbiology*. 6, 3343–3353.

Roossinck, M.J. (2003). Plant RNA virus evolution. *Current Opinion in Microbiology*. 6, 406–409.

Rosa, C., Kuo, Y.-W., Wuriyanghan, H., and Falk, B.W. (2018). RNA Interference Mechanisms and Applications in Plant Pathology. *Annual Review of Phytopathology*. 56, 581–610.

Roth, B.M., Pruss, G.J., and Vance, V.B. (2004). Plant viral suppressors of RNA silencing. *Virus Research*. 102, 97–108.

Roy, A., Zhai, Y., Ortiz, J., Neff, M., Mandal, B., Mukherjee, S.K., and Pappu, H.R. (2019). Multiplexed editing of a begomovirus genome restricts escape mutant formation and disease development. *PLOS ONE*. 14, e0223765.

Rubio, L., Galipienso, L., and Ferriol, I. (2020). Detection of Plant Viruses and Disease Management: Relevance of Genetic Diversity and Evolution. *Frontiers in Plant Science*. 11, 1–23.

Sampson, T.R., Saroj, S.D., Llewellyn, A.C., Tzeng, Y.L., and Weiss, D.S. (2013). A CRISPR/Cas system mediates bacterial innate immune evasion and virulence. *Nature*. 497, 254–257.

Sander, J.D., and Joung, J.K. (2014). CRISPR-Cas systems for editing, regulating and targeting genomes. *Nature Biotechnology*. 32, 347–355.

Sandhya, D., Jogam, P., Allini, V.R., Abbagani, S., and Alok, A. (2020). The present and potential future methods for delivering CRISPR/Cas9 components in plants. *Journal of Genetic Engineering and Biotechnology*. 18, 25.

Sanford, J.C., and Johnston, S.A. (1985). The concept of parasite-derived resistance-Deriving resistance genes from the parasite's own genome. *Journal of Theoretical Biology*. 113, 395–405.

Sastry, K.S., and A. Zitter, T. (2014). Management of Virus and Viroid Diseases of Crops in the Tropics. In Plant Virus and Viroid Diseases in the Tropics, (Dordrecht: Springer), pp. 149–489.

SAWIS (2018). South African Wine Industry Statistics (Annual Publication No. 43). *SA Wine Industry Information and Systems*. 1–32.

Scheben, A., Wolter, F., Batley, J., Puchta, H., and Edwards, D. (2017). Towards CRISPR/Cas crops - bringing together genomics and genome editing. *New Phytologist*. 216, 682–698.

Schmülling, T., and Schell, J. (1993). Transgenic tobacco plants regenerated from leaf disks can be periclinal chimeras. *Plant Molecular Biology*. 21, 705–708.

Shan-E-Ali Zaidi, S., and Mansoor, S. (2017). Viral vectors for plant genome engineering. *Frontiers in Plant Science*. 8, 2012–2017.

Shepherd, D.N., Mangwende, T., Martin, D.P., Bezuidenhout, M., Kloppers, F.J., Carolissen, C.H., Monjane, A.L., Rybicki, E.P., and Thomson, J.A. (2007). Maize streak virus-resistant transgenic maize: A first for Africa. *Plant Biotechnology Journal*. 5, 759–767.

Shi, Y., Wang, R., Luo, Z., Jin, L., Liu, P., Chen, Q., Li, Z., Li, F., Wei, C., Wu, M., et al. (2014). Molecular cloning and functional characterization of the Lycopene ε-cyclase gene via virus-induced gene silencing and its expression pattern in Nicotiana tabacum. *International Journal of Molecular Sciences*. 15, 14766–14785.

Shi, Y., Guo, J., Zhang, W., Jin, L., Liu, P., Chen, X., Li, F., Wei, P., Li, Z., Li, W., et al. (2015). Cloning of the Lycopene β-cyclase Gene in Nicotiana tabacum and Its Overexpression Confers Salt and Drought Tolerance. *International Journal of Molecular Sciences*. 16, 30438–30457.

Shmakov, S., Abudayyeh, O.O., Makarova, K.S., Wolf, Y.I., Gootenberg, J.S., Semenova, E., Minakhin, L., Joung, J., Konermann, S., Severinov, K., et al. (2015). Discovery and Functional Characterization of Diverse Class 2 CRISPR-Cas Systems. *Molecular Cell*. 60, 385–397.

Shmakov, S., Smargon, A., Scott, D., Cox, D., Pyzocha, N., Yan, W., Abudayyeh, O.O., Gootenberg, J.S., Makarova, K.S., Wolf, Y.I., et al. (2017). Diversity and evolution of class 2 CRISPR-Cas systems. *Nature Reviews Microbiology*. 15, 169–182.

Simón-Mateo, C., and García, J.A. (2011). Antiviral strategies in plants based on RNA silencing. *Biochimica et Biophysica Acta - Gene Regulatory Mechanisms*. 1809, 722–731.

Smargon, A.A., Cox, D.B.T., Pyzocha, N.K., Zheng, K., Slaymaker, I.M., Gootenberg, J.S., Abudayyeh, O.A., Essletzbichler, P., Shmakov, S., Makarova, K.S., et al. (2017). Cas13b Is a Type VI-B CRISPR-Associated RNA-Guided RNase Differentially Regulated by Accessory Proteins Csx27 and Csx28. *Molecular Cell*. 65, 618–630.

Song, G., Jia, M., Chen, K., Kong, X., Khattak, B., Xie, C., Li, A., and Mao, L. (2016). CRISPR/Cas9: A powerful tool for crop genome editing. *The Crop Journal*. 4, 75–82.

Sonoda, E., Hochegger, H., Saberi, A., Taniguchi, Y., and Takeda, S. (2006). Differential usage of non-homologous end-joining and homologous recombination in double strand break repair. *DNA Repair*. 5, 1021–1029.

Sun, T., Tadmor, Y., and Li, L. (2020). Pathways for Carotenoid Biosynthesis, Degradation, and Storage. In Plant and Food Carotenoids, M. Rodríguez-Concepción, and R. Welsch, eds. (New York: Springer), pp. 3–23.

Tabassum, B., Nasir, I.A., Khan, A., Aslam, U., Tariq, M., Shahid, N., and Husnain, T. (2016). Short hairpin RNA engineering: In planta gene silencing of potato virus Y. *Crop Protection*. 86, 1–8.

Taliansky, M., Samarskaya, V., Zavriev, S.K., Fesenko, I., Kalinina, N.O., and Love, A.J. (2021). RNA-Based Technologies for Engineering Plant Virus Resistance. *Plants*. 10, 82.

Tambe, A., East-Seletsky, A., Knott, G.J., Doudna, J.A., and O'Connell, M.R. (2018). RNA Binding and HEPN-Nuclease Activation Are Decoupled in CRISPR-Cas13a. *Cell Reports*. 24, 1025–1036.

Tashkandi, M., Ali, Z., Aljedaani, F., Shami, A., and Mahfouz, M.M. (2018). Engineering resistance against Tomato yellow leaf curl virus via the CRISPR/Cas9 system in tomato. *Plant Signaling and Behavior*. 13, 1–7.

Tavazza, M., Lucioli, A., and Ilardi, V. (2017). Gene Silencing Provides Efficient Protection against Plant Viruses. In Plant Gene Silencing: Mechanisms and Applications, T. Dalmay, ed. (Wallingford: CABI), pp. 193–205.

Tenllado, F. (2004). RNA interference as a new biotechnological tool for the control of virus diseases in plants. *Virus Research*. 102, 85–96.

Tian, J., Pei, H., Zhang, S., Chen, J., Chen, W., Yang, R., Meng, Y., You, J., Gao, J., and Ma, N. (2014). TRV-GFP: A modified Tobacco rattle virus vector for efficient and visualizable analysis of gene function. *Journal of Experimental Botany*. 65, 311–322.

Tripathi, J.N., Ntui, V.O., Ron, M., Muiruri, S.K., Britt, A., and Tripathi, L. (2019). CRISPR/Cas9 editing of endogenous banana streak virus in the B genome of Musa spp. overcomes a major challenge in banana

breeding. *Communications Biology*. 2, 1–11.

Tsai, S.Q., and Joung, J.K. (2016). Defining and improving the genome-wide specificities of CRISPR–Cas9 nucleases. *Nature Reviews Genetics*. 17, 300–312.

Uniyal, A.P., Mansotra, K., Yadav, S.K., and Kumar, V. (2019). An overview of designing and selection of sgRNAs for precise genome editing by the CRISPR-Cas9 system in plants. *3 Biotech*. 9, 223.

Varanda, C.M.R., Félix, M. do R., Campos, M.D., Patanita, M., and Materatski, P. (2021). Plant Viruses: From Targets to Tools for CRISPR. *Viruses*. 13, 141.

Wang, M., and Metzlaff, M. (2012). RNA silencing and antiviral defense in plants. *Methods in Molecular Biology*. 894, 17–38.

Wang, F., Wang, L., Zou, X., Duan, S., Li, Z., Deng, Z., Luo, J., Lee, S.Y., and Chen, S. (2019). Advances in CRISPR-Cas systems for RNA targeting, tracking and editing. *Biotechnology Advances*. 37, 708–729.

Wang, T., Iyer, L.M., Pancholy, R., Shi, X., and Hall, T.C. (2005). Assessment of penetrance and expressivity of RNAi-mediated silencing of the Arabidopsis phytoene desaturase gene. *New Phytologist*. 167, 751–760.

Wang, T., Deng, Z., Zhang, X., Wang, H., Wang, Y., Liu, X., Liu, S., Xu, F., Li, T., Fu, D., et al. (2018a). Tomato DCL2b is required for the biosynthesis of 22-nt small RNAs, the resulting secondary siRNAs, and the host defense against ToMV. *Horticulture Research*. 5, 62.

Wang, Z., Hardcastle, T.J., Pastor, A.C., Yip, W.H., Tang, S., and Baulcombe, D.C. (2018b). A novel DCL2-dependent miRNA pathway in tomato affects susceptibility to RNA viruses. *Genes and Development*. 32, 1155–1160.

Wessels, H.-H., Méndez-Mancilla, A., Guo, X., Legut, M., Daniloski, Z., and Sanjana, N.E. (2020). Massively parallel Cas13 screens reveal principles for guide RNA design. *Nature Biotechnology*. 38, 722–727.

Whitham, S., Dinesh-Kumar, S.P., Choi, D., Hehl, R., Corr, C., and Baker, B. (1994). The product of the tobacco mosaic virus resistance gene N: Similarity to toll and the interleukin-1 receptor. *Cell*. 78, 1101–1115.

Whitham, S., McCormick, S., and Baker, B. (1996). The N gene of tobacco confers resistance to tobacco mosaic virus in transgenic tomato. *Proceedings of the National Academy of Sciences of the United States of America*. 93, 8776–8781.

Wilson, T.M.A. (1993). Strategies to protect crop plants against viruses: Pathogen-derived resistance blossoms. *Proceedings of the National Academy of Sciences of the United States of America*. 90, 3134–3141.

Wolt, J.D., Wang, K., Sashital, D., and Lawrence-Dill, C.J. (2016). Achieving Plant CRISPR Targeting that Limits Off-Target Effects. *The Plant Genome*. 9, 1–8.

Woo, J.W., Kim, J., Kwon, S. Il, Corvalán, C., Cho, S.W., Kim, H., Kim, S.G., Kim, S.T., Choe, S., and Kim, J.S. (2015). DNA-free genome editing in plants with preassembled CRISPR-Cas9 ribonucleoproteins. *Nature Biotechnology*. 33, 1162–1164.

Xie, K., and Yang, Y. (2013). RNA-Guided genome editing in plants using a CRISPR-Cas system.

Molecular Plant. 6, 1975–1983.

Yadav, S., and Chhibbar, A.K. (2018). Plant–Virus Interactions. In Molecular Aspects of Plant-Pathogen Interaction, (Singapore: Springer Singapore), pp. 43–77.

Yan, M.-Y., Yan, H., Ren, G., Zhao, J., Guo, X., and Sun, Y.-C. (2017). CRISPR-Cas12a-Assisted Recombineering in Bacteria. *Applied and Environmental Microbiology*. 83, 1–13.

Yan, W.X., Chong, S., Zhang, H., Makarova, K.S., Koonin, E. V., Cheng, D.R., and Scott, D.A. (2018). Cas13d Is a Compact RNA-Targeting Type VI CRISPR Effector Positively Modulated by a WYL-Domain-Containing Accessory Protein. *Molecular Cell*. 70, 327–339.

Yepes-Molina, L., Bárzana, G., and Carvajal, M. (2020). Controversial regulation of gene expression and protein transduction of aquaporins under drought and salinity stress. *Plants*. 9, 1–18.

Yin, K., and Qiu, J.-L. (2019). Genome editing for plant disease resistance: applications and perspectives. *Philosophical Transactions of the Royal Society B: Biological Sciences*. 374, 20180322.

Yin, K., Han, T., Liu, G., Chen, T., Wang, Y., Yu, A.Y.L., and Liu, Y. (2015). A geminivirus-based guide RNA delivery system for CRISPR/Cas9 mediated plant genome editing. *Scientific Reports*. 5, 1–10.

Yin, K., Han, T., Xie, K., Zhao, J., Song, J., and Liu, Y. (2019). Engineer complete resistance to Cotton Leaf Curl Multan virus by the CRISPR/Cas9 system in Nicotiana benthamiana. *Phytopathology Research*. 1, 1–9.

Yu, B., Lydiate, D.J., Young, L.W., Schäfer, U.A., and Hannoufa, A. (2008). Enhancing the carotenoid content of Brassica napus seeds by downregulating lycopene epsilon cyclase. *Transgenic Research*. 17, 573–585.

Yu, Y., Wang, X., Sun, H., Liang, Q., Wang, W., Zhang, C., Bian, X., Cao, Q., Li, Q., Xie, Y., et al. (2020). Improving CRISPR-Cas-mediated RNA targeting and gene editing using SPLCV replicon-based expression vectors in Nicotiana benthamiana. *Plant Biotechnology Journal*. 18, 1993–1995.

Yue, J.-J., Hong, C.-Y., Wei, P., Tsai, Y.-C., and Lin, C.-S. (2020). How to start your monocot CRISPR/Cas project: plasmid design, efficiency detection, and offspring analysis. *Rice*. 13, 9.

Zaidi, S.S. e. A., Mahfouz, M.M., and Mansoor, S. (2017). CRISPR-Cpf1: A New Tool for Plant Genome Editing. *Trends in Plant Science*. 22, 550–553.

Zeng, J., Wang, C., Chen, X., Zang, M., Yuan, C., Wang, X., Wang, Q., Li, M., Li, X., Chen, L., et al. (2015). The lycopene β-cyclase plays a significant role in provitamin A biosynthesis in wheat endosperm. *BMC Plant Biology*. 15, 1–14.

Zetsche, B., Gootenberg, J.S., Abudayyeh, O.O., Slaymaker, I.M., Makarova, K.S., Essletzbichler, P., Volz, S.E., Joung, J., Van Der Oost, J., Regev, A., et al. (2015). Cpf1 Is a Single RNA-Guided Endonuclease of a Class 2 CRISPR-Cas System. *Cell*. 163, 759–771.

Zhan, X., Zhang, F., Zhong, Z., Chen, R., Wang, Y., Chang, L., Bock, R., Nie, B., and Zhang, J. (2019). Generation of virus-resistant potato plants by RNA genome targeting. *Plant Biotechnology Journal*. 17, 1814–1822.

Zhang, B., Ye, Y., Ye, W., Perčulija, V., Jiang, H., Chen, Y., Li, Y., Chen, J., Lin, J., Wang, S., et al. (2019a). Two HEPN domains dictate CRISPR RNA maturation and target cleavage in Cas13d. *Nature*

Communications. 10, 2544.

Zhang, C., Konermann, S., Brideau, N.J., Lotfy, P., Wu, X., Novick, S.J., Strutzenberg, T., Griffin, P.R., Hsu, P.D., and Lyumkis, D. (2018a). Structural Basis for the RNA-Guided Ribonuclease Activity of CRISPR-Cas13d. *Cell*. 175, 212–223.

Zhang, T., Zheng, Q., Yi, X., An, H., Zhao, Y., Ma, S., and Zhou, G. (2018b). Establishing RNA virus resistance in plants by harnessing CRISPR immune system. *Plant Biotechnology Journal*. 16, 1415–1423.

Zhang, T., Zhao, Y., Ye, J., Cao, X., Xu, C., Chen, B., An, H., Jiao, Y., Zhang, F., Yang, X., et al. (2019b). Establishing CRISPR/Cas13a immune system conferring RNA virus resistance in both dicot and monocot plants. *Plant Biotechnology Journal*. 17, 1185–1187.

Zhang, X.-H., Tee, L.Y., Wang, X.-G., Huang, Q.-S., and Yang, S.-H. (2015). Off-target Effects in CRISPR/Cas9-mediated Genome Engineering. *Molecular Therapy - Nucleic Acids*. 4, e264.

Zhang, Y., Shan, Q., Wang, Y., Chen, K., Liang, Z., Li, J., Zhang, Y., Zhang, K., Liu, J., Voytas, D.F., et al. (2013a). Rapid and efficient gene modification in rice and brachypodium using TALENs. *Molecular Plant*. 6, 1365–1368.

Zhang, Y., Zhang, F., Li, X., Baller, J.A., Qi, Y., Starker, C.G., Bogdanove, A.J., and Voytas, D.F. (2013b). Transcription activator-like effector nucleases enable efficient plant genome engineering. *Plant Physiology*. 161, 20–27.

Zherdev, A. V., Vinogradova, S. V., Byzova, N.A., Porotikova, E. V., Kamionskaya, A.M., and Dzantiev, B.B. (2018). Methods for the diagnosis of grapevine viral infections: A review. *Agriculture (Switzerland)*. 8, 1–19.

Zhu, H., Richmond, E., and Liang, C. (2018). CRISPR-RT: A web application for designing CRISPR-C2c2 crRNA with improved target specificity. *Bioinformatics*. 34, 117–119.

Zhu, H., Li, C., and Gao, C. (2020). Applications of CRISPR–Cas in agriculture and plant biotechnology. *Nature Reviews Molecular Cell Biology*. 21, 661–677.

APPENDIX A – RESEARCH OUTPUTS

Conference Attendance: Poster Presentations

Robertson GM, Campa M, Vivier MA and Burger JT. Establishing RNA targeting via the CRISPR/Cas13 system in *Vitis vinifera*. Plant Genome Editing & Genome Engineering II International Conference 5-6 July 2019. Vienna, Austria.

Robertson GM, Campa M, Vivier MA and Burger JT. Establishing the CRISPR/Cas13a system in *Vitis vinifera* for a virus interference application. Virology Africa, 10-14 February 2020. Cape Town, South Africa.

APPENDIX B - SUPPLEMENTARY MATERIAL

Supplementary Table 1. Oligonucleotides with the *Bbs*I-restriction sequences added at the 5'-end for cloning of the individual crRNAs.

Oligo name	Sequence (5' - 3')	crRNA purpose
LCYB/Target 1-F	aaacTTTGAGCTTCCTATGTATGACCCTTCAA	*LCYB* Target 1
LCYB/Target 1-R	aaaaTTGAAGGGTCATACATAGGAAGCTCAAA	
LCYB/Target 2-F	aaacGGGCCCAATAACTATGGTGTTTGGGTGGA	*LCYB* Target 2
LCYB/Target 2-R	aaaaTCCACCCAAACACCATAGTTATTGGGCCC	
TRBO-GFP/GFP Target-F	aaacGAACAGGTAGTTTTCCAGTAGTGCAAATA	TRBO-GFP GFP Target
TRBO-GFP/GFP Target-R	aaaaTATTTGCACTACTGGAAAACTACCTGTTC	

Supplementary Table 2. Gibson primers used to clone the respective LwaCas13a_NLS/NES fragments into the LwaCas13a_crRNA backbone.

Primer name	Sequence 5' (overlap/spacer/ANNEAL) 3'	Length (bp)	%GC
LwaCas13a-NLS_fwd	acgggggactcccgacatggAGCCCCAAAAAGAAGAGG	38	61
LwaCas13a-NLS_rev	aacacaaacttaagcacacaACCTACCTTGCGCTTTTTC	39	41
LwaCas13a-NES_fwd	acgggggactcccgacatggATGCTGTACCCTGAGCGG	38	66
LwaCas13a-NES_rev	aacacaaacttaagcacacaTGGGTAGGTCAGGATCCG	38	47

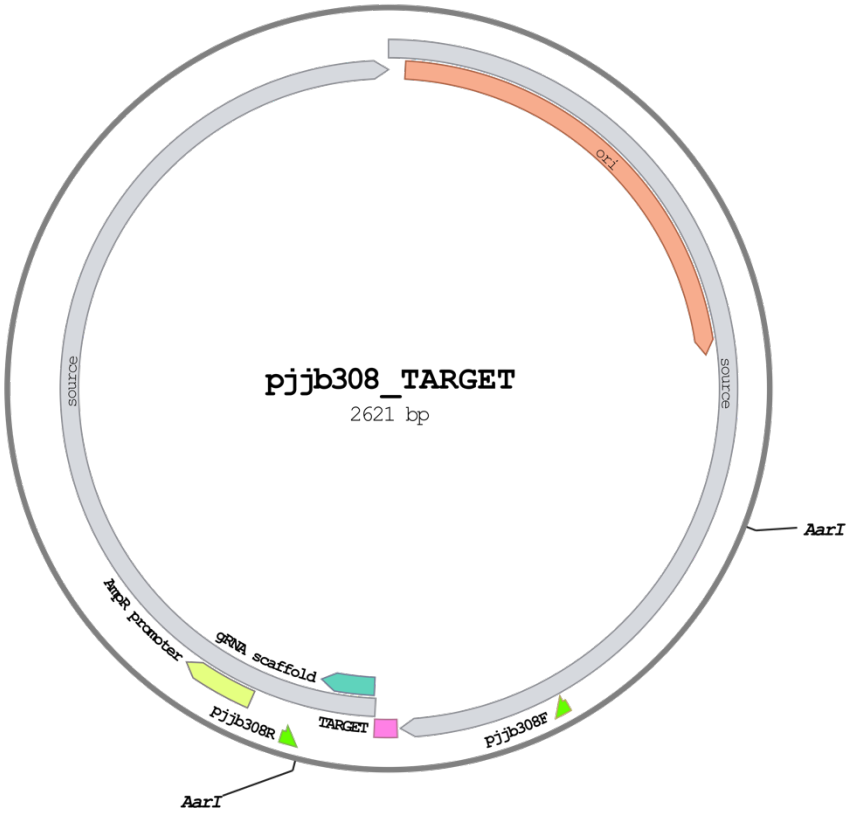

Supplementary Figure 1. Intermediate plasmid pjjb308_crRNA map annotated with primers and the important restriction enzyme sites.

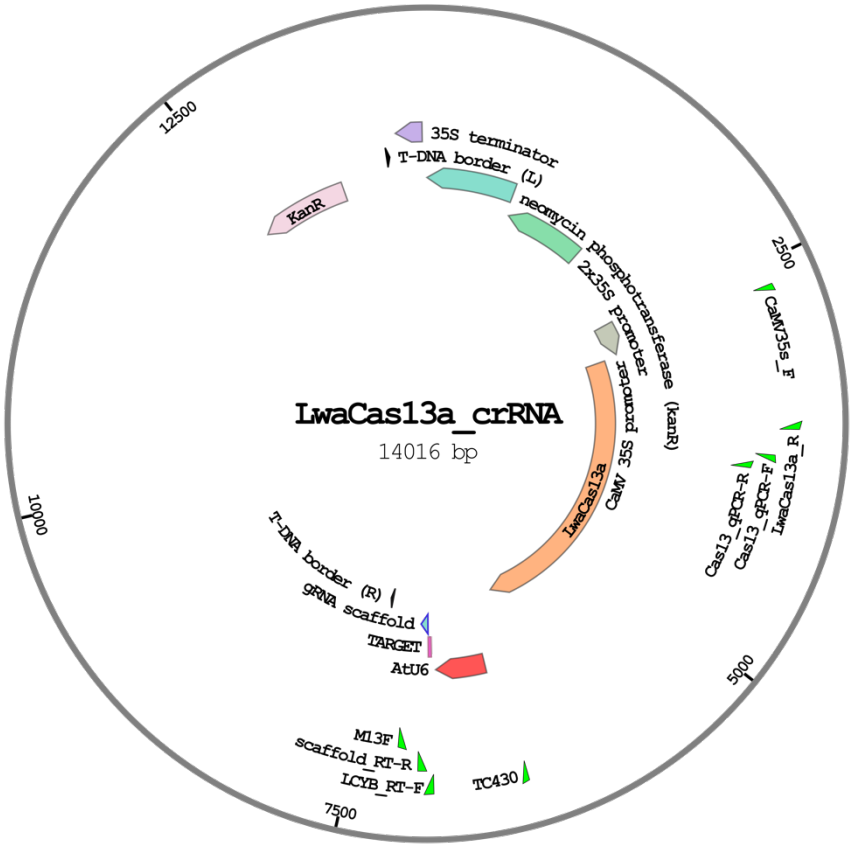

Supplementary Figure 2. LwaCas13a_crRNA plasmid map annotated with primers.

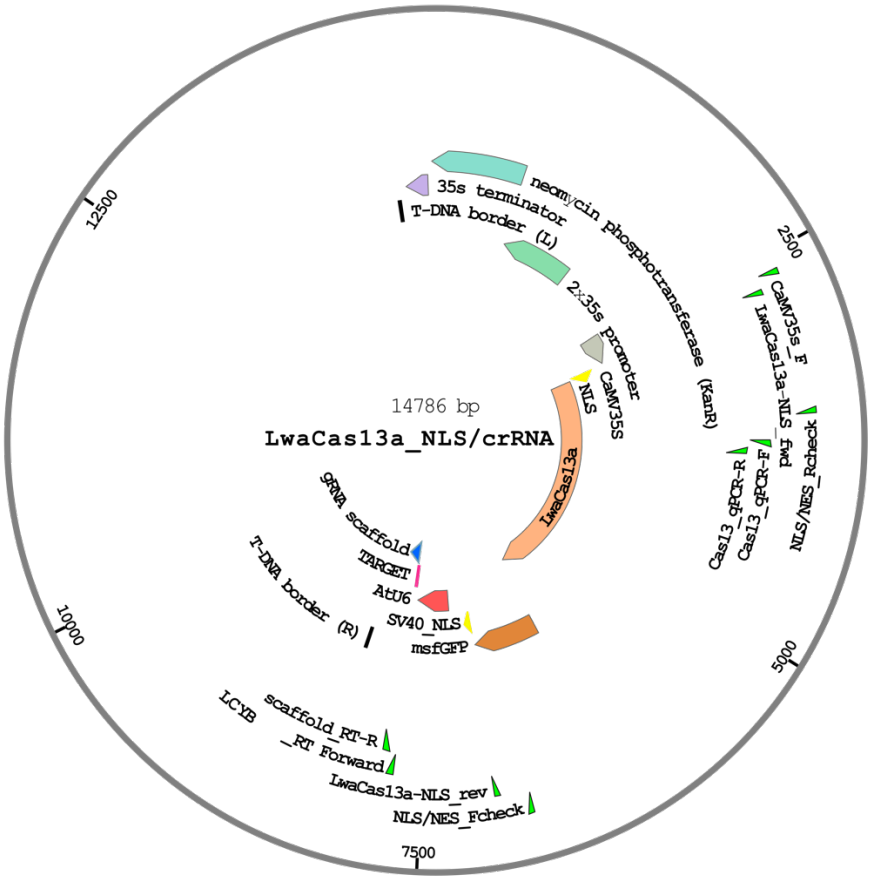

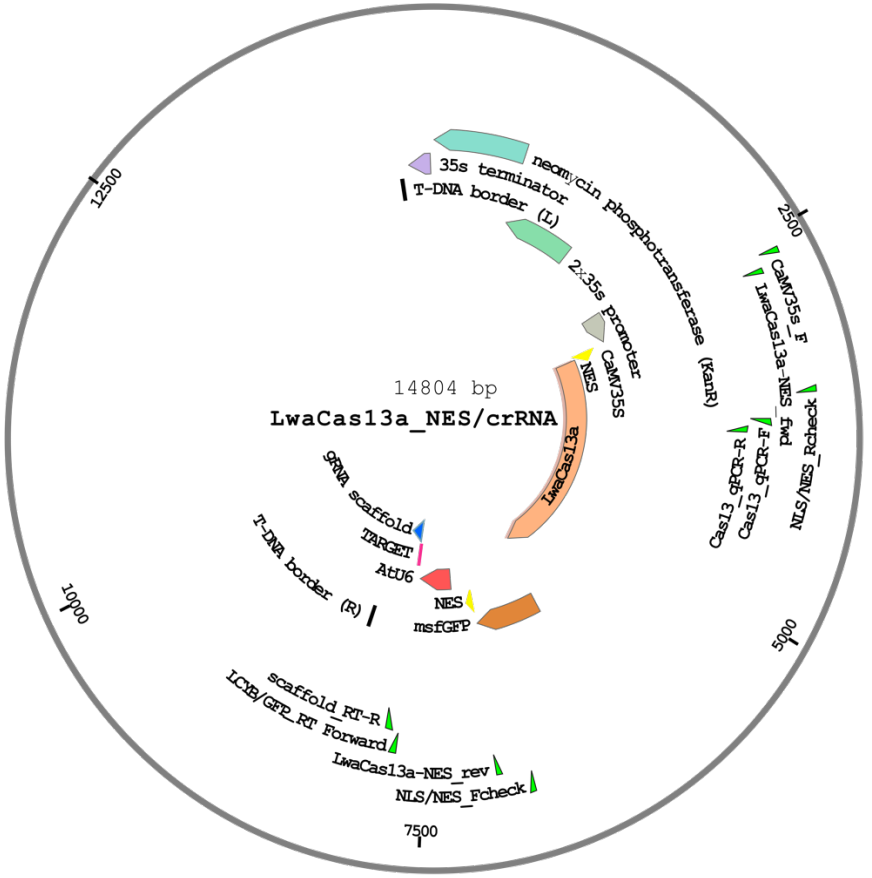

Supplementary Figure 3. LwaCas13a_NLS/crRNA and LwaCas13a_NES/crRNA plasmid maps annotated with primers.

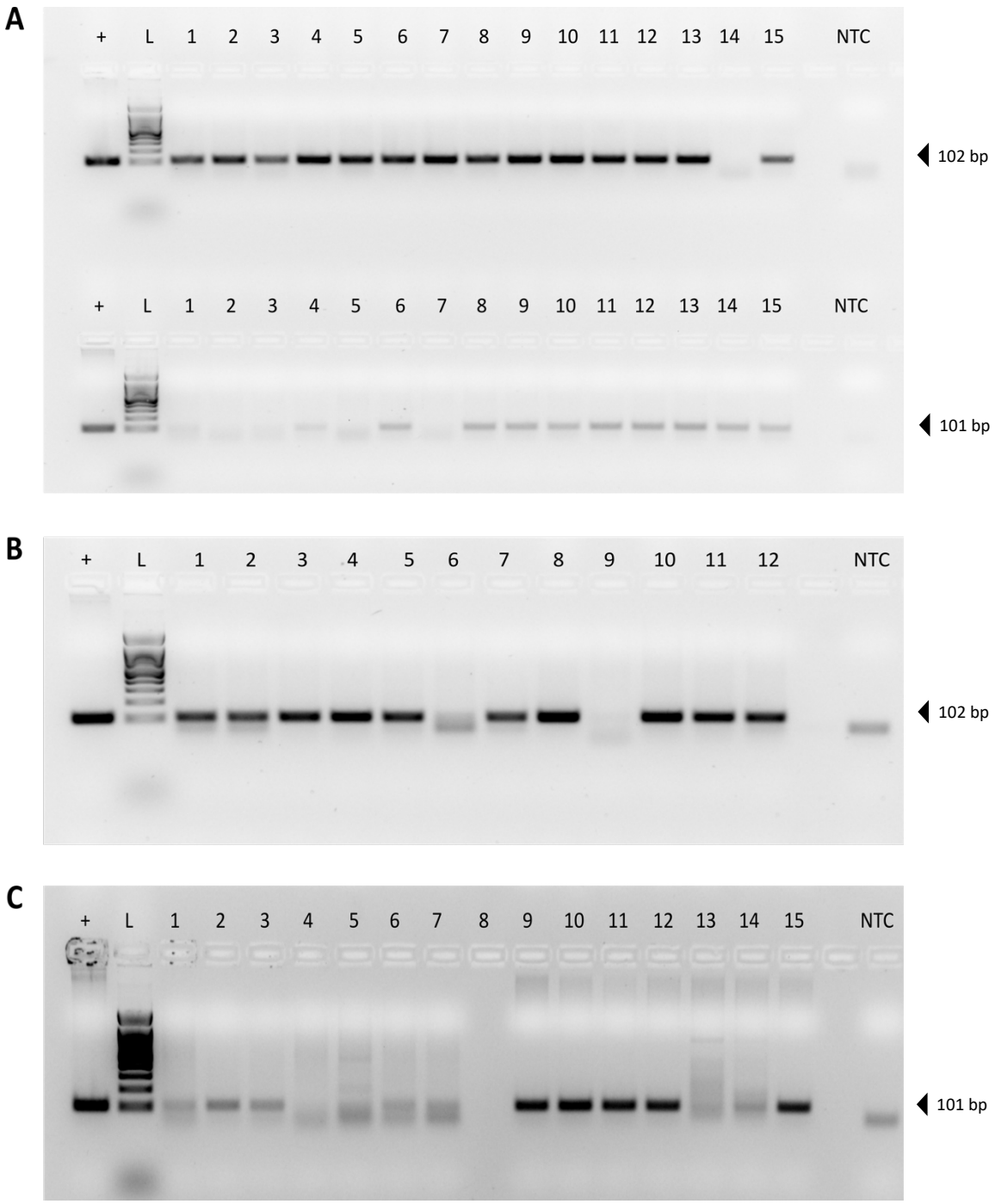

Supplementary Figure 4. Gene expression analysis by RT-PCR. (**A**) Detection of the expression of LwaCas13a (TOP) and the LCYB Target 1 crRNA (BOTTOM). PCR products are resolved on a 2% (w/v) agarose gel. Lanes 1- 5: samples E1-E5; Lanes 6-15: samples NLS1-NLS10. L: 100bp molecular weight marker (Cleaver Scientific, USA); Positive control: LwaCas13a/NLS-T1 target plasmid DNA; NTC: No template control. (**B**) Detection of the expression of LwaCas13a. PCR products are resolved on a 2% (w/v) agarose gel. Lanes 1- 5: samples E1-E5; Lanes 6-15: samples NES1-NES7. L: 100bp molecular weight marker (Cleaver Scientific, USA); Positive control: LwaCas13a/NES-T1 target plasmid DNA; NTC: No template control. (**C**) Detection of the expression of the LCYB Target 1 crRNA. PCR products are resolved on a 2% (w/v) agarose gel. Lanes 1- 7: NES1-NES7 crRNA samples; Lanes 9-15: NES1-NES7 DNA samples. L: 100bp molecular weight marker (Cleaver Scientific, USA); Positive control: LwaCas13a/NES-T1 target plasmid DNA; NTC: No template control.

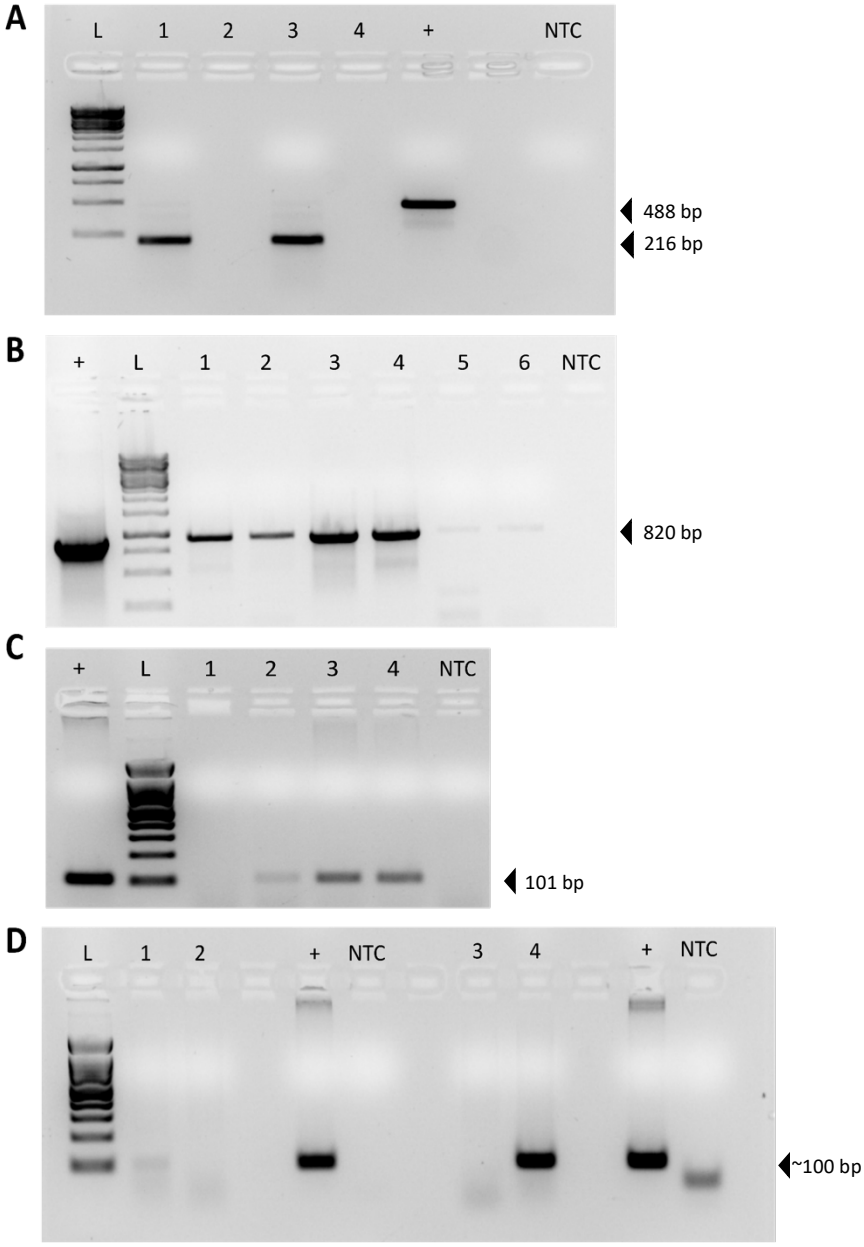

Supplementary Figure 5. RT-PCRs repeated for samples that did not amplify initially. (**A**) Detection of actin in cDNA sample E3 with an anticipated PCR product of 216 bp for cDNA and 488 bp for genomic DNA. PCR products are resolved on a 2% (w/v) agarose gel. Lanes 1 and 3: E3 cDNA ~50 ng/µl and E3 cDNA ~100 ng/µl, respectively; L: 1kb molecular weight marker (GeneRuler, Thermo Scientific); Positive control: wild-type *N. benthamiana* DNA sample; NTC: No template control. (**B**) Detection of LwaCas13a expression using the *Cas13a*-specific primers (~820 bp). PCR products are resolved on a 1% (w/v) agarose gel. Lanes 1 & 2: NLS 1 and 9 cDNA samples (~100 ng/µl); Lanes 3 & 4: NLS 1 and 9 DNA samples. Lanes 5 & 6: NLS 1 and cDNA samples (~50 ng/µl). L: 1kb molecular weight marker (GeneRuler, Thermo Scientific); Positive control: LwaCas13a/NLS-T1 target plasmid DNA; NTC: No template control. (**C**) Detection of *LCYB* Target 1 crRNA expression. PCR products are resolved on a 2% (w/v) agarose gel. Lanes 1 & 2: NLS 2 and 3 cDNA samples (~50 ng/µl) Lanes 3 & 4: NLS 2 and 3 cDNA samples (~100 ng/µl); L: 1kb molecular weight marker (GeneRuler, Thermo Scientific); Positive control: LwaCas13a/NLS-T1 target plasmid DNA; NTC: No template control. (**D**) Detection of the expression of the *LCYB* Target 1 crRNA (Lanes 1 & 2, cDNA samples NES 1 and 4) and LwaCas13a (Lanes 3 & 4, cDNA samples NES 4 & 5). PCR products are resolved on a 2% (w/v) agarose gel. L: 100bp molecular weight marker (Cleaver Scientific, USA); Positive control: LwaCas13a/NES-T1 target plasmid DNA; NTC: No template control.

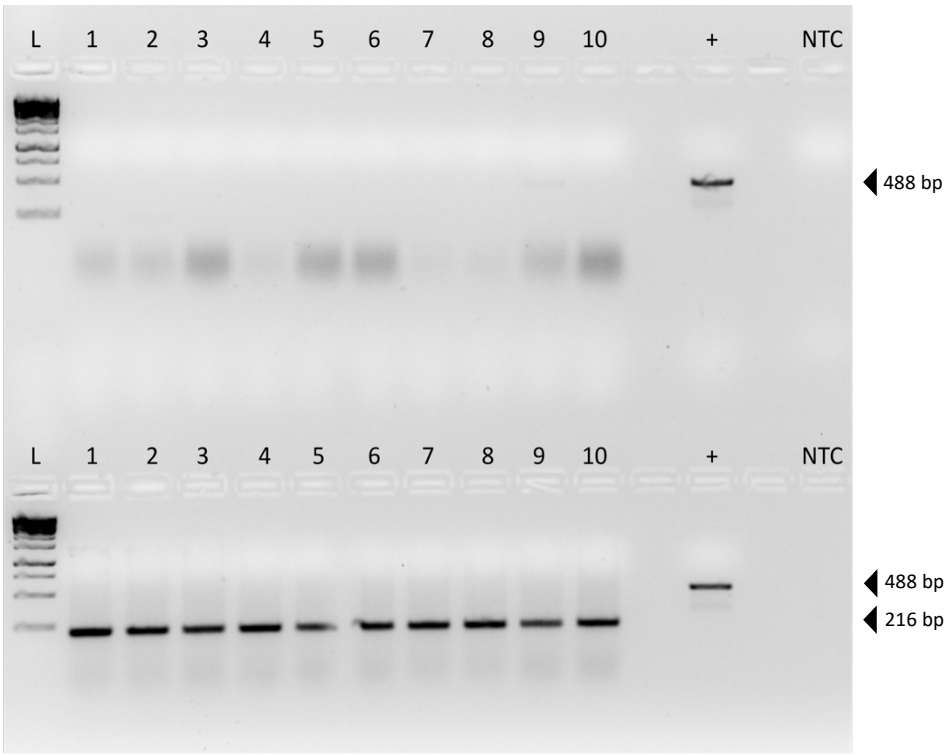

Supplementary Figure 6. Detection of actin in RNA samples (TOP row) and cDNA samples (BOTTOM row), with anticipated PCR products of 216 bp for cDNA and 488 bp for genomic DNA. PCR products are resolved on a 2% (w/v) agarose gel. Lanes 1 & 2: Samples NLS 1.1 and 1.2; Lanes 3 & 4: Samples NLS 6.1 and 6.2; Lanes 5 & 6: Samples NLS 8.1 and 8.2; Lanes 7 & 8: Samples NES 1.1 and 1.2; Lanes 9 & 10: Samples NES 7.1 and 7.2; L: 1kb molecular weight marker (GeneRuler, Thermo Scientific); Positive control: wild-type *N. benthamiana* DNA sample; NTC: No template control.

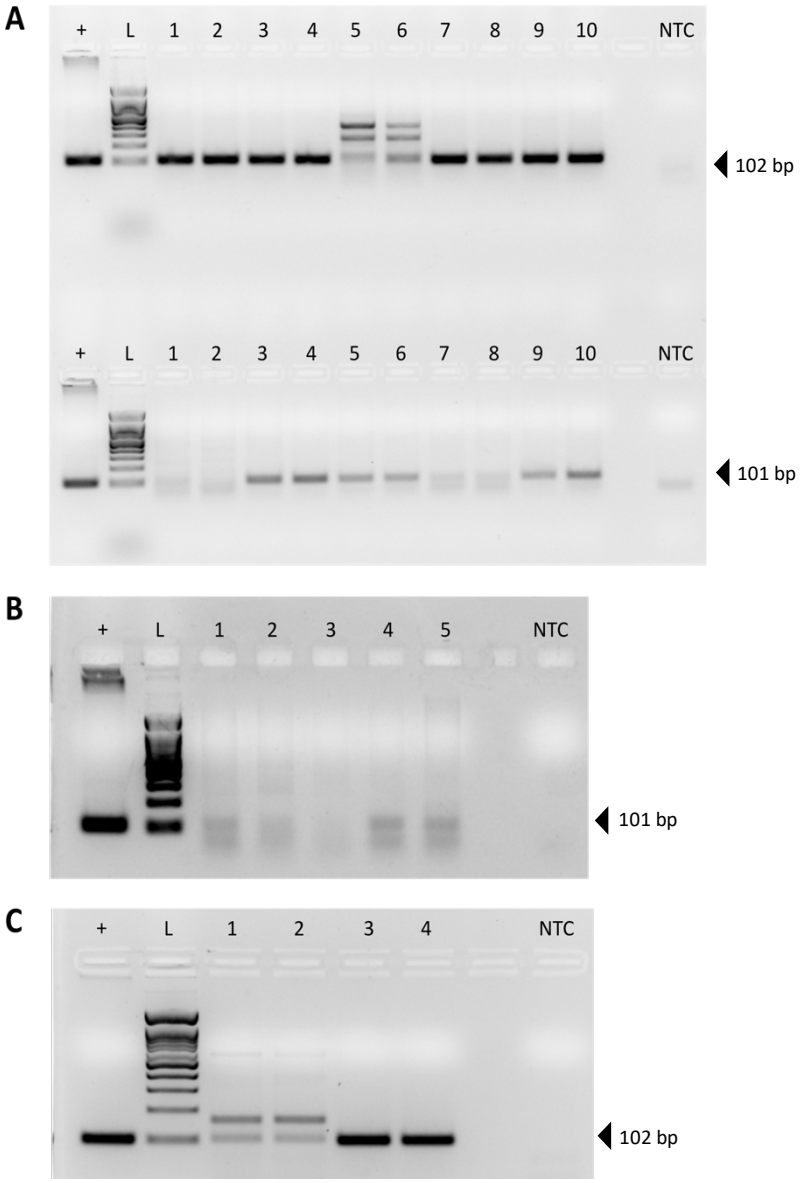

Supplementary Figure 7. Gene expression analysis by RT-PCR. All PCR products are resolved on 2% (w/v) agarose gels. (**A**) Detection of the expression of LwaCas13a (TOP) and the *LCYB* Target 1 crRNA (BOTTOM). Lanes 1 & 2: Samples NLS 1.1 and 1.2; Lanes 3 & 4: Samples NLS 4.1 and 4.2; Lanes 5 & 6: Samples NLS 6.1 and 6.2; Lanes 7 & 8: Samples NES 1.1 and 1.2; Lanes 9 & 10: Samples NES 7.1 and 7.2; L: 100bp molecular weight marker (Cleaver Scientific, USA); Positive control: LwaCas13a/NLS-T1 target plasmid DNA; NTC: No template control. (**B**) Detection of the expression of the *LCYB* Target 1 crRNA using a higher concentration of cDNA. Lanes 1 & 2: Samples NLS 1.1 and 1.2; Lanes 3 & 4: Samples NES 1.1 and 1.2. L: 100bp molecular weight marker (Cleaver Scientific, USA); Positive control: LwaCas13a/NLS-T1 target plasmid DNA; NTC: No template control. (**C**) Detection of the expression of LwaCas13a using a higher concentration of cDNA. Lanes 1 & 2: Samples NLS 6.1 and 6.2 (~50 ng/µl); Lanes 3 & 4: Samples NLS 6.1 and 6.2 (~100 ng/µl); L: 100bp molecular weight marker (Cleaver Scientific, USA); Positive control: LwaCas13a/NLS-T1 target plasmid DNA; NTC: No template control.

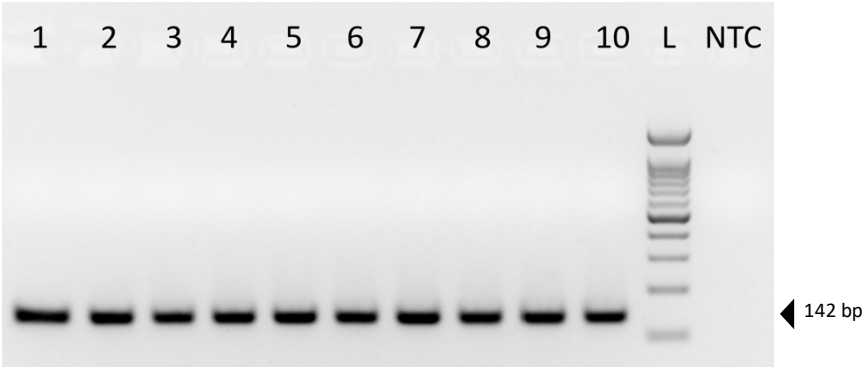

Supplementary Figure 8. Representative *ubiquitin* PCR on cDNA samples. PCR products (142 bp) are resolved on a 2% (w/v) agarose gel. Lanes 1- 5: samples 1.1-1.5; Lanes 6-10: samples 2.1-2.5. L: 100bp molecular weight marker (Cleaver Scientific, USA); NTC: No template control

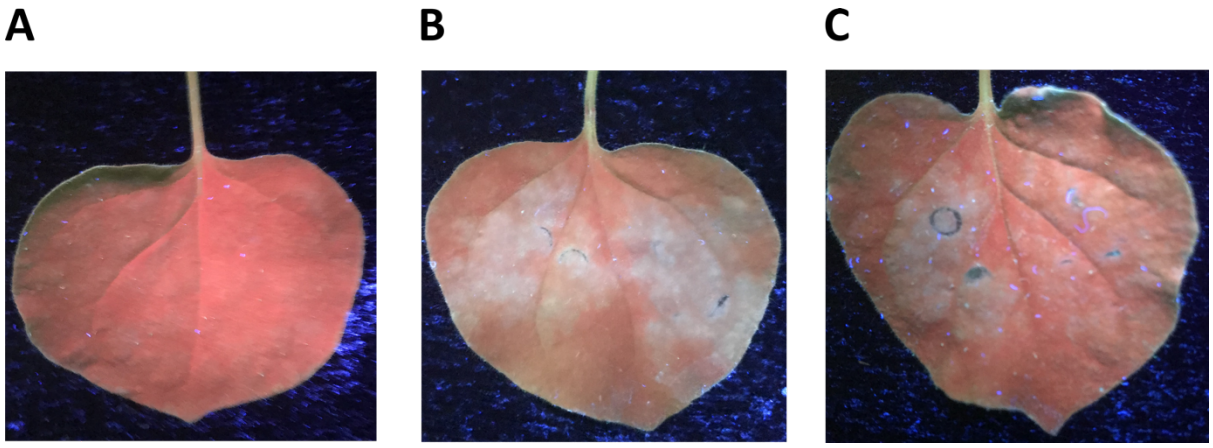

Supplementary Figure 9. Representative images of the *N. benthamaiana* 16C infiltration experiment visualised under UV light 4 days post-infiltration. (A) Non-infiltrated 16C leaf. (B) The left and right side of a 16C leaf infiltrated with the control LwaCas13a_NES EMPTY and the LwaCas13a_NLS/GFP construct, respectively. (C) The left and right side of a 16C leaf infiltrated with the control LwaCas13a_NES EMPTY and the LwaCas13a_NES/GFP construct, respectively.